THE UNIVERSITY *of* EDINBURGH

Low Complexity Radio Resource Management for Energy Efficient Wireless Networks

Rodrigo Alberto Vaca Ramirez

A thesis submitted for the degree of Doctor of Philosophy.
The University of Edinburgh.
April 2014

Abstract

Energy consumption has become a major research topic from both environmental and economical perspectives. The telecommunications industry is currently responsible for 0.7% of the total global carbon emissions, a figure which is increasing at rapid rate. By 2020, it is desired that CO_2 emissions can be reduced by 50%. Thus, reducing the energy consumption in order to lower carbon emissions and operational expenses has become a major design constraint for future communication systems. Therefore, in this thesis energy efficient resource allocation methods have been studied taking the Long Term Evolution (LTE) standard as an example.

Firstly, a theoretical analysis, that shows how improvements in energy efficiency can directly be related with improvements in fairness, is provided using a Shannon theory analysis. The traditional uplink power control challenge is re-evaluated and investigated from the view point of interference mitigation rather than power minimization. Thus, a low complexity distributed resource allocation scheme for reducing the uplink co-channel interference (CCI) is presented. Improvements in energy efficiency are obtained by controlling the level of CCI affecting vulnerable mobile stations (MSs). This is done with a combined scheduler and a two layer power allocation scheme, which is based on non-cooperative game theory. Simulation results show that the proposed low complexity method provides similar performance in terms of fairness and energy efficiency when compared to a centralized signal interference noise ratio balancing scheme.

Apart from using interference management techniques, by using efficiently the spare resources in the system such as bandwidth and available infrastructure, the energy expenditure in wireless networks can also be reduced. For example, during low network load periods spare resource blocks (RBs) can be allocated to mobile users for transmission in the uplink. Thereby, the user rate demands are split among its allocated RBs in order to transmit in each of them by using a simpler and more energy efficient modulation scheme. In addition, virtual Multiple-input Multiple-output (MIMO) coalitions can be formed by allowing single antenna MSs and available relay stations to cooperate between each other to obtain power savings by implementing the concepts of spatial multiplexing and spatial diversity. Resource block allocation and virtual MIMO coalition formation are modeled by a game theoretic approach derived from two different concepts of stable marriage with incomplete lists (SMI) and the college admission framework (CAF) respectively. These distributed approaches focus on optimizing the overall consumed power of the single antenna devices rather than on the transmitted power. Moreover, it is shown that when overall power consumption is optimized the energy efficiency of the users experiencing good propagation conditions in the uplink is not always improved by transmitting in more than one RB or by forming a virtual MIMO link. Finally, it is shown that the proposed distributed schemes achieve a similar performance in bits per Joule when compared to much more complex centralized resource allocation methods.

Declaration of originality

I hereby declare that the research recorded in this thesis and the thesis itself was composed and originated entirely by myself in the School of Engineering at The University of Edinburgh.

Rodrigo Alberto Vaca Ramirez

Acknowledgements

First and foremost, I would like to express my deepest gratitude and appreciation to my supervisors Prof. John S. Thompson and Dr. Victor M. Ramos Ramos for their insightful technical advice and excellent guidance during the course of my doctoral studies. Their unfailing patience and passion for the subject matter have been invaluable for my research.

I am also grateful to Prof. Eitan Altman for his invaluable support and advice during the six months that I spent at the French Institute for Research in Computer Science and Automation (INRIA). This has been a professional and personally enriching experience that I will never forget.

My family has been the most important support for me. I could not have complete my studies without their love, compassion, care and support. So, I would like to thank to my parents Jose Luis and Maria Luisa and to my brother Alejandro for always been looking after me during all these years.

A very special thank to my love Azadeh, whose care and support made of this journey such a wonderful and unforgettable experience.

Special thanks to my dear friends Jose Miguel, Alejandro and Julio Cesar for always been there no matter the physical distance between us.

I would like to thank the financial support of my sponsor the Consejo Nacional de Ciencia y Tecnologia (CONACYT), which gave me the opportunity to commence and complete these studies on time.

Last but not the least, I would like to thank to my friends at IDCOM: Dobro, Bogo, Harald, Nick, Stefan, Sakis, Chun Li and Myriam for their continuous help and friendship. I will never forget these three years at IDCOM.

Contents

List of figures

List of tables

Acronyms and abbreviations

3G	third generation
3GPP	third generation partnership project
4G	fourth generation
ANF	amplify-and-forward
ARBA	arbitrary RB allocation
AWGN	additive white Gaussian noise
BB	base band
BER	bit error ratio
BE	bandwidth expansion
BS	base station
BW	best worst
CAF	college admission framework
CCI	co-channel interference
CDF	cumulative distribution function
CDMA	code division multiple access
CIC	co-channel interference coordination
CSI	channel state information
EDGE	enhanced data rates for GSM evolution
FDD	frequency division duplexing
FDMA	frequency division multiple access
FSF	frequency selective fading
GSM	global system for mobile communications
GPRS	general packet radio service
HPA	high power amplifier
HSCSD	high speed circuit switches data
HSE	high spectral efficiency
HSUPA	high speed uplink packet access
LPA	low power amplifier
LSE	low spectral efficiency
LTE	Long Term Evolution

MIMO	multiple–input multiple–output
MISO	multiple–input single–output
MRH	minimum relaying hop
MS	mobile station
NCG	non-cooperative game
OFDMA	orthogonal frequency division multiple access
PDF	probability distribution function
QoS	quality of service
RB	resource block
RF	radio frequency
RRM	radio resource management
RS	relay station
SIMO	single–input multiple–output
SINR	signal to interference plus noise ratio
SISO	single–input single–output
SMI	stable marriage with incomplete lists
SNR	signal to noise ratio
SRS	sounding reference signals
SVD	singular value decomposition
TDD	time division duplexing
TDMA	time division multiple access
UL	uplink
WCDMA	wideband code division multiple access
ZMCSG	zero mean circulant symmetric complex

Nomenclature

A	constant value
b	priority levels in the system
B	bandwidth
B_m^n	user energy efficiency
$B_{m\_\text{capacity}}^n$	user energy efficiency when spatial multiplexing is implemented
B_{RB}	RB bandwidth
BS_d	the d-th BS
c^n	normalization for the pricing factor
C_m^n	Shannon's capacity of the m-th user in the n-th RB
d_m	distance from the cell center to the m-th user
$d_m(L)$	inverse relationship of the distance as function of pathloss
d_{mr}	distance between the m-th MS and the r-th RS
D	number of cells
E	the matching pair between the m-th MS and the n-th RB
E'	a tuple of one MS with a subset of one or more RSs
$\bar{E}$	The matching pair between the m-th MS and the r-th RS
$f_{d_m}(d_m)$	PDF of the distribution of the distances of the m-th MS from the center of the cell
$f_L(L)$	PDF of the pathloss
$f_{P_m^n}$	the PDF of the transmitted power for the spatial multiplexing case
$f_{P_{m\_\text{dBm}}^n}$	PDF of the transmitted power in [dBm] for the spatial multiplexing case
$f_{P_{m\_\text{mimo}}^n}$	PDF of the transmitted power for a MIMO user in the diversity case
$f_{P_{m\_\text{mimo\_capacity}}^n}$	PDF of the circuit consumed power for the spatial multiplexing case
$f_{P_{m\_\text{mimo\_dBm}}^n}$	PDF of the transmitted power in [dBm] for a MIMO user in the diversity case
$f_{P_{m\_\text{mimo\_diversity}}^n}$	PDF of the circuit consumed power for a MIMO user in the diversity case

$f_{P_m^{n*}}$	PDF of the transmitted power per antenna in [dBm] for the spatial multiplexing case
F	subset of spare RBs in the system
G	cooperative game
G_m^n	channel path gain between the m-th user and its serving BS
$h_{i,j}^n$	a ZMCSCG random variable
h_r	fading coefficient between the r-the RS and the BS
$\mathbf{h}_m^n$	$1 \times M_r$ channel matrix
H_m^n	channel transfer function between an outdoor MS and its serving BS in the n-th RB
$\mathbf{H}^H$	conjugate transpose of $\mathbf{H}$
$\mathbf{H}_m^n$	$M_t \times M_r$ channel matrix for the m-th user on the r-th RB
I_m^n	interference for the m-th user
$\mathcal{I}_m^n$	interfering set of users
J	the cardinality of the S'_m subset
k_{sc}	number of subcarriers per RB
$L(d_m)$	distance dependent path loss
$L(P_m^n)$	inverse relationship of the pathloss as function of the transmitted power for the spatial multiplexing case
$L(P_{m\_\mathrm{mimo}}^n)$	inverse relationship of the pathloss as a function of the transmitter power for a MIMO user in the diversity case
L_f	the f-th RB's preference list
L_m	the m-th MS's preference list
L_r	the r-th RS's preference list
M	number of MSs
MS_m	the m-th MS
M_r	number of transmitters
M_t	number of receivers
N	number of RBS
$\tilde{n_i}$	noise component in the i-th parallel subchannel after linear processing
n_m^{RB}	number of RBs assigned to MS_m
n_{sys}	total number of MSs in the system
$\mathbf{n}$	noise vector

$\tilde{\mathbf{n}}$	noise vector after linear processing
$\mathbf{p}^n$	vector of the power levels of the users at the equilibrium
$\mathbf{p}^n_{-m}$	vector of all the power levels except the m-th one
P	convex set of power values
P_{BB}	power consumed by the BB module
P^n_{circ}	circuit consumed power for a single antenna device such as RS or MS
P_{circop}	circuit consumed power for cooperation
P^n_m	transmitted power of the m-th user in the n-th RB
$P^n_m(P^n_{m\_\text{dBm}})$	inverse relationship of the transmitted power as a function of the transmitted power in [dBm]
$P^n_{m\_\text{BE}}$	power expenditure due to the BE scheme
$P^n_{m\_\text{BE}}{}^*$	power expenditure due to the BE in [dBm]
$P^n_{m\_\text{circ\_BE}}$	circuit power expenditure due to the BE scheme
P_{con}	base power consumption when connected to the BS
$P^n_{m\_\text{diversity}}$	circuit consumed power in the uplink when using spatial diversity
$P^n_{m\_\text{mimo}}$	inverse relationship of the transmitted power in function of the transmitted power in [dBm] for the diversity case
$P^n_{m\_\text{mimo\_capacity}}$	total consumed power in the uplink when spatial multiplexing is implemented
$P^n_{m\_\text{mimo\_capacity\_total}}$	overall total consumed power when spatial multiplexing is implemented
$P^n_{m\_\text{mimo\_diversity\_total}}$	overall circuit consumed power for a virtual MIMO user when using spatial diversity
P_{mr}	received power at the RS from the m-th MS
$P^n_{m\_\text{simo}}$	overall circuit consumed power for a SIMO user in the n-th RB
P_{m_total}	total power spent by the m-th user in its subset of allocated RBs
$P^n_{m\_\text{trans}}$	equals to $P^n_{m\_\text{mimo}}$ if the user forms a virtual MIMO link or to $P^n_{m\_\text{simo}}$ if the user transmits at its own
P_{min}	minimum transmit power
P_{max}	maximum transmit power
P_{tcop}	transmitted power for cooperation
P_Tx	base power that the RF chain consumes in transmission mode
P^{n*}_m	PDF of the transmitted power per antenna for the diversity case

P_m^{n*}	transmitted power spend by each single antenna device converted to [dBm]
$P_m^{n*}(P^n_{m\_\text{mimo\_capacity}})$	inverse relationship of the transmitted power per antenna in [dBm] as a function of the circuit consumed power
$P_m^{n*}(P_{m\_\text{mimo\_diversity}})$	inverse relationship of the transmitted power per antenna as a function of the circuit consumed power for the diversity case
$\bar{P}^n_{m\_\text{total}}$	total consumed power for the m-th user when spatial multiplexing is implemented
Pe_m^n	transmitted power level at the equilibrium for the m-th user
Pr_m^n	received power at the BS side
Pr_{mr}	the received power at the RS side transmitted from the m-th MS
R	radius of the cell
RS_c	the most efficient relay in the cooperative link for the MRH pathloss selection case
s	information symbol with unit energy
$\mathbf{s}$	information vector for transmission
S_{hpd}	set of high priority users in the d-th cell
S_m	subset of RSs close enough to cooperate with the m-th user
S'_m	the subset of RSs that have formed a coalition with the m-th MS
S_r	subset of MSs willing to cooperate with the n-th RS
t	time unit
T_m	total achieved throughput for the m-th user in its subset, Z, of allocated RBs
T_m^n	achieved throughput for the MS_m in the n-th RB
$T^n_{m\_\text{capacity}}$	total user throughput in the n-th RB when spatial multiplexing is implemented
$\bar{T}^n_{(i)}$	average throughput of the MS_m in the n-th RB
$\bar{T}_{(i)d}$	average throughput of the i-th MS in the d-th cell
U_{fm}	utility function used by the n-th RB to rank the available MSs
U_m^n	utility of the m-th user in the n-th RB
$\mathbf{U}_m^n$	output singular matrix of $\mathbf{H}_m^n$ through SVD
U_{mf}	utility function which computes the benefit obtained for the m-th user when using the BE scheme with the f-th spare RB

U_{mr_capacity}	utility function which the m-th MS uses to rank the RSs in the S_m subset
$U_{mr\_\text{diversity}}$	utility function which MSs use to rank its preferred subset of RSs, S_m
U_{rm}	utility function which RSs use to rank its preferred subset of MSs, S_r
U_{rm_capacity}	utility function which the r-th RS uses to rank the MSs in the S_r subset
$\mathbf{V}_m^n$	input singular matrix of $\mathbf{H}_m^n$ through SVD
$\mathbf{w}$	complex weight vector for MIMO spatial diversity
$\mathbf{y}_m^n$	received signal at the BS side
$\tilde{\mathbf{y}}_m^n$	received signal after linear processing
$\tilde{y}_i^n$	received signal in each i-th parallel sub-channel
X_σ	log normal shadowing value
Z	subset of RBs allocated to the m-th MS
$\|Z\|$	cardinality of the Z subset
ε	spectral efficiency
κ	the k-th power lost constant
κ_{id}^*	set of ordered throughput measurements in the d-th cell
$\lambda_{RB_n}^*$	set of ordered throughput measurements in the r-th RB
μ_m^n	power weighting factor
η	noise power
ϱ	symbols rate per subcarrier
Σ	diagonal matrix of $\mathbf{H}_m^n$ obtained through SVD
σ	standard deviation
σ_i	i-th singular value of the channel
σ_{max}^2	the maximum singular value of $\mathbf{H}_m^n$
τ	constant value for the water-pouring method
ν	constant which depends of the bit error ratio (BER)
ω	defines the rank of the channel H_m^n
$\gamma_{i\_\text{pipe}}^n$	SNR in the i-th pipe
$\gamma_{m\_\text{BE}}^n$	SNR of the m-th user when the BE scheme is used
γ_{mr}	SNR at the RS side
γ_m^n	SNR of the m-th MS in the n-tn RB

$\gamma^n_{m\_\text{simo}}$	SNR for the m-th SIMO user in the n-th RB
$\gamma^n_{m\_\text{mimo\_diversity}}$	SNR of the m-th user when spatial diversity is used
$\gamma^n_{m\_\text{mimo\_diversity\_alamouti}}$	SNR of the m-th user when the alamouti scheme is used
Γ	fairness index
ζ_i	transmitted power in the i-th parallel subchannel due to the waterpouring method

Chapter 1
Introduction

This thesis focuses on the energy efficient resource allocation design taking the Long Term Evolution (LTE) standard as an example. It is mainly devoted to uplink transmission techniques from mobile stations (MSs) to base stations (BS). The origin and motivation of this work is provided in Section 1.1. The overview of the organization of the remaining chapters is presented in Section 1.2. Finally, the main contributions of the thesis are summarized in Section 1.3.

1.1 Motivation

Energy consumption of wireless networks contributes significantly to global climate change as mobile data traffic continues growing dramatically [6, 7]. The growing energy costs also become a substantial operational expense for mobile operators [8]. Thus, reducing the energy consumption in order to lower carbon emissions and operational expenses has become an important design constraint for future communication systems [9]. The concept of green radio has arisen to reduce communication systems' energy expenses by developing environmentally friendly, energy efficient solutions. Hence, with the aim of reducing power expenditure a variety of techniques may be derived from the protocol stack viewpoint or the network architecture perspective.

Techniques across the protocol stack refers to radio resource management methods such as power and resource block (RB) allocation. Efficient power allocation is a main concern in LTE networks, since the demand for higher data rates coupled with full frequency reuse results in an interference limited-system, which is susceptible to co-channel interference (CCI). This can be prejudicial to the signal to noise plus interference ratio (SINR) of users across the cell but particularly for users close to the cell edge [10]. Therefore, the implementation of one or more viable interference mitigation/cancellation/coordination technique is envisioned to improve system's performance, while sacrificing minimal system capacity [4].

Significant research has been performed for resource block allocation and power allocation in orthogonal multiple access systems in order to achieve a fair distribution of the system resources [4, 11–13] or an energy efficient operating point [4, 11, 13–19]. In [18], an energy

efficient approach through BS coordination has been proposed for Orthogonal Frequency Division Multiple Access (OFDMA) networks. The proposed resource allocation maximizes the energy efficiency while considering a minimum required data rate. An energy efficient RB allocation scheme, which is coordinated at the base station (BS) side is proposed in [20]. The authors show that by allocating extra RBs to the mobile users it is possible to reduce the transmitted power expenditure in the downlink while maintaining a constant data rate. In addition, they demonstrate that increasing the number of allocated RBs always provides an increase in the energy efficiency metric for the system. In [4, 11], a co-channel interference coordination (CCIC) technique is proposed, it is based on the premise that the cell-edge performance improvement is almost linear while the degradation of the cell center users is logarithmic. The approaches in [4, 11] require a significant amount of intercell communication, in order to exchange the base-mobile and interference path gains for the optimization process, which leads to a high implementation cost and complexity. Therefore, it is necessary to study the design of distributed techniques, that can allow MSs to use the network resources efficiently, and also to maintain a low network complexity.

The network architecture aspect involves changes to the current network structure with the aim of reducing power expenditure. As an example in [21], the authors propose to modify the cell radius with the aim of improving the energy efficiency in the network. They show that by reducing the cell size, potential energy savings may be obtained. Nevertheless, when the cell size is reduced an increase in network infrastructure is required to maintain a similar performance in terms of network coverage, which increases mobile operators expenses. In [22] it is shown how macrocells and femtocells can coexist in order to reduce the energy consumption in the network. Femtocells are deployed to improve the coverage in the cell. However, since macrocells and femtocells may need to share the same spectral resource mutual interference problems arise. Thus, the authors present a game theory framework which aims to mitigate the interference in the system. The paper shows that when interference is reduced potential gains in energy efficiency can be obtained. The use of routing and multihop techniques may also be used as an effective way to improve the performance of communications systems as is shown in [23, 24]. Particularly, the use of relays stations (RSs) for reducing energy consumption is investigated in [25]. An approach to optimize the power allocation between transmitter and relay through the use of virtual antenna arrays by minimizing the overall consumed energy per bit in the system is presented. It is shown that by using an optimal power allocation, the virtual multiple input multiple output (MIMO) case achieves an energy efficiency performance close to the ideal MIMO system. The authors in [26, 27] illustrate the energy savings obtained when virtual

antenna arrays are used in wireless sensor networks. They argue that at certain distance ranges from the destination node the use of virtual MIMO results in a more energy efficient solution compared with single antenna transmission when circuit power consumption is optimized. As mentioned previously, most of the current research in energy efficient virtual MIMO [25–27] tackles the problem of "why to cooperate". Nevertheless, there are two questions that remain unanswered "when to cooperate" and "with whom to cooperate". Thereby, future research should aim to answer both questions by providing a framework that allows wireless entities to decide with whom to cooperate among their respective peers in order to obtain energy savings for the system. Moreover, low complexity distributed algorithms that allows the single antenna devices to *autonomously* decide when and with whom to cooperate are preferred over complex centralized methods. Since, centralized techniques entails extra implementation costs and an increase in system's complexity [28, 29].

1.2 Thesis Structure

As discussed above, for the protocol stack aspect current communications systems requirements are the development of low complexity resource management techniques for power and resource block allocation which allows the network to obtain power savings with a low implementation cost and complexity. In regard to the network architecture aspect, it is a matter of vital importance the study of distributed solutions that allow the MSs in the network to select the most suitable RSs to reduce the power consumption. In the case of the RS selection process the optimization in the presented work is based on the circuit consumed power rather than in the transmitted one, thus, the power consumption of radio frequency parts such as power amplifiers and the base band processing module are taken into account. By taking this in consideration the thesis structure is summarized as follows:

1.2.1 Background

This chapter provides a comprehensive basis for the research presented in following chapters. First, a general overview of radio resource management in Long Term Evolution (LTE) networks is given. Thus, a few key concepts in the area of scheduling, power allocation and routing and multihop are introduced. A study of the relevant solutions and the most common energy efficiency metrics will be illustrated. Moreover, the multiple input multiple output (MIMO)

system model will be described. A general overview of the benefits of MIMO when implementing the concepts of spatial diversity and spatial multiplexing will be given. In addition, an introduction to virtual MIMO is presented. Finally, the principles of non-cooperative and cooperative game theory are described.

1.2.2 Uplink Interference Mitigation

This chapter illustrates the close relationship between fairness and energy efficiency at the system level. The first contribution of this thesis is a mathematical derivation that shows how improvements in energy efficiency can directly be related with improvements in fairness. Moreover, the traditional uplink power control challenge is reevaluated and investigated from the view point of interference mitigation rather than power minimization. Thus, a low complexity distributed resource allocation scheme for reducing the uplink co-channel interference (CCI) is presented. Improvements in energy efficiency are obtained by controlling the level of CCI affecting vulnerable mobile stations (MSs). The proposed approach forces users with good propagation conditions to reduce transmission power, in order to protect users experiencing high levels of interference. Thus, the MSs' uplink throughputs are equalized under the max-min fairness optimization criterion. This is done with a combined scheduler and a two layer power allocation scheme, which is based on non-cooperative game theory. The scheme we propose works with minimum channel knowledge, since only base-mobile channel path gains are required for the optimization process. In addition we present extensive system level simulations that show that schemes that do not consider fairness as an optimization metric obtain a lower performance in energy efficiency than those that do.

1.2.3 A Stable Marriage Framework for Distributed Resource Allocation

This chapter illustrates the use of a cooperative game theory framework called stable marriage to allocate resources in the network in an energy efficient way, and is divided in two parts. In the first part, the proposed framework is used to enhance the energy efficiency by forming virtual MIMO coalitions between single antenna mobile and relay stations. The relay selection method optimizes the circuit power consumption of the mobiles and relays rather than the transmitted power by implementing spatial diversity in the uplink. Thus, the power consumption of the radio frequency (RF) parts such as the power amplifiers and the base band (BB) module is taken into account. Furthermore, it is shown by simulation that under certain conditions cooperation does not improve the energy efficiency metric of network users when circuit consumed power

is considered, thus single antenna devices prefer to transmit independently in order to maintain the users performance in the network.
In the second part, the aim is to reduce the power expenditure in the uplink during low network load periods by allocating extra resource blocks (RBs) to the mobile users. Thereby, the users rate demands are split among its allocated RBs in order to transmit in each of them by using a more energy efficient modulation scheme. This bandwidth expansion (BE) process is derived as well from the concept of stable marriage. Moreover, it is shown that when circuit power consumption is optimized, transmitting in more than one RB may not become an energy efficient solution for users experiencing favorable propagation conditions in the uplink.

1.2.4 A Distributed Virtual MIMO Coalition Formation Framework for Energy Efficient Wireless Networks

The stable marriage framework imposes restrictions regarding the number of elements that can participate in the coalitions, typically two entities. In this chapter, a more powerful tool is introduced called the college admissions framework for virtual MIMO coalition formation. This framework does not impose any restriction on the number of elements participating in the coalitions. In this chapter, we again focus on coalitions of antennas which enhance single user performance rather than multiuser performance by using a multiuser configuration. Moreover, power savings are obtained through the use of multiantenna arrays by implementing the concepts of spatial diversity and spatial multiplexing for uplink transmission. As in the previous chapter the proposed approach focuses on optimizing the circuit consumed power rather than just the transmitted power of the network devices. Furthermore, it is shown by system level simulations and mathematical derivations that when circuit consumed power is optimized the energy efficiency of the wireless entities is not always improved by forming a virtual MIMO array. Hence, single antenna devices may prefer to transmit at their own when channel conditions are favorable.

1.2.5 Conclusions

Finally, conclusions of the previous chapters and possible future work are presented.

1.3 Contributions

The main contributions for this research in energy efficient radio resource management are shown as follows:

- A low complexity game theory uplink cochannel interference (CCI) mitigation framework is proposed [7]. Improvements in energy efficiency are obtained by controlling the level of CCI affecting vulnerable mobile stations (MSs). Thus, the MSs uplink throughputs are equalized under the maxmin fairness optimization criterion. Moreover, It is shown that schemes that do not consider fairness in the optimization process obtain a lower performance in terms of energy efficiency when compared to those that do.

- By mathematical derivations and performance simulations, it is shown that improvements in energy efficiency are directly related with improvements in fairness at the system level [7]. Thus, an increase in the fairness index produces an increase in the system energy efficiency metric for the network.

- A low complexity resource allocation framework using game theory which reduces the power expenditure during low network load periods is proposed. Extra resource blocks (RBs) are allocated to the mobile users in the uplink. Thereby, the users rate demands are split among its allocated RBs in order to transmit in each of them by using a low level modulation scheme [30].

- The design of a relay selection distributed algorithm for energy efficient virtual Multiple-input Multiple-output (MIMO) coalition formation is studied. Cooperation between single antennas devices in modeled through the use of game theory Thus, single antenna devices such as MSs and RSs interact in a distributed way to form virtual MIMO coalitions to implement spatial diversity or spatial multiplexing respectively with the aim of reducing the power expenditure in the uplink. The proposed solution optimizes the circuit consumed power rather than the transmitter power [31, 32].

Chapter 2
Background

In this chapter, an essential basis for the understanding of the thesis is provided. First, a general overview of radio resource management in Long Term Evolution (LTE) networks is given. Thus, fundamental principles for scheduling, power control, interference coordination, routing and multihop are described. A study of the relevant solutions and the most common energy efficiency metrics will be illustrated. Moreover, the multiple input multiple output (MIMO) system model will be described. A general overview of the benefits of MIMO when implementing the concepts of spatial diversity and spatial multiplexing will be given. In addition, an introduction to virtual MIMO is presented. Finally, the principles of non-cooperative and cooperative game theory are described. The content of this chapter is divided in three main parts which includes: Radio resource management for LTE, MIMO wireless systems and game theory in wireless and communication networks. Thereby, this chapter provides the reader with the essential knowledge of the state of the art which will be used in the remainder of the thesis.

2.1 Radio Resource Management in Long Term Evolution (LTE) Networks

The Global System for Mobile communications (GSM) and its evolution is shown in Figure 2.1, through the General Packet Radio Service (GPRS), High Speed Circuit Switched Data (HSCSD), Enhanced Data Rates for GSM evolution (EDGE), Wideband Code Division Multiple Access (WCDMA) Frequency Division Duplexing (FDD), WCDMA Time Division Duplexing (TDD), High Speed Uplink Packet Access (HSUPA), High Speed Packet Access (HSPA) and Long Term Evolution (LTE) dominates 85% of the mobile phone global market [33]. LTE has been accepted as the current standard in mobile communications and it will be the basis on which future communication systems will be built. LTE aims to deliver high data rates and low latencies that current and future mobile applications will demand [34]. It delivers peak rates of 300 Mbps in the downlink and 75 Mbps in the uplink [33]. A key advantage

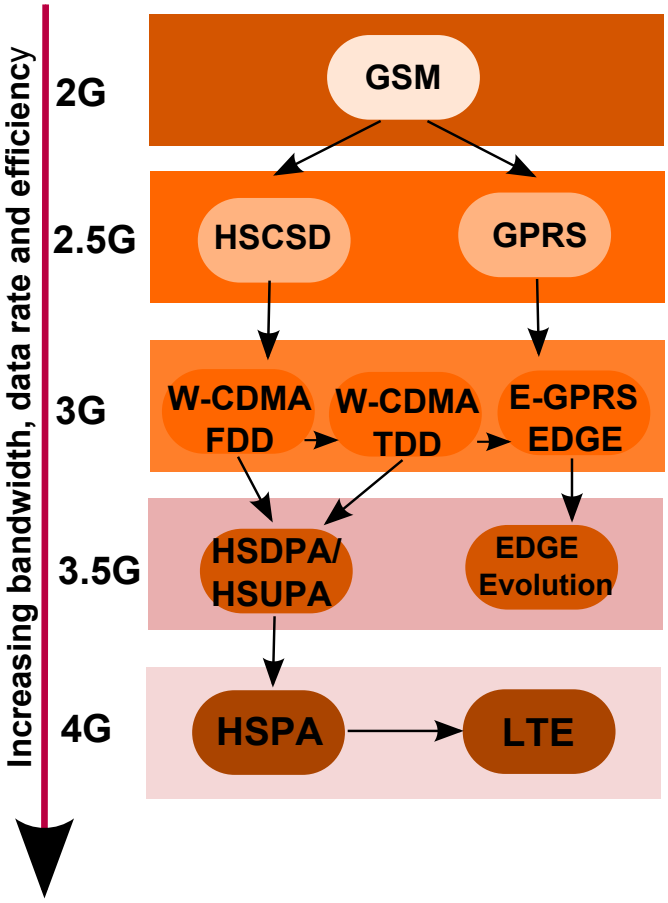

Figure 2.1: *Evolution of wireless standards.*

of LTE over previous standards such as WCDMA is that it supports spectral efficiencies three to four times higher than that offered by the last release of WCDMA in the downlink and two to three times higher in the uplink. It also supports scalable bandwidths of 1.25, 2.5, 5, 10, 15, and 20 MHz and implements both frequency division duplexing (FDD) and time division duplexing (TDD) modes [6]. Above all this, it provides inter-working with existing third generation (3G) systems and non third generation partnership project (3GPP) specified systems. To meet these ambitious demands, LTE implements advanced physical layer techniques such as orthogonal frequency division multiplexing (OFDM) in the downlink, MIMO, and radio resource management (RRM) techniques such as interference coordination (IC) [6]. By using multiple antennas at the transmitter and receiver side, schemes such as spatial diversity and spatial multiplexing are employed in LTE networks to achieve the high transmission rate demands. In the spatial multiplexing case, gains in the system's performance are obtained by sending different data streams over the same radio resource block and time slot. Interference coordination schemes apply restrictions to the RRM to improve the link quality of users that are severely affected by

high levels of interference to maintain an acceptable performance in terms of rate.

Radio resource management involves strategies and algorithms with the aim of utilizing the limited radio spectrum resources and network infrastructure as efficiently as possible. It deals with multi-user and multi-cell network capacity issues rather than just point to point communication links. Therefore, RRM is mostly used in systems that are limited by interference rather than noise such as wireless communications networks. It allows the network to control parameters such as power, carrier allocation, modulation order, handover criteria and error coding scheme to maximize the system's spectral efficiency in bits/Hz or the system's energy efficiency in bits/J under different practical constraints [35].

2.1.1 Multiple access schemes, mobile propagation and scheduling

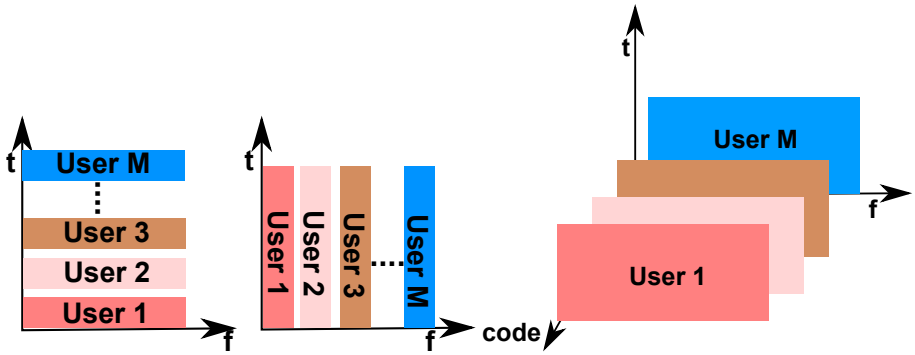

(a) TDMA (b) FDMA (c) CDMA

Figure 2.2: *Multiple access techniques.*

Due to limitations on the availability of wireless resources, while increasing the number of users it becomes necessary to share the physical communication medium within multiple users. Multiple access is a general strategy to allocate limited resources such as time and bandwidth to maintain the good performance of the network in terms of quality of service [36]. While multiple access allows the system to allocate limited resources to the users, scheduling decides when a specific user can have access to a certain spectrum.

Based on how to divide the available resources in the network the multiple access schemes can be classified in: time division multiple access (TDMA), frequency division multiple access (FDMA), code division multiple access (CDMA), and orthogonal division frequency multiple access (OFDMA). OFDMA is a combination between TDMA and OFDMA which allows a more efficient use of the available spectrum. Recently OFDMA has gained a significant interest

for use in 4G systems such as LTE [34]. Thus, this is a key technology for the research in this thesis.

1. **TDMA** As its name suggests, in TDMA the same frequency channel is used by dividing the signal into different time slots, at each time slot a single user has access to the whole available bandwidth of the system, as shown in Figure 2.2(a). TDMA requires a significant overhead for synchronization and guard intervals to prevent intracell interference.

2. **FDMA** This multiple access scheme divides the available system bandwidth into multiple non-overlapping narrowband channels, thus each user is assigned to a unique frequency band as shown in Figure 2.2(b). FDMA uses significant less information for synchronization when compared to TDMA, this due to the large symbol time of the narrowband signals, which reduces the inter-symbol interference [35].

3. **CDMA** This scheme differs from the previous schemes, since different transmitters are allowed to send information simultaneously over the total available bandwidth. In order to do that CDMA assigns each user an orthogonal pseudo-noise spreading signal or *code*. Since many users share the same spectrum resources, the utilization of the same resource is seen as noise by the other users. Thus, as the number of users increases in the system the noise floor of the system increases. Hence, CDMA is classified as an interference limited system [37].

4. **OFDMA** In this technique the available spectrum is divided into multiple orthogonal subcarriers [35]. Thus, a subset of subcarriers named resource block (RB), shown in Figure 2.3, is assigned exclusively to one user for transmission at any time, this subset cannot be reassigned to any other user in the same cell to avoid intra cell interference. Hence, in order to improve the system's performance different users transmit in different frequency-time slots by exploiting the multiuser diversity, time diversity and frequency diversity in the system, as shown in Figure 2.4.

2.1.1.1 Mobile propagation

Several difficulties may occur in mobile scenarios, which makes wireless channels extremely unpredictable and hard to analyze. Figure 2.5 shows a number of adverse effects that wireless devices should overcome to obtain a successful transmission and reception of data. These effects include but are not limited to [36]:

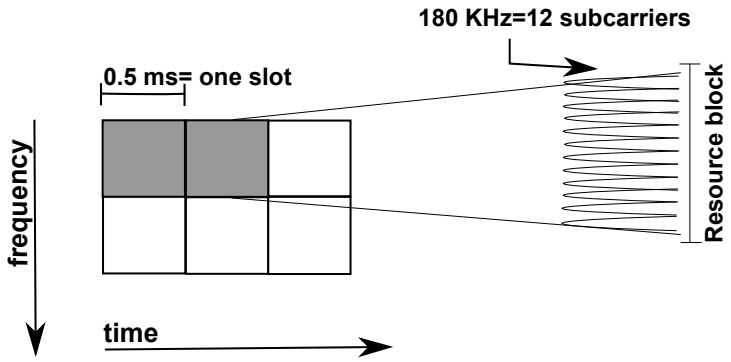

Figure 2.3: *An illustration of the RB in LTE.*

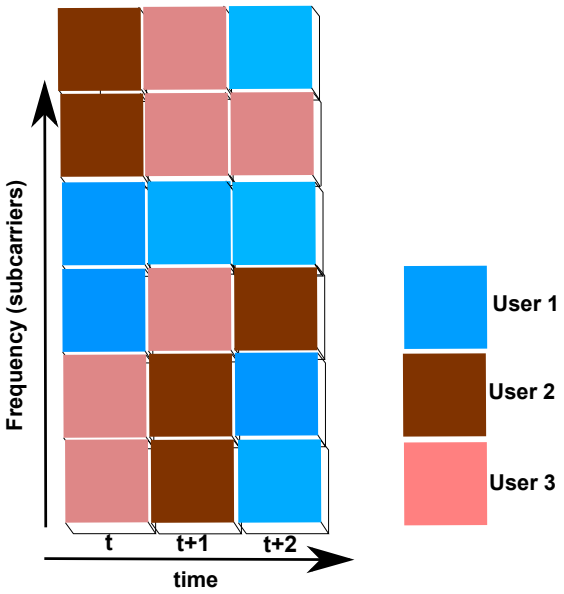

Figure 2.4: *Transmission in different frequency-time slots for OFDMA.*

- *Reflection* is the phenomenon that occurs when electromagnetic waves are reflected by a variety of surfaces such as buildings, terrain and vehicles. Thus, as result signals between transmitter and receiver will travel in different paths, called multipath propagation [1].
- *Diffraction* occurs when the signal finds an obstacle and bends around it. Then, the signal will be *shaded* by the obstacle. Diffraction tends to be more pronounced when the obstacle becomes sharper [1].
- *Delay*: signals at the receiver side may arrive at different time instants which can cause inter symbol interference. This is because, information from a previous transmission may arrive at the receiver when it is expecting the next transmission to start which generates interference.

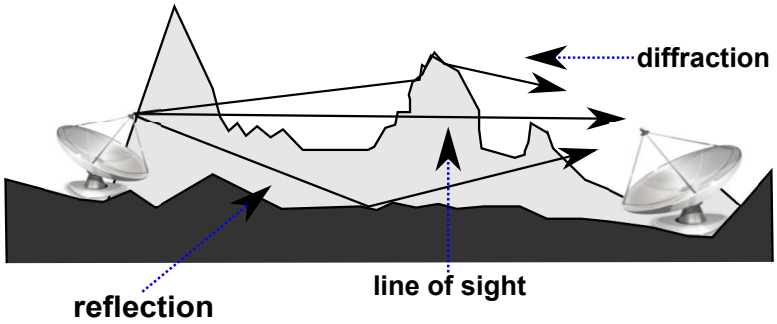

Figure 2.5: *Mobile propoagation scenario.*

Due to these difficulties, the design of wireless communication systems can become a quite challenging task. Path loss, shadowing and multi-path are the main propagation effects that affect the transmitted signal [7]. *Path loss* is defined as the attenuation that the signal experiences as a function of the distance between transmitter and receiver. *Shadowing* can be understood as the deviation of the attenuation from a fixed pathloss model and is mainly caused by large structures in the propagation path, such as buildings and hills. *Fast fading* is generated by the multiple propagation paths that the signal experiences due to phenomena such as diffraction and reflection. The multiple received copies on the signal are added at the receiver side in a destructive or constructive way which depends of their relative signal phases.

Generally, the channel path gain G^n_{md} between transmitter m and receiver d separated by a distance d_m [m] is a direct function of path loss, log normal shadowing, and channel variations caused by fading.

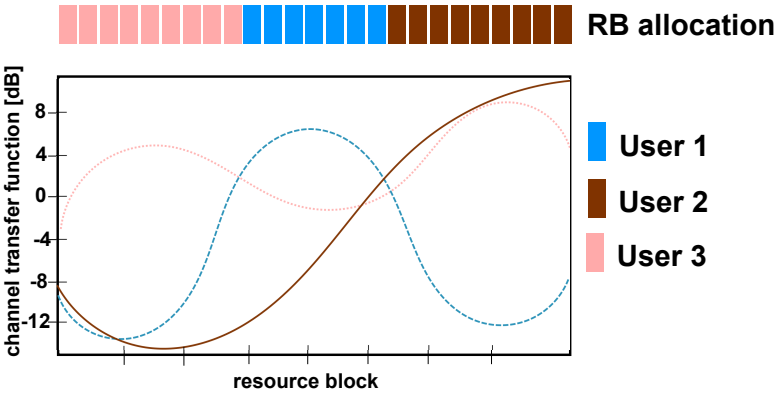

Figure 2.6: *RB allocation in OFDMA for a given time instant.*

2.1.1.2 Scheduling

Scheduling is a rule that specifies which user is allocated in a specific time, frequency, or time-frequency slot for transmission [37]. Users are scheduled based on: transmission needs, channel conditions, fairness, and other constraints, in order to maximize the performance of the network in terms of capacity, energy efficiency, delay or fairness. Figure 2.4 shows how users are allocated in time-frequency for an OFDMA system. Moreover, Figure 2.6 describes how each RB is allocated to a specific user in a given time instant based on the channel conditions between the users and the base station. Since, the channel in wireless communication systems may quickly change the scheduling method should be fast enough to adapt itself and take advantage of the channel variations. Each user will receive the information regarding which RBs will be allocated to him plus other transmission parameters such as modulation order and transmission power. This will allow the system to maximize the use of the available spectrum while maintaining a good quality of service for the users. In addition to the advantages of channel diversity, there are other design constraints that schedulers may consider. For example, energy consumption has become a major issue in wireless communications systems due to operational expenses and cost. Hence, the design of schedulers must consider to reduce the total energy expenditure in the network. Moreover, in a wireless network users pay the same price for getting access to a specific service, therefore fairness between them should also be considered. To define fairness we may utilize the concept of max-min fairness [7], proportional fairness or long term fairness [35]. Delay can also become an important constraint for some applications such as voice, which is an application that is not delay tolerant. Thus, the design of schedulers that are able to take into consideration the QoS of the wide variety of network application is a main issue for communication systems. Some examples of common scheduling approaches are presented below.

1. **Energy efficient scheduling** The problem of reducing the energy consumption in a network may be solved by: using a lower modulation order and increasing the duration of the transmission, or by using a lower modulation order and increasing the transmission bandwidth [38]. For the former case, the tradeoff between transmission time and transmission energy is convex, thus to save energy a packet should be transmitted over a longer period of time [39]. Therefore, a lower modulation order should be used while accommodating the delay constraint with the aim of minimizing the energy consumption. The authors in [13] propose a fair and energy efficient scheduling framework: their approach aims to reduce the users' energy consumption in the downlink by allocating the users the

spare RBs while maintaining a constant data rate. Thus, extra RBs are allocated to users in order to transmit with a more energy efficient modulation scheme.

2. **Joint scheduling and power control** This scheduling method has attract the interest of researchers as a suitable option to reduce interference in wireless networks. In [7], the authors present an interference mitigation framework which combines power management and resource block allocation. RBs are re-utilized in the network within users with favorable and bad propagation conditions. The power allocation framework forces users with good propagation conditions to reduce the transmission power in order to mitigate the interference levels for users experiencing unfavorable propagation conditions. Power control will be further discussed in Section 2.1.2. This proposed joint scheduling and power control method has been shown to increase the fairness and energy efficiency in the system.

3. **Max-min fairness** The rule in this method is to prioritize the users with the worst quality of service (QoS). Thus, the system resources are allocated to the user with the worst QoS. The advantage of this scheme is the extreme fairness in the resource distribution between the users in the system [35]. Nevertheless, this scheme may not be the most suitable option for a network that is only focused on maximizing the system's capacity. Since, this scheme achieves a trade-off between fairness and performance.

2.1.1.3 Resource block allocation

Resource block allocation allows wireless networks to assign single or multiple RBs to users for transmission in the uplink/downlink with the purpose of maintaining a good QoS in the network [35]. In LTE networks each user is able to adopt a different modulation and coding scheme (MCS) on the allocated RBs to achieve the network demands [10]. As shown in Figure 2.6, the RBs are allocated to specific users based on the channel conditions between the users and the BS. Multiple RBs can be allocated to a specific user with the purpose of improving capacity, energy efficiency or fairness in the network. In the energy efficiency case, authors in [30] propose a RB allocation method which allow users to increase the number of used RBs for uplink transmission with the aim of reducing the energy consumption. Thus, extra RBs are allocated to a specific user when transmission conditions are favorable, in order to reduce power consumption. Extra RBs are allocated under the condition that by increasing the allocated bandwidth transmission power is always reduced. When optimizing capacity, additional RBs may

be allocated to users to transmit in each of them with a different MCS. Hence, more aggressive target rates can be achieved.

2.1.2 Power allocation

Power is an essential resource in communication systems. Transmission power control involves schemes and strategies to adapt the power of base stations (BSs) and mobile stations (MSs) [40, 41] to increase the capacity of the system through interference management, managing the cell coverage or improving the MS's battery life.
In wireless networks, bandwidth is considered a limited resource, thus channels are reused for different transmissions. Wireless systems such as LTE use a frequency reuse of one, this implies that all the available resource blocks (RBs) in the system are reused in each of the cells forming part of the network. An RB defines the basic time-frequency unit in LTE as shown in Figure 2.3. Resource block reuse increases the capacity per area but at the same time tends to generate co-channel interference. Due to co-channel interference, the signal to interference noise ratio (SINR) may fluctuate at the receiver side in the range of 20-30 [dB]. This is prejudicial for all users across the cell but particularly for users close to the cell border. Therefore, the implementation of viable interference mitigation/cancellation/coordination techniques is envisioned to improve the systems performance. Power allocation is used as a suitable way to deal with these detrimental effects, since transmitted power can be controlled in order to maintain a certain link quality and minimize co-channel interference. Existing power control schemes can be classified as: centralized or distributed, downlink or uplink, open or closed loop etc [35]. The design of power control schemes is not a trivial task since there are many trade-offs and practical constraints that should be considered:

- Increasing the transmission power increases the SINR at the receiver side. Nevertheless, it also increases the level of interference of co-channel mobile stations [42].
- For power allocation in the uplink distributed methods are preferred over centralized ones. However, the converge time of the distributed schemes must be fast enough to deal with the time varying nature of the channel.
- Distributed methods should be able to allocated the power with only local information in order to reduce the communication overhead of the network.

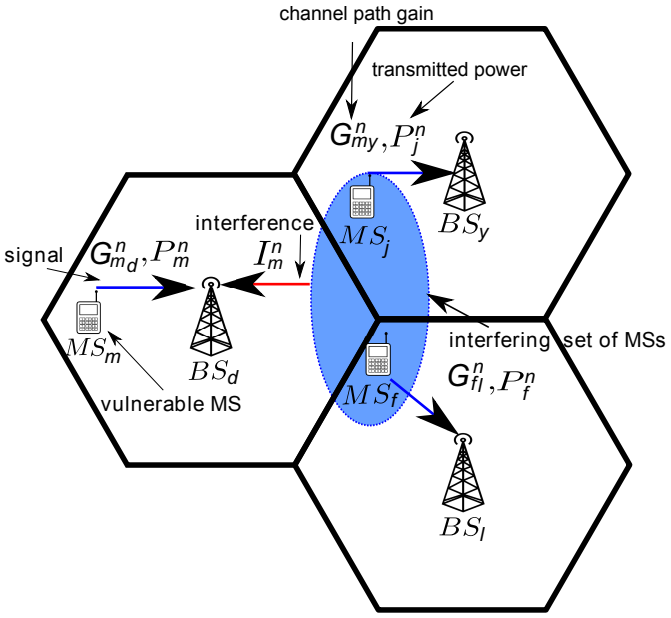

Figure 2.7: *Interference limited system.*

2.1.2.1 Power control basics

In the present section, the basic concepts to understand power control in wireless networks will be given.

(a) *Interference and noise limited systems*: On one hand, in Figure 2.7 the interference scenario for the uplink is presented, it should be noticed that a similar representation can be used for the downlink case. There are three mobile stations (MSs) transmitting at the uplink (UL) simultaneously in the same RB, which are served by three different base stations (BSs). The "vulnerable" MS_m is served by BS_d and the "interfering" set of users $\mathcal{I}^n_m$ transmitting at the n-th RB is served by the BSs located in the neighboring cells, where $n = \{1, 2, \ldots, N\}$ is the available set of RBs per cell. Vulnerable users represent users experiencing low SINR levels and interfering users are cell center users experiencing high SINR levels. In Chapter 3, we propose a joint scheduling and power allocation framework, which prioritizes users experiencing low SINR levels to transmit in high power regime. Moreover high SINR level users transmit with low power to reduce interference for vulnerable (low SINR level) users.

The uplink interference I^n_m that is caused by the set of "interfering" users $\mathcal{I}^n_m$ to the vulnerable MS_m will decrease the received SINR of the MS_m at its serving BS.

The SINR of MS_m at its serving base station BS_d is defined by

$$\gamma_m^n = \frac{P_m^n G_{md}^n}{\sum\limits_{j \in \mathcal{I}_m^n} P_j^n G_{jd}^n + \eta} = \frac{P_m^n G_{md}^n}{I_m^n + \eta}, \tag{2.1}$$

where G_{md}^n denotes the channel path gain between the "vulnerable", MS_m and its serving BS_d observed in the n-th RB. The scalar P_m^n denotes the transmit power of MS_m in the n-th RB, I_m^n is the received interference at BS_d from the MSs in neighboring cells transmitting in the n-th RB, and η is defined as the noise power. The co-channel interference I_m^n is defined as

$$I_m^n = \sum_{j \in \mathcal{I}_m^n} P_j^n G_{jd}^n, \tag{2.2}$$

where G_{jd}^n denotes the channel path gain of the interfering MSs, and P_j^n their respective transmission power. On the other hand, in Figure 2.8 a noise limited system is presented where the MS_m is served by BS_d. There are no other MSs transmitting in the same RB. Thus the signal at the receiver side is only affected by the noise power of the system η. Therefore, the SNR in the n-th RB at the receiver side is defined by:

$$\gamma_m^n = \frac{P_m^n G_{md}^n}{\eta}, \tag{2.3}$$

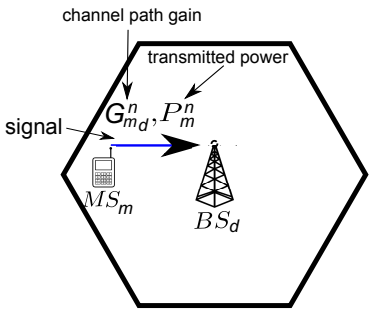

Figure 2.8: *Noise limited system.*

(b) *Power control in the downlink and uplink*: On one hand, in the downlink the transmitted power is mostly limited by the radio frequency parts at the BS side. Moreover, power control in the downlink is performed with the main purpose of interference mitigation and coverage enhancement [43]. In addition, the major limitation for the implementation of power control algorithms in the downlink is the com-

munication overhead rather than the computational complexity, since the downlink SINR measurements should be fed back from the user to the BS. On the other hand, in the uplink the transmitted power is limited mainly by the battery resources of the MSs [35]. Moreover, the computational complexity for the power allocation schemes in the uplink is constrained by the limited processing capabilities of the MSs. If no power allocation methods are applied, the effects of cochannel interference are typically more severe for users at the cell border than at the cell center, this is due to the not favorable propagation conditions for cell edge users, which is a direct consequence of pathloss [7].

(c) *Centralized and distributed power control*: Centralized power schemes are coordinated at the BS due to its high processing capabilities [30]. Centralized methods allocate all power levels in the network by gathering BS-mobile channel paths and interference path gains. However, to obtain this information a significant amount of communication overhead is required for the multicell scenario. Moreover, due to their high computational complexity, centralized methods may not be implemented in practice for multicell scenarios. They are useful however as performance upper bounds for the study of distributed approaches [35]. Distributed approaches are decentralized approaches that only required local information such as BS-mobile channel path gains for the optimization process, this characteristic allows them to be more scalable as the network grows [44]. Decentralized solutions are implementable in practice, nevertheless, the performance is limited by factors such as the convergence time of the solution and by the limited information that is used for the optimization process. In addition, distributed approaches always achieve a lower performance than their centralized counter parts [7, 31, 45].

(d) *Closed loop and open loop power control*: The closed loop power control requires constant feedback to adapt the transmitter power to the time-varying conditions of the communications link [46]. In the open loop case, the transmitter uses an estimate of the channel. For example, the MSs in the uplink estimate the channel attenuation in the downlink, and they use this measurement as an estimation for the channel in the uplink. This may be an accurate estimation for pathloss and shadowing. However, it should be remembered that for the fast fading case the downlink and uplink are not totally correlated in the case of FDD transmission.

2.1.2.2 Power control in data networks

In data networks, the main goal is to reduce the transmission errors in each communication link [47]. Moreover, there is no a minimum performance level below which the link is considered ineffective and above which improvement in performance is not required [48]. In practice, there is a tradeoff between the achieved SINR and the cost to achieve it, which in a multicell system is directly translated into co-channel interference. Thus, the network through power control decides the transmission levels in order to optimize the multiple metrics of the system. Therefore, each link adapts its transmission power to optimize its performance or utility, by possibly taking into consideration the consequences for other users.

Since, there are no specific SINR requirements in data links, a suitable approach from the operators point of view may be to set the power of the users through the BS in a way that maximizes the operator's profit. Another solution is to allow the users to define by themselves their own power strategies independently. Thus, a game theory treatment seems more natural with various entities competing among themselves for the network resources [48].

In [11], a SINR balancing method coordinated from the BS allocates similar transmission rates to all the users in the network. An optimal power vector is obtained by collecting the BS-mobile and interference path gains of all the users in the network. The proposed method reduces interference for users close to the cell edge by forcing users at the cell center to reduce their power transmission levels. In [7], an approach which allows each user to define independently its power strategy by the use of non-cooperative game theory is proposed. The proposed approach only requires local information (BS-mobile channel path gains) in order to perform the power allocation. Both schemes through the use of power control aim to reduce interference for users with not favorable propagation conditions or low SINR levels.

2.1.2.3 Power control in LTE

The power control method that is envisioned for utilization in LTE systems is discussed in this section. Hence, the power for a mobile station in the n-th RB is shown below [34,49].

$$P_m^n = argmin\{\gamma_{dB}^n + I_{avg,dBm}^n + \upsilon L_{des,dB}^n + (1-\upsilon)L_{int,dB}^n, P_{max,dBm}^n\}, \quad (2.4)$$

where

- P_m^n is the allocated power to the m-th user in the n-th RB.
- γ_{dB}^n is the nominal SNR user target, which mainly depends of the value of υ [49].
- υ allows the user to balance their transmission power which can vary from a selfish behavior to a more cooperative power management by considering the CCI generated to co-channel MSs. Thus, by making $\upsilon = 0$ a full power transmission mechanism is implemented and by making $\upsilon = 1, 2$, a cooperative power management scheme is used.
- $I_{avg,dBm}^n$ is the time-average interference in the n-th RB, this parameter allows the system to cope with co-channel interference from neighboring cells.
- $L_{des,dB}^n$ is the desired link pathloss.
- $L_{int,dB}^n$ is the interfering link pathloss.
- $P_{max,dBm}^n$ is the maximum transmission power that can be allocated to the m-th user in the n-th RB.

2.1.3 Routing and multihop

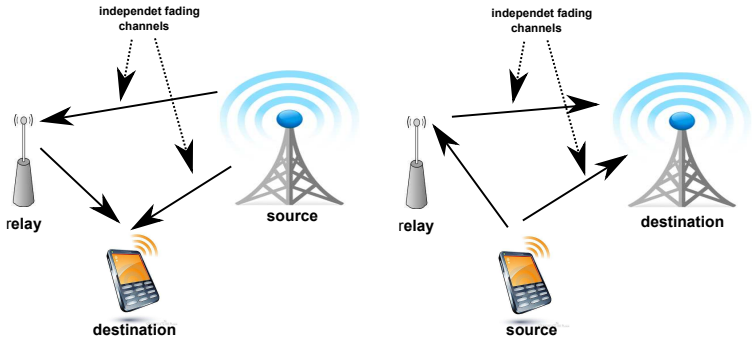

(a) Downlink multihop (b) Uplink multihop

Figure 2.9: *Classic relay scheme for the downlink and uplink.*

Previously, we have presented two resource allocation approaches that work at the protocol stack level. In this section, we consider techniques derived from the network architecture perspective. Since, significant performance gains may be achieve by a smart allocation of infrastructure resources such as RSs for improving the transmission in uplink and downlink [32]. Thus, transmission distances can be reduced, therefore, an increase in data rates and a reduction in power consumption are obtained. In addition, the use of RSs to implement spatial diversity may be utilized to obtain significant performance gains with a limited use of infrastructure [31].

This is because in networks such as Long Term Evolution (LTE), a base station (BS) may support multiple antennas. However, mobile stations (MSs) may not be equipped with more than one single antenna due to physical constraints [25, 34]. Hence, implementing effective solutions that allow MSs to benefit from the advantages of multi-antenna systems without the extra burden of having multiple antennas physically present at the users' side, has become a major issue for current communication systems. For an explanation of basic ideas, we refer to the model shown in Figure 2.9, which shows the basic configuration for the downlink and uplink. Moreover, Figure 2.9(a) presents a BS which transmits information to a MS. The MS has a single antenna, thus it cannot individually generate diversity. However, due to the broadcast nature of the wireless communication channel, it might be possible for the RS to receive the information intended for the MS and downlink this information to the BS in order to generate diversity. Diversity is generated since the fading in the channels between the MS-BS and RS-BS is statistical independent. The uplink case which is shown in Figure 2.9(b) is analogous to the downlink.

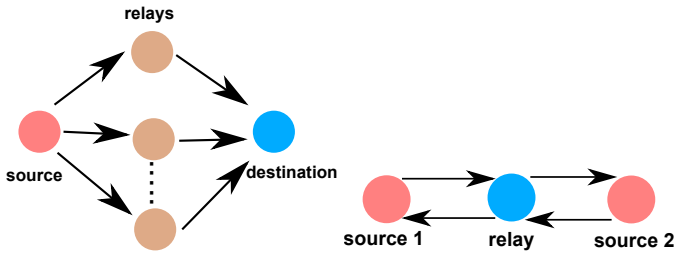

(a) Parallel relay channel (b) Two way relay channel

Figure 2.10: *Other cooperative multihop schemes, after [1].*

2.1.3.1 Configuration and operation types

As shown previously in Figure 2.9, the classic relay channel consists of three elements: a source, a relay and a destination. Moreover, the classic relay concept can be extended to a more challenging scenarios [1, 50]. In Figure 2.10, two different relay configurations are shown. Figure 2.10(a) and Figure 2.10(b) show the one way relay and the two way relay configuration respectively. The two way relay scenario is modeled as two sources that exchange information with the help of a RS. In the one way relay configuration, the source only uses the relays to transmits information to the destination. For the two way relay case source and destination use the relays to transmit information mutually [1].

The operation types for the one way relay configuration are show in Table 2.1. For type 1, source transmits information to the RS and the destination in the first slot, in the second slot, RS and source transmit the information to destination. For type 2, source transmits to the RS in the first slot, in the second one, RS and source transmits to the destination.

Operation type	Slot 1	Slot 2
Type 1	$S \rightarrow RS, S \rightarrow D$	$RS \rightarrow D, S \rightarrow D$
Type 2	$S \rightarrow RS$	$S \rightarrow D, RS \rightarrow D$

Table 2.1: *Operation types for one way relay schemes, where S and D stands for source and destination respectively and $A \rightarrow B$ means communication between A and B, after [1].*

2.1.4 Energy Efficiency Metrics

In order to assess the performance of energy efficient solutions, it is important to identify suitable metrics to understand what gains are achieved [51, 52]. Since, the concept of energy efficiency only becomes meaningful when is measured, energy efficient metrics should provide quantified information to evaluate efficiency. Energy efficiency metrics are mainly used for three proposes [51]: to compare the difference in power consumption between components and systems of the same class; to set specific long term targets in research and development; to allow the optimization of current communication systems based on energy efficiency constrains. Energy efficiency metrics have been widely discussed in literature [53], thus for this work there are two particular important metrics that we will use. The first and absolute metric can be defined as the power that is spent by a transmitter to achieve a particular transmission rate. Thus, the energy consumption ratio (ECR) is defined as $ECR = P/T \ \ [\mathrm{W/bps}]$, where P represents the transmitter power consumption in order to achieve a specific transmission rate T. Moreover, one system becomes more energy efficient when compared to another when its ECR factor is lower than the compared system, since it means that less energy is consumed to transport the same amount of data. ECR is an useful metric to measure the energy efficiency performance of telecommunications equipment as well as communication networks [36]. In addition, the ECR can be further modified to consider the circuit consumed power of the radio devices rather that only the transmitted power.

The second metric is a relative measurement rather that a quantitative one, this is utilized to compare the performance of two different systems [53]. Thus, the energy consumption gain (ECG) is defined as the ratio of the energy consumed by a baseline system over the energy of the system under test, $ECG = E_t/E_b$, where E_t represents the energy spent by the test system

and E_b represents the energy spent by the baseline scheme. The greater is the ratio of ECG, the better is the performance of the system under test when compared to the baseline.

2.2 MIMO Wireless Systems

The main design goals behind the fourth generation (4G) of wireless systems are higher user bit rates, lower delays and increased energy efficiency. These requirements call for new techniques to enhance the communications systems performance. The use of multiple antennas at both the transmitter and receiver side has result in a useful technique to improve the performance of wireless systems in terms of capacity and reliability [2]. In this section the concept of Multiple-input Multiple Output (MIMO) system will be introduced. Furthermore, we will study the concepts of spatial multiplexing and spatial diversity in MIMO communication systems. To conclude, an introduction to the concept of virtual MIMO will be given.

2.2.1 MIMO system model

We focus on the MIMO system presented in Figure 2.11 where the m-th transmitter is equipped with M_t transmit antennas and the receiver with M_r antennas. A Rayleigh fading channel is considered, thus the fading coefficients for an $M_t \times M_r$ MIMO channel in the n-th RB can be represented by a matrix as:

$$\mathbf{H}_m^n = \begin{bmatrix} h_{1,1}^n & h_{1,2}^n & \cdots & h_{1,M_t}^n \\ h_{2,1}^n & h_{2,2}^n & \cdots & h_{2,M_t}^n \\ \vdots & \vdots & \ddots & \vdots \\ h_{M_r,1}^n & h_{M_r,2}^n & \cdots & h_{M_r,M_t}^n \end{bmatrix}, \tag{2.5}$$

where each matrix element defines a Zero Mean Circular Symmetric Complex Gaussian (ZM-CSCG) random variable with unit variance [2]. The input-output relation of the system shown in Figure 2.11 is given by:

$$\mathbf{y}_m^n = \mathbf{H}_m^n \mathbf{s} + \mathbf{n} \tag{2.6}$$

where $\mathbf{s} = [s_1, s_2, ..., s_{M_t}]^T$ is the transmitted signal vector, $\mathbf{y}_m^n = [y_1^n, y_2^n, ..., y_{M_r}^n]^T$ represents the signal at the receiver side, and $\mathbf{n} = [n_1, n_2, ..., n_{M_t}]$ is the $M_t \times 1$ noise vector. It is assumed that the channel state information (CSI) is known at the receiver and the transmitter side. State of the art wireless standards such as LTE may implement closed loop techniques to obtain

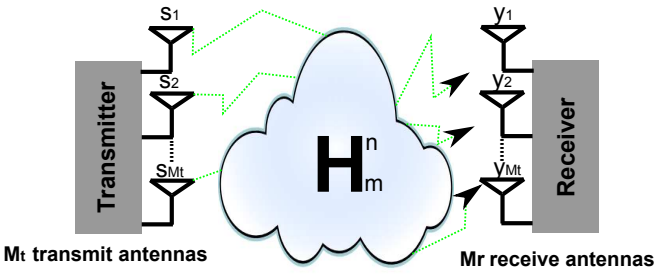

Figure 2.11: *MIMO communication model.*

current channel state information [54]. If CSI is present at the transmitter side, optimal power allocation methods such as the water-pouring scheme [2] may be utilized for allocating the power of each transmit antenna. In the case than CSI is not available at the transmitter, the most optimal solution is to assign equal power level to all the transmit antennas.

2.2.2 Spatial Diversity and Spatial Multiplexing

Compared to the traditional single input-single output (SISO) model, the MIMO systems offer substantial increase in performance due to the implementation of concepts such as spatial diversity and spatial multiplexing.

2.2.2.1 Spatial diversity

Wireless links suffer from random fluctuations in signal level known as fading. The implementation of spatial diversity techniques at the transmitter side provides the receiver with multiple copies of the signal. Each copy of the signal constitutes a diversity branch. Thus, as the number of branches grows the probability of all the branches being in fade decreases drastically. Hence, it can be understood that the use of diversity leads to substantial improvements in link reliability or error rate. The way in which diversity is implemented depends if channel state information is available or not at the transmitter side.

1. **Channel unknown to the transmitter** When CSI is not available at the transmitter side the best option to generate diversity is by the use of the Alamouti scheme. With the advent of space-time coding schemes, such as the Alamouti scheme [55] shown in Figure 2.12,

implementing transmit diversity without CSI information becomes possible. We assume two transmit and receive antennas, thus two symbols s_1 and s_2 are transmitted simultaneously from antenna 1 and 2 respectively during the first symbol period. At the second time slot, the symbols $-s_2^*$ and s_1^* are transmitted from antenna 1 and 2 respectively. Let the 2×2 channel matrix of Figure 2.12 being represented by:

$$\mathbf{H}_m^n = \begin{bmatrix} h_{1,1}^n & h_{1,2}^n \\ h_{2,1}^n & h_{2,2}^n \end{bmatrix}, \tag{2.7}$$

The signal at the receiver side over the first symbol period can be described by [2]

$$\mathbf{y}_1^n = \sqrt{\frac{Pr_m^n}{2}} \mathbf{H}_m^n \left[s_1 \;\; s_2 \right]^T + \left[n_1 \;\; n_2 \right]^T, \tag{2.8}$$

For the second time slot, the received signal is given by

$$\mathbf{y}_2^n = \sqrt{\frac{Pr_m^n}{2}} \mathbf{H}_m^n \left[-s_2^* \;\; s_1^* \right]^T + \left[n_3 \;\; n_4 \right]^T, \tag{2.9}$$

where s_1, s_2 are the transmitted signal symbols, n_1, n_2, n_3, n_4 are uncorrelated ZMC-SCG noise samples, and Pr_m^n is the received power of the m-th user in the n-th RB. Moreover, the receiver forms a signal vector equal to

$$\mathbf{y}_m^n = \sqrt{\frac{Pr_m^n}{2}} \begin{bmatrix} h_{1,1}^n & h_{1,2}^n \\ h_{2,1}^n & h_{2,2}^n \\ {h_{1,2}^n}^* & -{h_{1,1}^n}^* \\ {h_{2,2}^n}^* & -{h_{2,1}^n}^* \end{bmatrix} \left[s_1 \;\; s_2 \right]^T + \left[n_1 \;\; n_2 \;\; n_3^* \;\; n_4^* \right]^T, \tag{2.10}$$

$$\mathbf{y}_m^n = \sqrt{\frac{Pr_m^n}{2}} \mathbf{H}_{proc}^n \mathbf{s} + \mathbf{n}. \tag{2.11}$$

It is easy to see that $\mathbf{H}_{proc}^n$ is orthogonal to one channel realization, thus if we multiply $\mathbf{y}_m^n$ by ${\mathbf{H}_{proc}^n}^H$ where $\mathbf{A}^H$ represent the conjugate transpose of $\mathbf{A}$. The obtained signal is as follows [2].

$${\mathbf{y}_m^n}^* = \sqrt{\frac{Pr_m^n}{2}} \|\mathbf{H}_m^n\|_F^2 \mathbf{I}\mathbf{s} + \mathbf{n}^*, \tag{2.12}$$

where $\mathbf{I}$ represents the identity matrix, $\mathbf{n}^*$ is the noise after processing, and $\|\mathbf{H}_m^n\|_F^2$ represents the squared Frobenious norm of $\mathbf{H}_m^n$. Thus, from Eq. (2.12), it can be seen

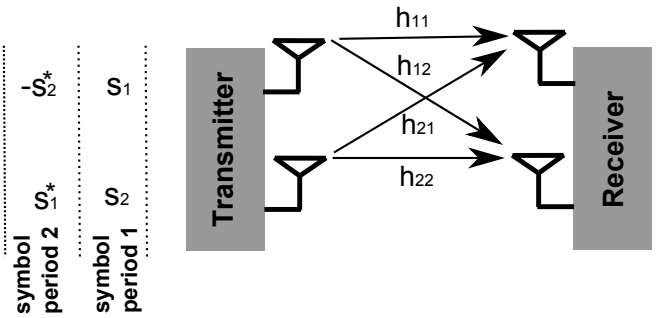

Figure 2.12: *A schematic transmission of the Alamouti scheme for a* 2×2 *system, after [2].*

that the SNR of each symbol at the receiver side is given by

$$\gamma^n_{\text{m\_mimo\_diversity\_alamouti}} = \frac{Pr^n_m}{2\eta}\|\mathbf{H}^n_m\|^2_F. \tag{2.13}$$

where η is the noise power. Hence, it can be observed that the Alamouti scheme extracts a diversity of order of $\|\mathbf{H}^n_m\|^2_F = M_t M_r$, for each transmitted symbol [2].

2. **Channel known to the transmitter** When CSI is available at the transmitter side spatial diversity can be obtained by using the dominant eigenmode transmission. Thus, the same signal is transmitted by all the transmit antennas and weighted by a vector. By considering a system of $M_t \times M_r$ antennas as proposed in Figure 2.11. The received signal at the BS side is given by

$$\mathbf{y^n_m} = \sqrt{\frac{Pr^n_m}{M_t}}\mathbf{H}^n_m\mathbf{w}s + \mathbf{n}, \tag{2.14}$$

where s is the information symbol transmitted by each antenna, and $\mathbf{w}$ is the weight vector. Moreover, the SNR is given by [2]

$$\gamma^n_{\text{m\_mimo\_diversity}} = \frac{\sigma^2_{max} Pr^n_m}{\eta}, \tag{2.15}$$

σ^2_{max} represents the maximum eigenvalue of $\mathbf{H}^n_m$. Furthermore, $\frac{\|\mathbf{H}^n_m\|^2_F}{\omega} \leq \sigma^2_{max} \leq \|\mathbf{H}^n_m\|^2_F$, where ω represents the rank of $\mathbf{H}^n_m$ [2]. Thus, by comparing Eq. (2.13) and Eq. (2.15). It can be understood the the performance of spatial diversity when having channel knowledge will outperform the Alamouti scheme due to the higher array gain. The concept of spatial diversity when channel is known at the transmitter side will be studied in Section 4.3. For now it is only important to understand that there is a difference between the two presented schemes due to the array gain.

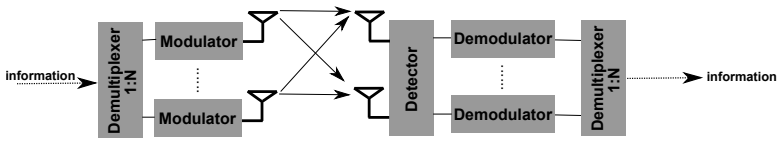

Figure 2.13: *A schematic transmission of the spatial multiplexing scheme for a $M_t \times M_r$ system.*

2.2.2.2 Spatial multiplexing

The main concept of spatial multiplexing is presented at Figure 2.13. The information stream is demultiplexed into N parallel sub-streams which are modulated and transmitted simultaneously from the antennas. At the receiver side each antenna gets a superposition of the transmitted signals sub-streams. The detector decodes the signals and combine them into the original information stream.

All the transmitted sub-streams contain different data, hence the system has no transmit diversity as in the spatial diversity case. The main advantage when using spatial multiplexing is that the capacity of the systems becomes proportional to the number of transmit and receive antennas. Thus, as lager is the number of transmit and receive antennas the greater is the capacity of the system [2].

2.2.3 Virtual MIMO

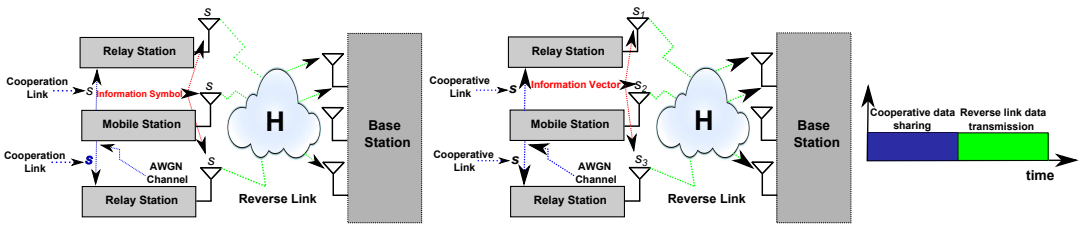

(a) Enhancing Diversity (b) Enhancing Capacity

Figure 2.14: *A Virtual $M_t \times M_r$ MIMO link.*

In networks such as Long Term Evolution (LTE), a base station (BS) may support multiple antennas. However, mobile stations (MSs) may not be equipped with more than one single antenna due to physical constraints [25, 34]. Hence, implementing effective solutions, that allow MSs to benefit from the advantages of multi-antenna systems without the extra burden of having multiple antennas physically present at the users' side, has become a major issue for current communication systems. Cooperative communications have recently attracted signifi-

cant attention as an effective way to improve the performance of wireless networks [29]. By the use of cooperative techniques wireless devices are allowed to share and utilize the network resources in a more efficient way [3, 6, 27, 29, 56–58]. An important application of cooperative techniques is the formation of virtual multi-antenna arrays. In this context, a number of single antenna devices may cooperate with each other by forming virtual Multiple-input Multiple-output (MIMO) transmitters or receivers to reap some of the benefits of multi-antenna systems [59].

2.2.3.1 Virtual MIMO Link

Figure 2.14(a) and Figure 2.14(b) show a virtual $M_t \times M_r$ MIMO link which implements spatial diversity and spatial multiplexing in the uplink respectively [32]. At the first time slot, the MS forwards the information symbol s or vector $\mathbf{s}$ to its peers by using the cooperative link. In the following slot, the MS and RSs will transmit the information symbol s or vector $\mathbf{s}$ at the uplink through the MIMO channel $\mathbf{H}_m^n$. In addition, to avoid mutual interference the uplink and the cooperative link should be designed orthogonal to each other. When spatial multiplexing is implemented as shown in Figure 2.14(b), it is assumed that the cooperative link is fast enough on information transmission, thus MSs can transmit their signal vector $\mathbf{s}$ to the cooperating peers and they can demultiplex it into independent information streams for simultaneous transmission. For the downlink case a similar analogy to the uplink case can be done.

2.3 Game Theory for Communication Networks

The main design goals behind the fourth generation (4G) of wireless systems are higher user bit rates, lower delays and increased energy efficiency. However, many technical challenges should be addressed before this wireless vision becomes a reality. Hence, to support tomorrow's wireless systems demands, it is essential to develop solutions which are able to provide an optimal cost-resource-performance tradeoff for the next generation of wireless systems [29].
Game theory has been used as a tool to explain complicated economic behavior for decades. Moreover, it has been employed as a way to model a large variety of engineering problems such as scheduling mechanisms for smart grid [60], distributed control in robotics and transportation analysis [61]. Nowadays, it has become a powerful framework to model and analyze state of the art communication systems. This is because, the use of internet as a global platform

for communications has led to the development of large scale, distributed, and heterogeneous communication systems.
The use of game theory as a framework for developing distributed and low cost efficient wireless algorithms is highly desirable but challenging in practice. On one hand wireless users are selfish by nature, since they aim to maximize their own performance in the system without considering other users needs. On the other hand, in some scenarios cooperation between the users is required rather than competition in order to improve the system's performance [62–64]. Therefore, researches have adopted the use of non-cooperative and cooperative game theory approaches to model and study competition and cooperation in communication systems.

2.3.1 Non-cooperative games

Non-cooperative game (NCG) theory is one of the main branches of game theory which studies competitive decision-making involving several players. It provides a natural framework to characterize the players interactions in a wireless network, because each individual competes with each other in an effort to achieve its own goals.
In communication systems, non-cooperative schemes may model the behavior and interaction of selfish users in a wide range of scenarios such as: allocation of resources, allocation of frequencies, transmit power, packet forwarding and interference management [29, 35]. It should be pointed out that the term *non-cooperative* game does not mean that users do not cooperate, cooperation is always possible through self enforcement, but it should be done without any coordination or communication between the players.
Non-cooperative users maximize their own utility function, which represents directly the users performance and controls the outcomes of the game [45]. A non-cooperative game is mainly defined by three components $G = [M, \{P\}, \{U(\cdot)\}]$ where:

- G represents the NCG.
- M represents a finite set of players e.g., {1,2,....,M}.
- P describes the set of available strategies for each player.
- $U(\cdot)$ is the utility function which represents the payoff of the user in the network.

Non-cooperative games are further divided into static and dynamic games [29]. This division is made depending on weather each player has or does not have information of the other's players decisions.

1. **Static:** In this case there is no sense of time since players only take actions once. Hence, players never have an understanding of how the strategies of the other players affect their own performance.

2. **Dynamic:** In this case the players have some knowledge of the strategies of the others and can act more than once to adapt their strategies and react to the other player's decisions.

Solving non-cooperative games is not easy in practice. The most widely accepted solution for the majority of non-cooperative games is the one introduced by John Nash in his seminal work, which is known as the *Nash Equilibrium* [65]. At equilibrium, all the users should be satisfied with the utilities that they obtain from the NCG.
Definition 1: The solution $\mathbf{p} = (p_1 \dots p_M)$ is a *Nash equilibrium* of the non-cooperative game, $G = [M, \{P\}, \{U(\cdot)\}]$, if for every $m \in M$, $U(p_m, p_{-m}) \geq U(p'_m, p_{-m})$ for all $p_m \in P$.
Where $p'_m \in P$ and $p_m \neq p'_m$. Thus, the *Nash Equilibrium* can be understood as a state where no player can improve its payoff from the system without a change in the other players strategies [45, 66, 67].

2.3.2 Cooperative games

On one hand, non-cooperative game theory studies the interaction and the resulting actions between competing players. One the other hand, cooperative game theory provides an analytical framework to study the nature of players when they cooperate. This is because, with the aim of increasing their utilities players are allowed to establish agreements between them. Cooperative games are divided in two main branches:

- **Bargaining games** This branch of cooperative game theory focuses on players that have to achieve an agreement over the share of a resource but face a conflict of interest in the conditions and terms to reach this agreement [29]. All the players must mutually agree how the resource will be distributed. Moreover, a decision cannot be made without the consensus of any of the players. In communication networks the Nash bargain concept can be used to model how to share a specific resource (e.g., spectrum, time, infrastructure) between a set of users. In [68], the Nash bargain is used to model spectrum sharing in an interference limited channel. When multiple antenna systems share the same spectrum band, it is shown that when systems do not cooperate the corresponding performances are always bounded regardless of how much power they spend. Moreover, when the

agreement is achieved through Nash bargain, the outcome can be on average similar to the max-sum-rate performance.

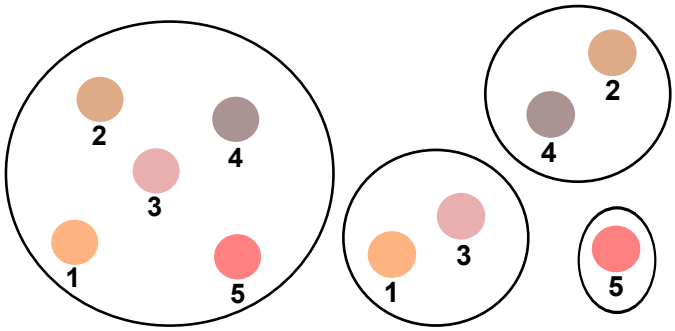

(a) Canonical coalitional games (b) Coalition formation games

Figure 2.15: *Classification of coalitional games, after [3].*

- **Coalitional games** Describes the framework that allows users to form coalitions with the aim of increasing their own profits in the game [29]. Hence, coalitional games have become a powerful tool for modeling cooperation in wireless communication systems. Coalitional games involves a set of M players which aim to cooperate with each other by forming coalitions with the aim of strengthening their position in a given situation. A coalition represents a subset of $S \in M$ players which have decided to cooperate and form a single entity. Coalitional games can be divided in two main branches:
  a) Canonical coalitional games: In this kind of game the formation of a grand coalition is seen as the optimal structure for the game, as shown in Figure 2.15(a). Thus, all the users cooperate as a single entity to enhance their performance in the game. The main question for this kind of game is under which circumstances the grand coalition can be formed [3, 29].
  b) Coalition formation games: The formation of different coalition groups, as shown in Figure 2.15(b), is based on the performance gains and the cost of cooperation between the players. The main issue in coalition formation games is to design the rules that allow the players to maximize the benefit of coalition formation. In Chapter 4, we utilize coalitional games for forming virtual MIMO links to reduce the power consumption in the network. Moreover, we show that forming a virtual MIMO coalition when optimizing overall power consumption only becomes a feasible option when mobiles experience not favorable propagation conditions in the uplink.

2.4 Summary

In this chapter some basic concepts for Radio resource management for LTE, MIMO wireless systems and game theory for wireless networks have been introduced. In the first part radio resource management techniques such as scheduling, power control and routing and multihop are presented. In the second part a general overview of MIMO is given followed by a description of the concepts of spatial multiplexing and spatial diversity. Moreover, some general concepts of virtual MIMO are studied. Finally, a brief review of game theory concepts and how they can be utilized for the study of communication systems is presented. Thereby, this chapter provides the reader with the essential knowledge of the state of the art and this information will be used in the remainder of the thesis.

Chapter 3
Uplink Interference Mitigation

3.1 Introduction

This chapter illustrates the close relationship between fairness and energy efficiency at the system level. It shows a mathematical derivation that shows how improvements in energy efficiency can directly be related with improvements in fairness. Moreover, the traditional uplink power control challenge is reevaluated and investigated from the view point of interference mitigation rather than power minimization. Thus, a low complexity distributed resource allocation scheme for reducing the uplink co-channel interference (CCI) is presented. Improvements in energy efficiency are obtained by controlling the level of CCI affecting vulnerable mobile stations (MSs). The proposed approach forces users with good propagation conditions to reduce transmission power, in order to protect users experiencing high levels of interference. Thus, the MSs' uplink throughputs are equalized under the max-min fairness optimization criterion. This is done with a combined scheduler and a two layer power allocation scheme, which is based on non-cooperative game theory. The scheme we propose works with minimum channel knowledge, since only base-mobile channel path gains are required for the optimization process. In addition, we present extensive system level simulations that show that schemes that do not consider fairness as an optimization metric obtain a lower performance in energy efficiency that the ones that do it.

The rest of the chapter is structured as follows: Section 3.2 presents a literature review, Section 3.3 describes the interference scenario, performance metrics, and channel model. In Section 3.4 the scheduling method is presented. Section 3.5 explains the two layer power allocation framework. A two layer max-min approach, which achieves a more optimal solution in fairness and energy efficiency is given in Section 3.6. A summary of the comparison schemes and the simulation scenario are described in Section 3.7. Simulation results are presented in Section 3.8. Finally, Section 3.9 offers concluding remarks.

3.2 Literature Review

The main design goals behind the fourth generation (4G) of wireless systems are higher user bit rates, lower delays, and increased energy efficiency [6]. How to accommodate all these requirements simultaneously has become an important research issue in wireless networks. On one hand, a fair distribution of the system resources is a major concern in communication systems, since current research has been focused on maximizing the system's data throughput [69]. Thus, users close to the base station are prioritized over users close to the cell edge, which makes the resource distribution unfair [29]. On the other hand, energy efficiency is an important area of study to reduce network expenses, carbon emissions and to improve current and future network sustainability [70]. The telecommunications industry is currently responsible for 0.7% of the total carbon emissions, a figure which is increasing at rapid rate [6, 71, 72]. The data volume of communication networks is expected to grow by a factor of ten every five years, which brings a doubling of energy consumption over the same time period [4, 6, 73]. By 2020, is expected that the CO_2 emissions can be *reduced* by 50% [74]. Thus, a clear demand exists for energy efficient resource allocation techniques [53, 70].

Orthogonal Frequency Division Multiple Access (OFDMA) has been chosen as the main multiple access technique for 4G systems such as Long Term Evolution (LTE) [29]. LTE networks must serve a large number of users efficiently while providing seamless connectivity and access to a wide range of applications and services. In these networks, the demand for higher data rates coupled with full frequency reuse results in an interference limited-system, which is susceptible to co-channel interference (CCI). This can be prejudicial to the Signal to Interference plus Noise Ratio (SINR) of users across the cell but particularly for users close to the cell edge [10]. Therefore, the implementation of one or more viable interference mitigation/cancellation/coordination techniques is envisioned to improve the system's performance in terms of energy efficiency and fairness while sacrificing minimal system capacity [4].

Significant research has been performed for resource and power allocation in orthogonal multiple access systems in order to achieve a fair distribution of the system resources [4, 11–13] or to achieve an energy efficient operating point [4, 11, 13–19, 75]. In [18], an energy efficient approach through base station (BS) coordination has been proposed for OFDMA networks, the proposed resource allocation maximizes the energy efficiency while considering a minimum required data rate. In [75], the authors propose an energy aware interference coordination scheme through femtocell cooperation in the uplink. It is shown that the proposed method reduces the interference levels and outage probability. The authors in [13] propose a fair and energy efficient resource block (RB) allocation framework: their approach aims to reduce the

users' energy consumption by allocating them more RBs while maintaining a constant data rate. In [4, 11], a co-channel interference coordination (CCIC) technique is proposed, which is based on the premise that the cell-edge performance improvement is almost linear while the degradation of the cell center users is logarithmic. The approaches in [4, 11] require a significant amount of intercell communication, in order to exchange the base-mobile and interference path gains for the optimization process, which leads to a high implementation cost and complexity. Therefore, it is necessary to study the design of distributed techniques to allow MSs to use the network resources efficiently, and also to reduce the network complexity [31]. These constraints combined with the large scale nature of wireless systems is a motivation for the use of game theoretic approaches.

Non-cooperative game (NCG) theory provides a natural framework to characterize the players interactions in a resource allocation problem, because each individual competes with each other in an effort to achieve its own goals. [45, 76, 77]. In [66, 78, 79], a game-theoretic approach for distributed power allocation is presented. However, these papers only deal with a single cell model. So, the effect of the interference affecting cochannel MSs is not considered. In [45, 77, 80], the authors propose a game theory framework to address the problem of CCI in a multi-cell scenario, nevertheless their approach is mainly focused on maximizing system capacity rather than on energy efficiency. Game theory approaches, which improve the energy efficiency metric for MSs in the system, have already been investigated in [15, 78, 81, 82]. However, those papers do not take into consideration the tradeoff between energy efficiency and fairness, because the authors work under the premise that energy efficiency increases with the channel power gain, thus users close to the cell center are prioritized over users at the cell boundary.

In non-cooperative game theory, the users try to maximize their own utility function, which represents directly the users' performance and controls the outcomes of the game [45]. In [45, 66, 67], a utility function, which works at the user level, is defined for power and rate allocation, however the use of a single utility function can result in achieving only a local optimum point for the optimization process. It has been shown in [80, 83] that joint power control and rate allocation can be formulated by two interconnected optimization layers, which act at the user and system levels respectively.

In this chapter, a game theory approach is presented to optimize the energy efficiency and fairness based on two interconnected optimization layers, which act at the user and system levels respectively [80]. The user's utility function is defined as the difference between its spectral efficiency and a pricing function. Hence, a non-cooperative game is designed at the user level,

where users try to maximize their own utility function until convergence is achieved. After convergence, the system level modifies the utility function pricing to move the outcome of the system to a fairer and more energy efficient operation point.

3.3 Interference Scenario, Performance Metrics and Channel Model

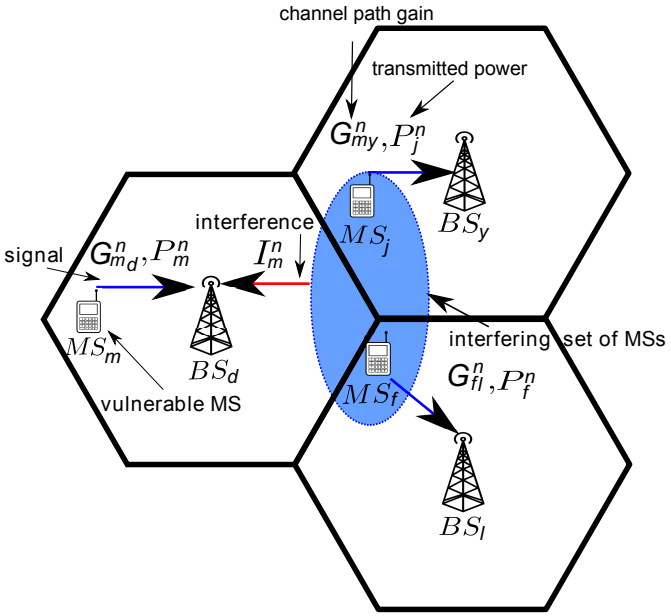

Figure 3.1: *Interference limited system.*

The model adopted in this chapter for a multiple cell OFDMA system with a total of D base stations is described. The system bandwidth B (Hz) is divided into N resource blocks (RBs). An RB defines the basic time-frequency unit with bandwidth $B_{RB} = B/N$ (Hz). Full frequency reuse is assumed, thus each cell uses the full set of N RBs. Moreover, the set of N RBs is assigned by each BS to their associated MSs. In the proposed system, each RB is assigned to a single MS per cell, hence each RB is used across the D cells. Furthermore, in this chapter the system is assumed to be fully loaded, thus the system serves a total of $N \times D$ users. In Figure 3.1 the interference scenario for the uplink is presented, it should be noticed that a similar representation can be used for the downlink case. There are three mobile stations (MSs) transmitting at the uplink (UL) simultaneously in the same RB, which are served by three different base stations (BSs). The "vulnerable" MS_m is served by BS_d and the "interfering" set of users $\mathcal{I}^n_m$ transmitting at the n-th RB is served by the BSs located in the neighboring cells, where $n = \{1, 2, \ldots, N\}$ is the available set of RBs per cell. The uplink interference I^n_m that

is caused by the set of "interfering" users $\mathcal{I}_m^n$ to the vulnerable MS_m will decrease the received SINR of the MS_m at its serving BS. The SINR of MS_m at its serving base station BS_d is defined by

$$\gamma_m^n = \frac{P_m^n G_{md}^n}{\sum\limits_{j \in \mathcal{I}_m^n} P_j^n G_{jd}^n + \eta} = \frac{P_m^n G_{md}^n}{I_m^n + \eta}, \tag{3.1}$$

where G_{md}^n denotes the channel path gain between the "vulnerable" MS_m and its serving BS_d observed in the n-th RB. The scalar P_m^n denotes the transmit power of MS_m in the n-th RB, I_m^n is the received interference at BS_d from the MSs in neighboring cells transmitting in the n-th RB, and η is defined as the noise power. The co-channel interference I_m^n is defined as

$$I_m^n = \sum_{j \in \mathcal{I}_m^n} P_j^n G_{jd}^n, \tag{3.2}$$

where G_{jd}^n denotes the channel path gain of the interfering MSs, and P_j^n their respective transmission power.

3.3.1 Performance Metrics

The achievable throughput on the link between MS_m and BS_d using adaptive modulation and coding is calculated as follows [84]:

$$T_m^n(\gamma_m^n) = n_m^{RB} k_{sc} \varrho \varepsilon(\gamma_m^m) \left[\frac{\text{bits}}{\text{s}}\right], \tag{3.3}$$

where n_m^{RB} is the number of RBs assigned to MS_m, k_{sc} is the number of subcarriers per RB, ϱ is the symbol rate per subcarrier, and $\varepsilon(\gamma_m^n)$ is the spectral efficiency given in Table 3.1, which is based on LTE [4, 84]. The user energy efficiency β_m^n measures the data rate per unit of transmitted power of MS_m, which is defined as follows:

$$\beta_m^n = \frac{T_m^n}{P_m^n} \left[\frac{\text{bits}}{\text{J}}\right]. \tag{3.4}$$

Furthermore, the system energy efficiency is defined as the ratio between the total user throughput and the total power spent by all the users in the system:

$$\beta_{sys} = \frac{\sum\limits_{m=1}^{n_{sys}} T_m}{\sum\limits_{m=1}^{n_{sys}} P_m} \ [\text{bits/J}]. \tag{3.5}$$

where T_m and P_m are the m-th user's throughput and transmitted power respectively. Moreover, n_{sys} indicates the number of MSs in the system. The Jain's fairness index [85] is used to

CQI index	min SINR [dB]	Modulation	Code rate	Spectral efficiency ε [bits/symbol]
0	-	None	-	0
1	-6	QPSK	0.076	0.1523
2	-5	QPSK	0.12	0.2344
3	-3	QPSK	0.19	0.3770
4	-1	QPSK	0.3	0.6016
5	1	QPSK	0.44	0.8770
6	3	QPSK	0.59	1.1758
7	5	16QAM	0.37	1.4766
8	8	16QAM	0.48	1.9141
9	9	16QAM	0.6	2.4063
10	11	64QAM	0.45	2.7305
11	12	64QAM	0.55	3.3223
12	14	64QAM	0.65	3.9023
13	16	64QAM	0.75	4.5234
14	18	64QAM	0.85	5.1152
15	20	64QAM	0.93	5.5547

Table 3.1: *Adaptive Modulation and Coding Table, after [4].*

calculate the throughput fairness of the system in each time slot and is given by:

$$\Gamma = \frac{(\sum_{m=1}^{n_{sys}} T_m)^2}{n_{sys} \sum_{m=1}^{n_{sys}} T_m^2}. \tag{3.6}$$

3.3.2 Channel Model

Generally, the channel gain G_{md}^n between transmitter *m* and receiver *d* separated by a distance d_m [m] is determined by path loss, log normal shadowing, and channel variations caused by slow fading. In this work, it is considered the channel model previously proposed in [4], which is stated as follows:

$$G_{md}^n = \mid \bar{H}_{md}^n \mid^2 10^{\frac{-L(d_m)+X_\sigma}{10}}, \tag{3.7}$$

where $\bar{H}_{md}^n$ describes the channel transfer function between an outdoor MS_m and its serving BS_d in the n-th RB, X_σ is the log-normal shadowing value (dB) with standard deviation σ and

L(d_m) is the distance-dependent path loss (dB), which is calculated as [86]:

$$L(d_m) = 15.3 + 37.6\log_{10}(d_m). \tag{3.8}$$

Additionally, in order to generate the channel transfer function G^n_{md}, a frequency selective fading based on a clustered delay model scenario is incorporated as described in [87] for an Urban Micro-cell model.

3.4 SINR Scheduling Based on a Three Level Priority Status Scheme

In this section, a scheduler which separates out vulnerable (low SINR) MSs from interfering (high SINR) MSs is introduced. Thus, in order to protect interference-prone users, a three priority status scheme is exploited: high priority, mid priority, and low priority as proposed in [4]. Hence, high and mid priority users are the ones experiencing low and medium SINR levels, and low priority users are the users experiencing high SINR levels. This priority status is allocated in an orthogonal fashion, hence for a RB that has assigned a MS with high priority status in one cell, the same RB is assigned to MSs with mid and low priority status in neighboring cells.
The users are scheduled based only on local BS information. Hence, each BS sorts its users based on the average uplink throughput as follows:

$$\begin{aligned} \kappa^*_{id} &= \{\bar{T}_{(1)d}, \bar{T}_{(2)d}, \ldots, \bar{T}_{(M)d}\}, \\ \text{s.t } \bar{T}_{(1)d} &\leq \bar{T}_{(2)d} \leq \ldots \leq \bar{T}_{(M)d,} \end{aligned} \tag{3.9}$$

where κ^*_{id} is the set of ordered throughput measurements in the d-th cell. The scalar $\bar{T}_{(i)d}$, denotes the average throughput of the i-th mobile, where $i = \{1, 2, \ldots, M\}$ is the set of MSs transmitting in the coverage area of the same BS. High priority status is allocated to the $\left[\frac{M}{b}\right]$ MSs with the lowest SINR. Low priority status is allocated to the $\left[\frac{M}{b}\right]$ MSs with the highest SINR. Finally, mid priority status is allocated to the remaining $\left[\frac{M}{b}\right]$ mobiles, where b defines the number of priority bands in the system.
After the users have been scheduled, each RB will contain a combination of MSs with high, mid, and low priority status across all cells, as shown in Figure 3.2. Therefore, in order to reduce CCI for vulnerable users, in Section 3.5 a power allocation framework, that forces users with *good propagation conditions* (low and mid priority status) to reduce their transmission

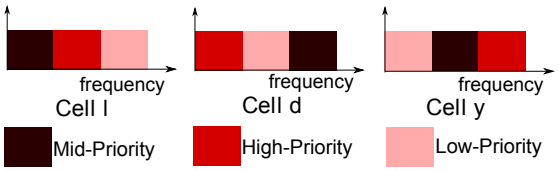

Figure 3.2: *Orthogonal allocation for high, mid, and low priority users across the cells.*

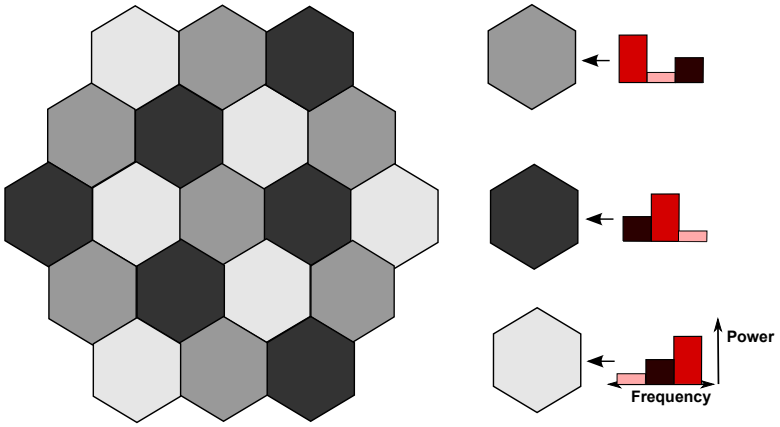

Figure 3.3: *Power allocation for each orthogonal segment in a multicell system using the three priority classes.*

power, is presented. In order to protect *vulnerable* users (high priority status) which are allowed to transmit up to their maximum power level, in Figure 3.3 it can be observed how the transmitted power should be allocated in each orthogonal segment in a multicell system to provide protection to interference prone users. In this way, each cell may use the entire bandwidth by reducing interference to its neighboring cells. This *three priority class* reuse scheme, as mentioned in [10], is a suitable way to improve the SINR level of users with unfavorable propagation conditions. Additionally, it can be noticed from Figure 3.3 that if the number of priority bands is reduced in the system (e.g., $b = 2$), adjacent cell-edge regions will share frequency segments, thereby resulting in higher levels of CCI for interference-prone users, which consequently diminishes their performance in the network.

3.5 Two Layer Framework for Power Allocation

In the uplink of OFDMA, interference is generated by co-channel MSs, e.g., users transmitting in the same RB. Furthermore, the power allocation in a wireless network can be modeled as an non-cooperative game (NCG). However, the power allocation vector which results from a NCG might not be an optimal solution from the system's perspective [45]. The authors in [83] present a joint optimization which considers users and network constraints. It has been shown

in [80] that joint power control and rate allocation can be formulated by two interconnected optimization layers, which act at the user and system levels respectively. Hence at the user level, MSs try to maximize their own utility function until convergence is achieved. Furthermore, the system level interacts with the user level in order to modify the price of the utility function so that the outcome of the NCG can be moved to a more favorable operating point.

3.5.1 User Level Framework

The proposed model is for a multiple cell OFDMA system with up to D users transmitting in the same resource block (RB). In this work, it is considered that each RB is allocated to a single MS per cell. Therefore, let $G = [D, \{P\}, \{U_m^n(\cdot)\}]$ denote the non-cooperative game, where $m = \{1, 2, \ldots, D\}$ is the set of mobiles transmitting in the n-th RB, P is a bounded convex set of power values $P \in \{0, P_{\max}\}$, which is bounded by the maximum $P_{\max}$ and zero transmitted power, and U_m^n is the utility function of the MS_m transmitting in the n-th RB. The outcome of the game will be the vector $\mathbf{p}^n = (P_1^n, \ldots, P_D^n) \in P$, which is a vector composed by the selected power levels of the D users. Furthermore, the utility function of MS_m is defined as the difference between its spectral efficiency and its pricing function. Accordingly, the utility function is defined as:

$$U_m^n(P_m^n, \mathbf{p}_{-m}^n, \mu_m^n) = \log_2(1 + \nu\gamma_m^n) - \mu_m^n P_m^n, \tag{3.10}$$

where $P_m^n \geq 0$ and $\mathbf{p}_{-m}^n$ denotes the vector of power levels for all users except the m-th one, and ν is a constant which depends of the bit error ratio (BER) of the system as follows [88]:

$$\nu \approx -1.5/\ln(\mathrm{BER}/0.2) \tag{3.11}$$

In this work, ν is set to 0.5 to match the Shannon's capacity with the spectral efficiency of the LTE system presented in Table 3.1. In equation (3.10), the user spectral efficiency function is a logarithmic function of the MS's SINR, which is denoted by γ_m^n. Furthermore, the pricing function defines the "price" μ_m^n that is paid by the MS_m for using power P_m^n to transmit in the n-th RB. This means that the pricing term linearly reduces the utility by a factor of $\mu_m^n P_m^n$, where $\mu_m^n \geq 0$. The "price" μ_m^n is used to penalize the users for the amount of interference that is caused to the other users in the n-th RB. In [14, 66], a similar utility function considering the cost of power expenditure has been used to perform the power allocation in multiple access systems. Furthermore, in [14] it is shown that the utility function (3.10) may be a reasonable

choice for power allocation in energy aware communications.

In this chapter, the power control scheme is conceived as a utility maximization problem, where the users play an NCG in order to get the highest payoff from the network. This premise can be formulated as:

$$\max U_m^n(P_{m,}^n \mathbf{p}_{-m}^n, \mu_m^n)\ P_m^n\ \in\ P. \tag{3.12}$$

After the users are scheduled as shown in Section 3.4, a pricing method based on the uplink throughput allocation is applied in order to control the transmit power of each MS. At this stage, the throughput $\bar{T}_m^n$ of each MS must be exchanged between the adjacent BSs in order to set the price for each user, which can be implemented with limited signaling. Hence, the users' throughput in the n-th RB for the D cells is sorted as follows:

$$\begin{aligned} \lambda_{RB_n}^* &= \{\bar{T}_{(1)}^n, \bar{T}_{(2)}^n, \ldots, \bar{T}_{(D)}^n\}, \\ \text{s.t } \bar{T}_{(1)}^n &\leq \bar{T}_{(2)}^n \leq \ldots \leq \bar{T}_{(D)}^n, \end{aligned} \tag{3.13}$$

where $\lambda_{RB_n}^*$ is the set of ordered throughput measurements in the n-th RB, $\bar{T}_{(m)}^n$ denotes the average throughput of the MS_m in the n-th RB, and D represents the number of available cells in the system. Hence the price of the m-th user can be defined by:

$$\mu_m^n = y(\lambda_{RB_n}^*) = \left\{ \frac{\bar{T}_{(1)}^n}{c^n}, \frac{\bar{T}_{(2)}^n}{c^n}, \ldots, \frac{\bar{T}_{(D)}^n}{c^n} \right\}, \tag{3.14}$$

where $c^n = \bar{T}_{(1)}^n \times\ P_{\max}$. This pricing factor will be higher for users which are less *vulnerable* to interference, thus it will be more costly for them to transmit in a high power regime than for *interference prone* users. Consequently, this pricing factor will reduce CCI for vulnerable MSs. Once the price is set, the MSs will play an NCG until all the users are satisfied with the utilities that they obtain from the NCG. This point of convergence, if it exists, is called the *equilibrium* [45, 66]. Appendix A shows the conditions under which the *equilibrium* exists for the user level framework in a multi-cell OFDMA scenario. In the proposed NCG, users optimize their utility functions until convergence is achieved. The equilibrium exists for the proposed game since the utility function 3.10 is continuous in P and quasi-concave. Moreover, P is a nonempty, convex, and compact subset of some Euclidean space $\Re^n$. Thus, both conditions are enough to ensure that the NCG will converge to an equilibrium point.

3.5.2 System Level Framework

In order to achieve the system goals, it is necessary to design rules that force the non-cooperative users to enhance the global system performance. This is because the chosen power weighting factor μ_m^n might not be suited to fulfill the system's optimization goals. Hence, the network should be able to modify this parameter based on its own optimization criteria. Thus, the outcome of the system will be shifted towards a better solution from the network's perspective.
Adaptive modulation allows the system to match the spectral efficiency ε, to the interference or channel conditions for specific users [80, 88]. In the proposed model, coded $\bar{M}$-ary quadrature amplitude modulation ($\bar{M}$-QAM) is used, in which the number of bits transmitted per symbol is a finite number as shown in Table 3.1. Therefore, the user spectral efficiency ε based on $\bar{M}$-QAM may be approximated by:

$$\varepsilon(\gamma_m^n) \approx \log_2(1 + \nu\gamma_m^n), \tag{3.15}$$

Equation (3.15) is used to match the Shannon's capacity with the spectral efficiency of the LTE system presented in Table 3.1. Furthermore, as is shown in [88], equation (3.15) is a valid way to approximate the capacity curve when an $\bar{M}$-QAM modulation is used. Thus, the required k-th user's SINR for a required ε may be expressed as:

$$\gamma_m^n(\varepsilon) \approx \frac{2^\varepsilon - 1}{\nu}, \tag{3.16}$$

Therefore, by combining equations (3.1) and (3.16) an expression for the m-th user's required power for a certain choice of ε is obtained:

$$P_m^n(\varepsilon) \approx \frac{(I_m^n + \eta)(2^\varepsilon - 1)}{\nu G_{md}^n}. \tag{3.17}$$

Once the NCG converges, each BS can exchange the total interference metric that is received by the MS_m, which is defined as $(I_m^n + \eta)$. This information may be obtained easily from equation (3.1) based only on local BS information, if the channel path gain G_{md}^n, the m-th user's SINR γ_m^n, and the users' transmit power levels at the *equilibrium* Pe_m^n are known:

$$I_m^n + \eta = \frac{Pe_m^n G_{md}^n}{\gamma_m^n}, \tag{3.18}$$

Hence, once $(I_m^n + \eta)$ is obtained, the system can adapt the MS's transmitted power P_m^n by using equation (3.17) in order to fulfill the system optimization goals. It can be seen that each user

in the n-th RB should select their transmit power according to the selected symbol efficiency ε, previously shown in Table 3.1.

3.6 Optimization for max-min fairness

The system may have multiple possible operating points, the choice of which depends directly on its optimization criteria. Thus, the system goals may vary from maximizing the total transmission rate without considering fairness to minimizing the total transmitted power under some constraints. However, in this chapter the system goal is to equalize the uplink user throughput for users transmitting in the same RB. Hence, the max-min fairness optimization criteria is applied. So, the worst-case user's throughput is optimized in order to improve fairness as follows.

$$\max \min \, T_m^n \quad \text{s.t} \quad P_m^n \in \, P. \tag{3.19}$$

This means that users with good SINR levels or high spectral efficiency (HSE) reduce their transmitted power, in order to reduce CCI to vulnerable users.
Theorem 1: Based on the users' ordered rates in equation (3.13), improvements in total system fairness and energy efficiency can be achieved if users with good SINR levels or high spectral efficiency (HSE) change their power strategy P_m^n to $P_m^n - \Delta P_m^n$, where $P_m^n - \Delta P_m^n \leq P_m^n$ and $P_m^n - \Delta P_m^n \in \, P$, which is proved in Appendix B.

3.6.1 Two layer algorithm for max-min fairness

At the beginning of the algorithm, the MSs in the system should start transmitting at maximum power. This means that users close to the cell center will achieve higher rates than users at the cell edge. Furthermore, the MSs are initially scheduled as described in Section 3.4. The power allocation technique at the user level, previously shown in Section 3.5.1 is applied, thus the power weighting factor μ_m^n is set for each user in the n-th RB. This choice of μ_m^n ensures that users more vulnerable to interference transmit at higher power levels when compared to less vulnerable users. The MSs will update their powers at time instants given by $t = \{t_1, t_2, \ldots\}$. Set $s = 1$, for all s such that $t_s \in t$ and for all terminals compute $P_m^n(t_s) = \max U_m^n(P_{m,}^n, \mathbf{p}_{-m}^n, \mu_m^n)$. The NCG should then converge to the *equilibrium*. Once the *equilibrium* is reached, each BS can compute $(I_m^n + \eta)$ for each MS_m in the n-th RB with equation (3.18). The system matches the MS_m's power at the *equilibrium* Pe_m^n with the clos-

est $P_m^n(\varepsilon)$, which is obtained using equation (3.17), based on the different bits/symbol options presented in Table 3.1.

$$\zeta(\varepsilon^*) = \min|Pe_m^n - P_m^n(\varepsilon)|. \tag{3.20}$$

From *Theorem 1* and *Definition 3* (see Appendix B), users with the highest symbol efficiency (HSE) reduce their transmission power. Hence, their new power values P_{HSE}^* are computed based on equation (3.17), where ε^* is replaced by $\varepsilon^* - \Delta\varepsilon^*$, where $\varepsilon^* - \Delta\varepsilon^* \leq \varepsilon^*$. By *Definition 4* (see Appendix B), and since the MS utility maximization starting point is the power weighting factor μ_m^n, this will allow us to change the parameter μ_m^n for HSE users in the following way.

$$\mu_{HSE}^n = \frac{1}{P_m^n(\varepsilon^* - \Delta\varepsilon^*)}. \tag{3.21}$$

Furthermore, due to the convergence to the equilibrium for the user layer framework, if the power weighting factor μ_m^n is changed according to *Theorem 1* and *Definition 4* (see Appendix B), the users should achieve a *fairer* distribution of the user's throughput after each iteration of the system level layer, hence iteratively the two layer algorithm for max-min fairness will satisfy the optimization metric presented in equation (3.19). The two layer algorithm for max-min fairness is shown in Table 3.2.

3.7 Comparison Schemes and Simulation Scenario

To compare the performance of the proposed algorithm, five power allocation schemes are discussed in this section. On one hand, three schemes, which try to achieve a fair allocation of the limited system resources, are presented in Section 3.7.1. On the other hand, two baseline schemes, which prioritize users with good channel conditions over users close to the cell boundary, are proposed in Section 3.7.2. These comparisons are helpful, in order to understand if prioritizing users with good channel conditions will bring improvements in energy efficiency at the expense of lower system fairness. The scheduling for all these schemes is performed as described in Section 3.4.

3.7.1 Schemes considering a fair distribution of the system resources

These schemes provide an equal distribution of the resources for all the users in the network. Their aim is to maintain a good quality of service (QoS) for users in both cell center and cell edge.

1. User Level Framework (Initialization)
Mobiles transmit at $P_{\max}$.
The users are scheduled as defined in Section 3.4.
Set the user's price μ_m^n in the n-th RB as defined in Section 3.5.1.
2. User Level Framework (Optimization)
The users play an NCG until the *equilibrium* is achieved.
3. System Framework (Initialization)
After convergence, the system can collect the interference metric $(I_m^n + \eta)$.
The system matches the power at the *equilibrium* Pe_m^n with the different entries from Table 3.1 as follows: $\zeta(\varepsilon^*) = \min\|Pe_m^n - P_m^n(\varepsilon)\|$.
4. System Framework (Optimization)
Users with the highest spectral efficiency reduce their transmission rate.
Their new power values are computed based on equation (3.17), where ε^* is replaced by $\varepsilon^* - \Delta\varepsilon^*$.
The new μ_m^n is computed as: $\frac{1}{P_m^n(\varepsilon^* - \Delta\varepsilon^*)}$.
The users play an NCG until the *equilibrium* is achieved.
5. Iterations for the System Framework
Repeat steps 3 and 4 until the optimization metric shown in equation (3.19), is satisfied.

Table 3.2: *Power Allocation Algorithm.*

a) Centralized SINR balancing Scheme

The authors in [11] introduce the concept of SINR balancing, which equalizes the SINR levels across the users transmitting in the same RB, allowing a fair distribution of the system's resources. However, this scheme requires full knowledge of base-mobile and interference path gains. Hence, interference path gains should be obtained and communicated to the adjacent BSs, which implies a significant amount of information exchange and an increase in complexity. Additionally, the authors in [89] show that if a distributed version of the SINR balancing scheme is implemented, it converges in approximately 51 iterations (time slots), which is a large number of iterations, specially for practical applications where the channel varies in time.

b) One Layer Framework

To understand the performance differences, the proposed method is compared with the *user level framework*, which works without the system optimization layer. Hence, the

performance of this framework is decided by the users selfish interest, without considering the network optimization goals.

c) Two layer framework for max-min fairness

The two layer optimization algorithm presented in Section 3.6, which optimizes the system fairness under the max-min optimization criteria, is constructed. Hence, the outcome of the NCG is modified in order to achieve a fair distribution of the system resources.

3.7.2 Schemes prioritizing users with good channel conditions

These schemes prioritize users close to the BS rather than users at the cell edge, due to the good propagation conditions for users at the cell center. Moreover, these schemes aim to achieve a high transmission rate rather than a tradeoff between capacity-energy efficiency and fairness.

d) Two layer framework for rate maximization without considering fairness

Another option for the system optimization criteria is to maximize the throughput sum in each RB as: max $\sum_{m=1}^{D} T_m^n$ s.t $P_m^n \in P$. Furthermore, the price μ_m^n is calculated in a way to allow users less vulnerable to interference or with good SINR levels to transmit at higher power levels, in order to improve system capacity at the expense of generating higher CCI levels for vulnerable users.

e) Benchmark case

Additionally, a maximum power transmission scheme is implemented as a benchmark, in which all the mobiles transmit at maximum power in each RB.

3.7.3 Simulation Scenario

To compare the performance of the schemes presented above, Monte Carlo simulations considering the simulation parameters in Table 3.3 are performed. The simulation is comprised of a single-tier, tessellated hexagonal cell layout of seven cells. However, statistics are only taken from the center cell. Each cell is served by a single omnidirectional BS with the MSs uniformly distributed in the cell. Additionally, all MSs in the network are required to transmit continuously. Finally, 10000 simulations are run over 20 time slots.

For comparison, the required channel path gains for the optimization process are shown in Table 3.4, for each of the schemes presented above, where M is the number of available MSs per cell, and D is the number of mobiles sharing the same RB in different cells.

Parameter	Value
MSs per macro-cell, M	6
Intersite-site distance	200 m
Number of available RBs, N	6
Number of cells, D	7
RB bandwidth, B_{RB}	180 kHz
Subcarriers per RB, k_{sc}	12
Symbol rate per subcarrier, ϱ_s	15 ksps
Subframe duration	1ms
Thermal noise, η	-174 dBm/Hz
Total MS transmit power	23 dBm
Shadowing, Std. Dev., σ	4 dB
BER (for computing ν)	10^{-2}
Fading	frequency selective fading
$\Delta\varepsilon^*$	$\approx$ 1 bit/symbol

Table 3.3: *Simulation parameters.*

Method	Propagation paths
Centralized SINR Balancing	$M \times D^2$
Benchmark	$M \times D$
One and Two Layer Framework	$M \times D$

Table 3.4: *Required number of channel path gains for performing power allocation.*

3.8 Results

From the simulations, the cumulative distribution functions (CDFs) and the graphs which show the distribution of the system resources at different distances from the BS, are generated for the algorithms presented in the last section. In Figure 3.4, the overall user throughput, given by equation (3.3), is displayed. It can be observed at 65^{th} percentile and at 70^{th} percentile that the CDF of the two layer (max-min fairness) scheme has an intersection point with the two layer (rate maximization) and the benchmark scheme respectively. This means that the max-min framework allows higher throughputs for 65% and 70% of the users in the network, when compared with these two baseline schemes. Additionally, important throughput improvements of 152%, 68%, 7% and 5% are obtained at the 10^{th} percentile, when the two layer approach (max-min fairness) is compared with the other four approaches respectively: the two layer (rate maximization), the benchmark, the one layer framework, and the SINR balancing scheme. Thus, the proposed scheme allows vulnerable MSs to achieve more favorable transmission conditions than the other approaches. Furthermore, in Figure 3.5 it is shown that the two layer (max-min fairness) scheme allows a fairer distribution of the uplink user throughput,

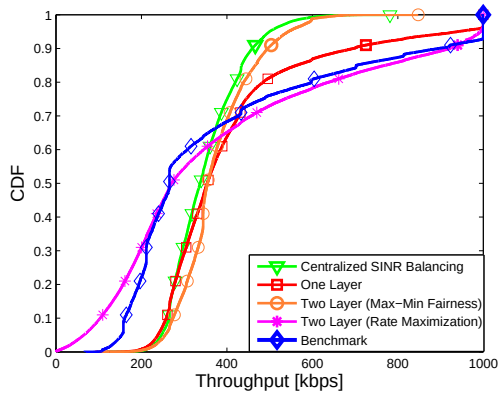

Figure 3.4: *User average CDF throughput.*

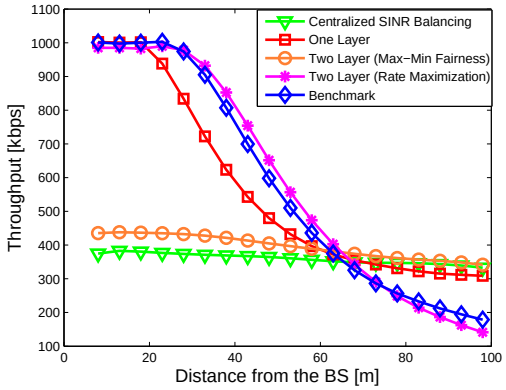

Figure 3.5: *User throughput vs distance from the BS.*

equation (3.3), at different distances from the BS, which goes from 450 kbps at the proximity of the BS to 350 kbps at the cell edge, which contrasts with the distribution of the two layer (rate maximization) scheme which goes from 1 Mbps at the cell center to 150 kbps at the cell border. This fair resource distribution for the two layer (max-min fairness) scheme is related to the power reductions applied to cell center MSs, which consequently reduce CCI significantly for vulnerable users. Thus, users close to the cell border achieve a more favorable uplink throughput in the system.

In Table 3.5, the fairness index, equation (3.6), of the two layer (max-min fairness) scheme is compared with the SINR balancing, the one layer framework, the benchmark and, the two layer (rate maximization) respectively. Thus important improvements in system fairness of 2%, 9%, 27%, and 36% can be achieved.

In Figure 3.6, it can be seen that the two layer (max-min fairness) scheme sacrifices the transmitted power expenditure for users close to the center, which transmit in a low power regime (e.g., 0.01 W at 33 m from the cell center), in order to allow users with less favorable propaga-

Scheme	Jain's index
Centralized SINR Balancing	0.96
One Layer Framework	0.88
Two Layer Framework (max-min fairness)	0.97
Two Layer Framework (rate maximization)	0.71
Benchmark	0.76

Table 3.5: *Jain's fairness index.*

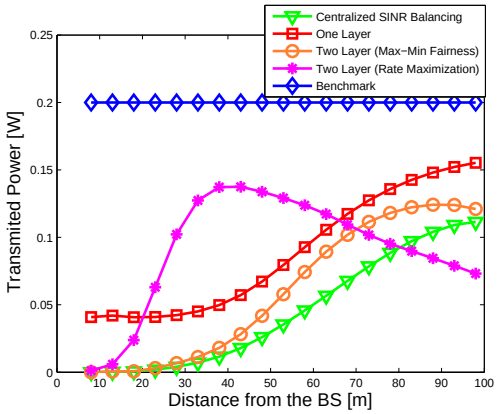

Figure 3.6: *User power vs distance from the BS.*

tion conditions to transmit in a high power regime (e.g., 0.12 W at 93 m from the cell center). By contrast, it is also shown in Figure 3.6 that the two layer (rate maximization) framework allows cell center users to work in a high power regime (e.g., 0.12 W at 33 m from the cell center) at the expense of increasing CCI for users close to the cell edge (which transmit at 0.07 W at 93 m from the cell center).

For the system energy efficiency, equation (3.5), in Figure 3.7 at the 50^{th} percentile, it can be noticed that the two layer (max-min fairness) scheme is more energy efficient compared to the benchmark, the one layer, and the two layer (rate maximization) framework with improvements of 116%, 16% and 7% respectively. Nevertheless, the two layer scheme (max-min fairness) has losses of 19% compared to the SINR balancing scheme. These losses are tolerable in practice due to the significant reductions in communications overhead shown in Table 3.4.

Furthermore, Figure 3.8 shows that the user energy efficiency, equation (3.4), for all the MSs in the network is higher for the SINR balancing and the two layer (max-min fairness) framework than for the other three approaches. Additionally, from the simulations it can be confirmed that after power reductions are applied to HSE users, the system has representative improvements in energy efficiency and fairness, as shown in Figure 3.7 and Table 3.5. Thus, the results presented

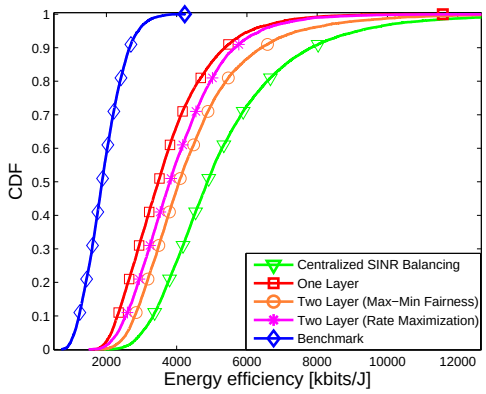

Figure 3.7: *System CDF energy efficiency performance.*

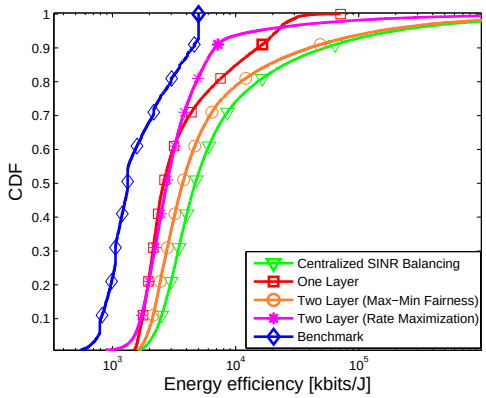

Figure 3.8: *User CDF energy efficiency performance.*

in *Theorem 1* are confirmed. Furthermore, it can be understood that by using the system level layer which optimizes max-min fairness, the outcome of the user level framework (one layer framework) is changed to a more energy efficient and fair operating point.

One important result that can be seen from the simulations is that, while the two layer (rate maximization) algorithm is the one that allows higher transmission rates, the loss in fairness cannot be justified. This is because this algorithm also achieves a lower performance in energy efficiency than the two layer (max-min fairness) framework and the SINR balancing scheme.

In Table 3.4, it is presented the required channel knowledge to perform the power allocation for the schemes presented above, thus the number of channel path gains that have to be estimated are: 42 for the proposed scheme and 294 for the centralized SINR balancing approach. Therefore, the two layer (max-min fairness) scheme only uses 14% of the channel path gains that the centralized scheme requires for its optimization process. It is found that the two layer optimization framework converges on average after four iterations, which are measured in time slots, for the system level and four for the user level. Hence, the total number of iterations for

the two layer framework is $4 \times 4 = 16$, which are significantly lower than the 51 iterations needed for the distributed version of the SINR balancing scheme.

3.8.1 Computational Complexity

To conclude the comparison, the complexity of the centralized SINR scheme compared to the two layer (max-min fairness) method and the one layer framework is discussed. Big $\mathcal{O}$ notation is used to describe the growth rate for the two schemes. The complexity analysis focuses on the power allocation framework, since the scheduling is performed using the same procedure for both schemes. The centralized SINR method requires a matrix inversion operation to compute the power allocation vector for the D MSs allocated in each RB inducing a complexity proportional to $\mathcal{O}(D^3)$. For the two layer (max-min fairness) case, each user maximizes its utility function, equation (3.10), which computes the best response of each user to other users strategies, equation (A.3), which requires arithmetic operations with a complexity of order $\mathcal{O}(D^2)$. After reaching the equilibrium, the system level interacts in order to change the outcome of the game to a better operational point, equations (3.20) and (3.21), thus an arithmetic operation and a binary search are needed, which requires a complexity of order $\mathcal{O}(D^2)$ and $\mathcal{O}(\log(D))$ respectively. Furthermore, as $\mathcal{O}(D)$ increases the dominant factor will be the term with the largest exponent, thus the complexity of the two layer (max min fairness) is upper bounded by $\mathcal{O}(D^2)$. For the one layer framework case, its complexity is only bounded by the complexity of the user level framework since the system level layer does not change the outcome of the NCG. Hence its complexity is given by $\mathcal{O}(D^2)$. Additionally, the complexity of these methods increases linearly with the number of MSs per cell, M. Hence, the centralized SINR scheme has a complexity $\mathcal{O}(M \times D^3)$, which is a higher order complexity compared with a complexity $\mathcal{O}(M \times D^2)$ for the two layer (max-min fairness) scheme and a complexity of $\mathcal{O}(M \times D^2)$ for the one layer framework. As stated before, the complexity for the one layer framework and the two layers scheme remains the same, nevertheless it should be remembered that the convergence time for the two layer framework is four times the one required for the one layer case.

3.9 Summary

In this chapter, we present a resource allocation scheme based on a SINR scheduler and a two layer power allocation technique for the uplink. The proposed scheme forces interfering users to reduce their transmission power, in order to reduce CCI for vulnerable users. Thus, interfered users achieve higher transmission rates, when compared to other approaches previously proposed. Aside from the fact that the proposed algorithm is easy to implement (only mobile-base path gains are required for its optimization process), a further benefit of the framework is an increase in energy efficiency for all MSs in the system. Furthermore, it has been shown analytically and by extensive simulations that improvements in system fairness are related with gains in energy efficiency, which is a direct result of the throughput displacement from the cell center to the cell edge. Additionally, it has been shown that the proposed power allocation framework combined with the SINR scheduler achieves improvements of 116% and 27% in system energy efficiency and fairness respectively, when compared with the benchmark. There is also a substantial increase in user throughput of 68% for interference prone users. Finally, it can be understood that the proposed framework achieves a fair tradeoff between complexity, capacity, energy efficiency, and fairness. Hence, it may be used as suitable way to obtain energy savings at the protocol stack level. In the following chapters different techniques which may deliver similar performance gains at the protocol stack level will be studied. In addition, schemes that take advantage of the changes in the network infrastructure to obtain power savings will be considered.

Chapter 4
A Stable Marriage Framework for Distributed Resource Allocation

4.1 Introduction

This chapter illustrates the use of a cooperative game theory framework called stable marriage to allocate resources in the network in an energy efficient way. The chapter is divided in two parts. In the first part, the proposed framework is used to enhance the energy efficiency by forming virtual MIMO coalitions between single antenna mobile and relay stations. The relay selection method optimizes the circuit power consumption of the mobiles and relays rather than the transmitted power by implementing spatial diversity in the uplink. Thus, the power consumption of the radio frequency (RF) parts such as the power amplifiers and the base band (BB) module is taken into account. Furthermore, it is shown by simulation that under certain conditions cooperation does not improve the energy efficiency metric of network users when circuit consumed power is considered, thus single antenna devices prefer to transmit independently in order to maintain the users performance in the network.

In the second part, the aim is to reduce the power expenditure in the uplink during low network load periods by allocating extra resource blocks (RBs) to the mobile users. Thereby, the users rate demands are split among its allocated RBs in order to transmit in each of them by using a more energy efficient modulation scheme. This bandwidth expansion (BE) process is derived from the concept of stable marriage. Moreover, it is shown that when circuit power consumption is optimized, transmitting in more than one RB may not become an energy efficient solution for users experiencing favorable propagation conditions.

The rest of the chapter is structured as follows: Section 4.2 presents the literature review. Section 4.3 describes the problem scenario and performance metrics. An analysis of the consequences that arise when overall power consumption is optimized rather than transmitted power is shown in Section 4.4. In Section 4.5, a cooperative framework is described. The summary of

the comparison schemes and the simulation scenario are described in Section 4.6. Results are presented in Section 4.7. Finally, Section 4.8 offers concluding remarks.

4.2 Literature Review

Significant research has been performed in the context of green radio [7, 30, 31, 45]. As an example in [53], the authors describe the most promising research directions to improve energy efficiency in wireless networks. Radio resource management techniques such as: *interference mitigation*, *resource block* (RB) *allocation* and the *use of multiple antennas* as a way to enhance the diversity in the uplink are proposed as an efficient way to reduce power consumption in the network. In the previous chapter, a scheme for intercell *interference reduction* which trades capacity for energy efficiency is proposed. Capacity is reduced for users at the cell center which consequently reduces interference for users close to the cell edge. Thus, significant gains in energy efficiency can be obtained with a minimal reduction in the system's throughput. The authors in [90] study the fundamental tradeoffs between deployment efficiency-energy efficiency and bandwidth efficiency-energy efficiency. They suggest that the bandwidth and the network infrastructure can be traded to obtain potential energy savings at the system level. In [91], the authors further study the concept of trading bandwidth for high energy efficiency. They conclude that bandwidth expansion can be used as an energy efficient alternative when low to moderate traffic low loads are present in the network. A framework for an energy efficient *resource block allocation* scheme, which is coordinated at the base station (BS) side, is presented in [20]. The authors show that by allocating extra RBs to the mobile users it is possible to reduce the transmitted power expenditure in the downlink while maintaining a constant data rate. In addition, they demonstrate that increasing the number of allocated RBs always provides an increase in the energy efficiency metric for the system.

In [2], the use of spatial diversity and spatial multiplexing through the use of *multiple antennas* is illustrated as an useful technique to reduce the power expenditure in wireless networks. In fourth generation (4G) networks such as Long Term Evolution (LTE), a base station (BS) may be equipped with multiple antennas. Nevertheless, mobile stations (MSs) may not support more than one single antenna due to physical constraints [25, 34]. Hence, cooperation between the network devices in information transmission may be used to obtain important gains in spectral and energy efficiency [31]. In [92], the authors propose a cooperation scheme between source and relay stations by the use of the amplify-and-forward (ANF) technique. Thus, potential energy savings are obtained due to the increase of diversity generated by multiple sources of

signal reception. Cooperative techniques such as virtual MIMO may also be used to reduce delay and power consumption in the network as presented in [25, 93]. In [93], the authors justify the increase in communication overhead and complexity for the system due to the substantial reductions in delay and power expenditure of using virtual MIMO in wireless sensor networks. In [25], an approach to optimize the power allocation between transmitter and relay is presented in order to minimize the overall energy per bit consumption in the system. Moreover, it is shown that by using an optimal power allocation, the virtual MIMO case achieves an energy efficiency performance close to the ideal MIMO system.

An important consideration in the design of resource allocation techniques such as the ones proposed previously in [20, 93] is the complexity and communication overhead that is required to implement these solutions due to the large scale nature of wireless systems [35]. This is because the complexity and implementation cost of centralized schemes such as that described in [20] tend to be a limiting factor in the network performance [7]. Thus, the design of *distributed* algorithms that allows the network to autonomously allocate its bandwidth and infrastructure resources is highly challenging but desirable in practice [28].

Game theory has been successfully used as a powerful tool for the design of low complexity resource allocation techniques [94]. Non-cooperative game theory tends to focus on the multiuser competitive nature of the problem and on the users interaction as previously seen in Chapter 3. Cooperative game theory provides a framework to study the behavior of players when they cooperate. In this context players are allowed to form agreements among themselves. Furthermore, these agreements may impact the strategies and the payoff that the players obtain from the network. In [3, 29], an overview of cooperative game theory approaches for resource allocation in communication systems is presented. In [28], the use of cooperative game theory for virtual MIMO coalition formation is described. The aim of the work is to maximize the users data rate while accounting for the cost of cooperation in terms of the overall power consumption.

The main contribution in this chapter is to model the virtual MIMO coalition formation process and the RB allocation process by using a low complexity cooperative game theory framework derived from the concept of stable marriage with incomplete lists (SMI) [95]. We focus on the optimization of the overall consumed power among devices rather than the transmitted power. In addition, it is shown that under certain conditions allocating extra resources such as RBs or RSs to a mobile station for information transmission does not provide an energy efficient solution, when the overall power consumption is considered.

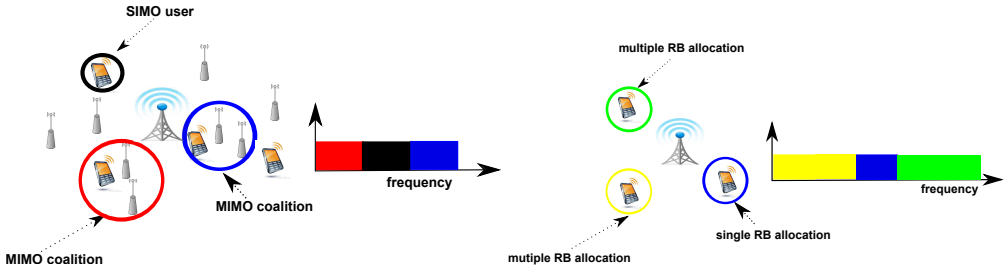

(a) Virtual MIMO coalition formation (b) Bandwidth expansion process

Figure 4.1: *Virtual MIMO coalition and bandwidth expansion scenarios*

4.3 System Scenario and Performance Metrics

For the *virtual MIMO coalition* case, we consider M single antenna mobile stations (MSs) sending data on the uplink to a multiple antenna base station (BS). The system bandwidth B (Hz) is divided into N resource blocks (RBs) as shown in Figure 4.1(a). Hence, an orthogonal frequency division multiple access (OFDMA) system is constructed. Moreover, we consider R single antenna relay stations (RSs) uniformly distributed through the cell, assuming $R \gg M$. Thus, virtual MIMO coalitions are formed between MSs and RSS to increase the energy efficiency metric for the uplink transmission. In the *bandwidth expansion* case, MSs transmit in the uplink to a multiple antenna BS. It is assumed that the network experiences low load $N \gg M$, thus spare RBs can be allocated to the users with the aim of reducing the power consumption. In Figure 4.1(b), an illustration of the system scenario is presented.

4.3.1 System Model

In Figure 4.2(a) a virtual $2 \times M_r$ MIMO link is shown. At the first time slot, the MS forwards the information symbol s to the RS using the cooperative (short range) link. In the following slot, the MS and RS transmit the symbol s in the uplink through the MIMO channel $\mathbf{H}_m^n$. The uplink and cooperative link are designed orthogonal to each other, in order to prevent mutual interference. Thus, when transmitting in the cooperative link the MS uses a different frequency set that when transmitting in the reverse link. Hence, additional bandwidth is required when implementing the cooperative link.

For the bandwidth expansion process case, cooperation between mobile devices is not required. Thus, MSs only transmit in the uplink, as presented in Figure 4.2(b), in one or multiple RBs. The channel model for the cooperative link and the uplink is explained below.

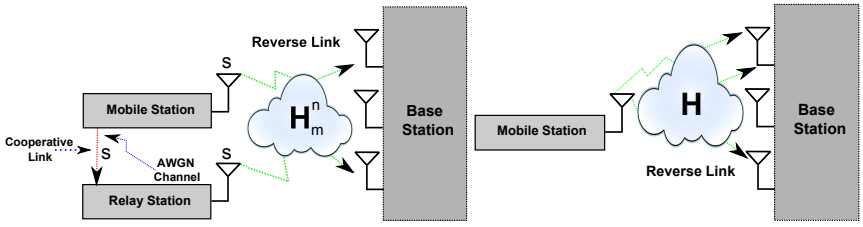

(a) A Virtual $2 \times M_r$ MIMO link.

(b) Uplink transmission for the BE method

Figure 4.2: *Transmission scenario*

4.3.2 Channel Model

4.3.2.1 Cooperative Link

If RSs and MSs cooperate between each other by forming multi-antenna arrays, the cooperative link between the MS_m and the r-th relay station is modeled as following κ^{th}-power path loss (loss $\approx \frac{1}{d_{mr}^{\kappa}}$) with Additive White Gaussian Noise (AWGN). Hence, the received power P_{mr} from the signal transmitted from the MS_m to the r-th RS is expressed by:

$$P_{mr} = \frac{P_{\mathrm{tcop}}}{d_{mr}^{\kappa}} \tag{4.1}$$

where P_{tcop} is the transmitted power for cooperation and d_{mr} is the distance between the MS_m and the r-th RS. Hence, the signal-noise ratio (SNR) at the RS side is given by

$$\gamma_{mr} = \frac{P_{mr}}{\eta} \tag{4.2}$$

4.3.2.2 Uplink

The uplink received signal at the base station (BS) separated by a distance d_m from the MS_m is determined by path loss, log-normal shadowing, and channel variations caused by frequency selective fading. The channel exhibits Rayleigh fading, whose power delay profile has been taken from [96]. Path loss and shadowing are modeled as a power fall off that subsequently attenuates the power of the transmitted signal. Thus, the average power of the received signal on the n-th RB can be expressed by [7]:

$$Pr_m^n = P_m^n \; 10^{\frac{-L(d_m)+X_\sigma}{10}}, \tag{4.3}$$

where P_m^n denotes the signal transmitted power for the m-th user in the n-th RB, X_σ is the m-th user log-normal shadowing value (dB) with standard deviation σ, and $L(d_m)$ is the distance-dependent path loss (dB), which is calculated as follows:

$$L(d_m) = 15.3 + 37.6 \log_{10}(d_m). \tag{4.4}$$

We assume the channel is known at the transmitter and receiver. Therefore, the received signal at the BS side on the n-th RB for the m-th Single-input Multiple-output (SIMO) user is given by:

$$\mathbf{y}_m^n = \sqrt{Pr_m^n}\mathbf{h}_m^n s + \mathbf{n}, \tag{4.5}$$

where $\mathbf{h}_m^n$ is the $1 \times M_r$ channel matrix on the n-th RB, s is the information scalar symbol with unit energy, and $\mathbf{n}$ is the $M_r \times 1$ noise factor. Hence, the received signal to noise ratio (SNR) at the BS side in the n-th RB may be expressed by [2]:

$$\gamma_{m\_\text{simo}}^n = \frac{\|\mathbf{h}_m^n\|_F^2 Pr_m^n}{\eta}, \tag{4.6}$$

where η is the noise power. In addition, by combining Eqs. (4.3), and (4.6) and by defining $G_m^n = \|\mathbf{h}_m^n\|_F^2 10^{\frac{-L(d_m)+X_\sigma}{10}}$, Eq. (4.6) may be written as follows:

$$\gamma_{m\_\text{simo}}^n = \frac{Pr_m^n G_m^n}{\eta}, \tag{4.7}$$

where G_m^n represents the channel path-gain between the BS and the MS_m in the n-th RB. If single antenna RSs and MSs cooperate to form multi-antenna coalitions for information transmission in the uplink, Eq. (4.5) may be re-written by

$$\mathbf{y}_m^n = \sqrt{\frac{Pr_m^n}{M_t}}\mathbf{H}_m^n \mathbf{w} s + \mathbf{n}, \tag{4.8}$$

where $\mathbf{y}_m^n$ is the received signal at the BS from the m-th MIMO coalition, $\mathbf{H}_m^n$ is the $M_t \times M_r$ channel matrix on the n-th RB, M_t is the number of transmitting antennas per *coalition*, s is the information symbol with unit energy, $\mathbf{n}$ is the noise, and $\mathbf{w}$ is a complex weight vector, that must satisfy $\|\mathbf{w}\|_F^2 = M_t$ to constrain the total average transmitted power, where $\|\cdot\|_F^2$ is the Frobenius norm. Furthermore, the signal-to-noise ratio (SNR) for a MIMO coalition is given by [2]:

$$\gamma_{m\_\text{mimo\_diversity}}^n = \frac{\|\mathbf{g}^H \mathbf{H}_m^n \mathbf{w}\|_F^2 Pr_m^n}{M_t \|\mathbf{g}\|_F^2 \eta}, \tag{4.9}$$

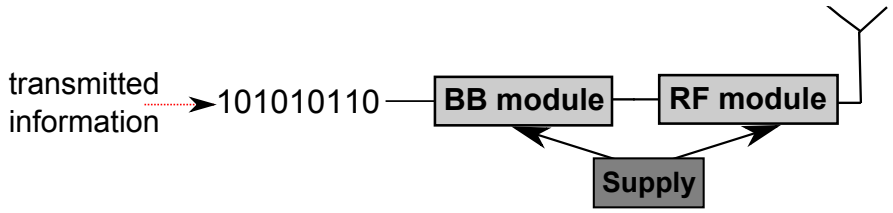

Figure 4.3: *Block diagram of the power consumption model.*

where $\mathbf{g}$ is an $M_r \times 1$ vector of complex weights which multiplies $\mathbf{y}_m^n$ at the BS side and η is the noise power. Hence, maximizing the SNR at the receiver is equivalent to maximizing $\|\mathbf{g}^H \mathbf{H}_m^n \mathbf{w}\|_F^2 / \|\mathbf{g}\|_F^2$. By using the singular value decomposition (SVD) the channel matrix can be represented as $\mathbf{H}_m^n = \mathbf{U}_m^n \Sigma \mathbf{V}_m^{n\,H}$, where the columns of $\mathbf{V}_m^n$ and $\mathbf{U}_m^n$ are known as the input and output singular value vectors respectively, and $\Sigma = \text{diag}\{\sigma_1, \sigma_2, ..., \sigma_\omega\}$ with $\sigma_i \geq 0$, where σ_i is the i-th singular value of the channel, and ω is the rank of $\mathbf{H}_m^n$. Thus, the right choice of $\mathbf{w}/\sqrt{M_t}$ and $\mathbf{g}$ that maximizes the SNR are the corresponding input and output singular value vectors corresponding to the maximum singular value σ_{max} of $\mathbf{H}_m^n$ [2]. Therefore, the received SNR at the BS side from the m-th MIMO coalition may be expressed as follows:

$$\gamma_{m\_\text{mimo\_diversity}}^n = \frac{\sigma_{max}^2 Pr_m^n}{\eta}, \tag{4.10}$$

4.3.3 Power Consumption Model

In this work, we take into account the overall power expenditure caused by information transmission in the uplink. The uplink power expenditure mainly depends on components such as the baseband (BB) module and the radio frequency (RF) module as shown in Figure 4.3. The former encloses the power expenditure due to the baseband signal processing (e.g., channel coding and decoding), and the latter includes the power consumption of the radio frequency parts (e.g., the power amplifier). Therefore, to model the power consumption for both modules, we use the model proposed in [97], where an analysis of the power consumption for these modules in a Long Term Evolution (LTE) mobile station is presented. Thus, the overall consumed power for a SIMO user $P_{m\_\text{simo}}^n$ only depends on the transmitted power in the uplink P_m^n. Hence, it is modeled as follows:

$$P_{m\_\text{simo}}^n(P_m^n) = P_{\text{circ}}^n(P_m^n) \tag{4.11}$$

Additionally, the uplink consumed power to form a virtual MIMO link which implements spatial diversity becomes a function of the total transmitted power in the uplink P_m^n, and how this is distributed between the MS and the RSs, which is due to the weight vector $\mathbf{w}$. Thus, the total consumed power for a virtual m-th MIMO user in the uplink is given by:

$$P^n_{m\_\text{mimo\_diversity}}(P_m^n) = \sum_{i=1}^{M_t} P^n_{\text{circ}} \left(\frac{P_m^n \|w_\text{i}\|^2}{M_t} \right) \tag{4.12}$$

where P^n_{circ} defines the circuit power in the uplink spent by each of single antenna device such as MSs or RSs forming the virtual MIMO link. In addition, the circuit power expenditure due to the cooperative link, P_{circop}, which is a direct function of the transmitted power for cooperation, P_{tcop}, should be added to Eq.(4.12). Thereby, the total power expenditure to form the virtual MIMO link when implementing spatial diversity is given by:

$$P^n_{m\_\text{mimo\_diversity\_total}}(P_m^n, P_{\text{tcop}}) = P_{\text{circop}}(P_{\text{tcop}}) + \sum_{i=1}^{M_t} P^n_{\text{circ}} \left(\frac{P_m^n \|w_\text{i}\|^2}{M_t} \right) \tag{4.13}$$

To model the circuit consumed power of the RF module, a power amplifier array [97,98] which is based on four power amplifiers is considered: a low power amplifier (LPA) and three high power amplifiers HPA 1, HPA 2 and HPA 3 as presented in Fig 4.4. The power amplifier efficiency is assumed equal for both high power amplifiers; however HPA 1 and 2 are designed to transmit up to one fourth and to one half of the maximum transmitted power of HPA 3 respectively. Thus, the circuit power expenditure at the uplink P^n_{circ} [W] is given by:

$$P^n_{\text{circ}}(P_m^{n*}) = \begin{cases} 2 + 0.005(P_m^{n*}) - A & 14 \geq P_m^{n*} \\ \frac{1.2+0.12(P_m^{n*})-(A-\frac{3}{4}P_{BB})}{4} & 17 \geq P_m^{n*} > 14 \\ \frac{1.2+0.12(P_m^{n*})-(A-P_{BB})}{2} & 20 \geq P_m^{n*} > 17 \\ 1.2 + 0.12(P_m^{n*}) - A & 24 \geq P_m^{n*} > 20 \end{cases} \tag{4.14}$$

where the P_m^{n*} [dBm] is the input value of P^n_{circ} in Equations (4.11), (4.12), (4.13) and A comprises a set of constant values defined by [97]:

$$A = P_{Tx} + P_{\text{con}} - P_{BB}\ [W], \tag{4.15}$$

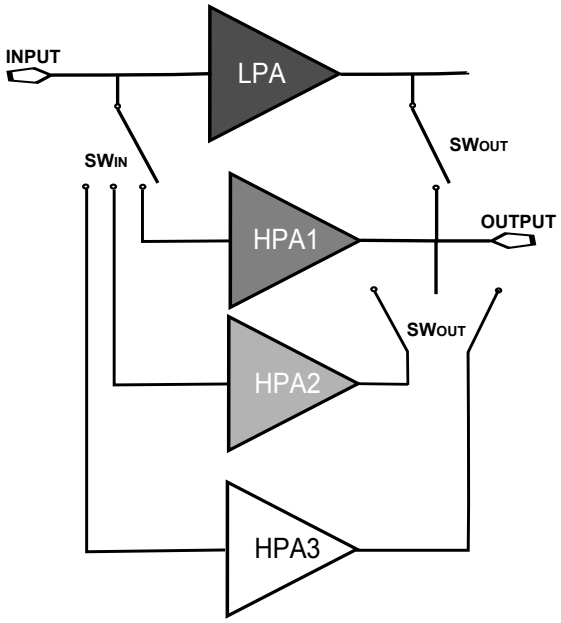

Figure 4.4: *Internal model of the power amplifier for the RF module.*

The value P_{Tx} is minimum power that the RF chain consumes in transmission mode, P_{con} is the MS's power consumption when connected to the BS, and P_{BB} is the power consumed by the BB module [97]. As we have stated, the cooperative link is a short range communications link, thus in order to model its circuit power consumption P_{circop}, we use the LPA model:

$$P_{\text{circop}}(P_{\text{tcop}}) = 2 + 0.005(P_{\text{tcop}}) - A\ [W] \quad 14 \geq P_{\text{tcop}}(\text{dBm}) \tag{4.16}$$

4.3.4 Performance Metrics

The throughput between the MS_m and the BS in the n-th RB using adaptive modulation and coding is computed by [7]:

$$T_m^n(\gamma_m^n) = k_{sc}\varrho_s\varepsilon(\gamma_m^n)\ \ [\text{bits/s}]\,, \tag{4.17}$$

where k_{sc} is the number of subcarriers per resource block, ϱ_s is the symbol rate per subcarrier, and $\varepsilon(\gamma_m^n)$ is the spectral efficiency for a Long Term Evolution (LTE) system [7]. Moreover, γ_m^n in (4.17) must be replaced by (4.10) when the user transmits in MIMO or by (4.7) when the user transmits in SIMO mode.

Moreover, the total user throughput for the m-th user can be obtained by:

$$T_m = \sum_{n \in Z} T_m^n \ \text{[bits/s]}\,, \tag{4.18}$$

where $Z \in N$ represents the subset of RBs allocated to the MS_m, whose cardinality defines the bandwidth expansion factor denoted as $|Z|$. Additionally, the total user consumed power for the MS_m is represented by:

$$P_{m\_\mathrm{total}} = \sum_{n \in Z} P_{m\_\mathrm{trans}}^n(P_m^n) \ [W]. \tag{4.19}$$

where $P_{m\_\mathrm{trans}}^n(P_m^n)$ in Eq. (4.19) should be replaced by $P_{m\_\mathrm{mimo\_diversity\_total}}^n(P_m^n, P_{\mathrm{tcop}})$ (4.13) if the user forms a virtual MIMO link or by $P_{m\_\mathrm{simo}}^n(P_m^n)$ (4.11) if the user transmit at its own. The user energy efficiency β_m measures the user throughput per unit of consumed power:

$$\beta_m = T_m / P_{m\_\mathrm{total}} \ \text{[bits/J]}\,. \tag{4.20}$$

Furthermore, the system energy efficiency β_{sys} describes the correspondence between the total user throughput and the total power spent by all the users in the system.

$$\beta_{sys} = \sum_{m=1}^{M} T_m / \sum_{m=1}^{M} P_{\mathrm{m\_total}} \ \text{[bits/J]}\,, \tag{4.21}$$

where M is the number of total users in the system.

4.4 Theoretical Analysis

In the present section, we show the consequences in terms of power consumption that arise when transmitting with multiple antennas or transmitting in more than one RB.

4.4.1 Virtual MIMO Coalition Formation

A complete analysis that studies the consequences in transmitted and overall power consumption when increasing the number of transmit antennas in the uplink is presented in Section 5.6.1.

4.4.2 Bandwidth Expansion Process

In order to show the gains in energy efficiency when adding extra RBs to the MS_m for transmission in the uplink, Shannon's capacity formula will be used. Thereby, the capacity for the n-th RB may be written as follows:

$$C_m^n = B_{RB}\log_2(1+\gamma_{m\_\mathrm{simo}}^n), \tag{4.22}$$

where B_{RB} represents the n-th's RB bandwidth. Moreover, assume that for the bandwidth expansion (BE) scheme, we aim to have the same overall transmission rate after more RBs are allocated to the m-th user. This requirement may be represented by:

$$|Z|(B_{RB}\log_2(1+\gamma_{m\_\mathrm{BE}}^n)) = B_{RB}\log_2(1+\gamma_{m\_\mathrm{simo}}^n), \tag{4.23}$$

where $\gamma_{m\_\mathrm{BE}}^n$ is the SNR of the MS_m in the n-th RB when the bandwidth expansion scheme is used. Recall that in an OFDMA system all the operations are always performed on an RB basis. Hence, by algebraic manipulations (4.23) becomes:

$$(1+\gamma_{m\_\mathrm{BE}}^n)^{|Z|} = 1+\gamma_{m\_\mathrm{simo}}^n, \tag{4.24}$$

By combining Eqs. (4.7) and (4.24), we may obtain the transmit power expenditure due to the BE scheme [20].

$$P_{m\_\mathrm{BE}}^n = \frac{\eta}{G_{m\_\mathrm{BE}}^n}\left((1+\gamma_{m\_\mathrm{simo}}^n)^{1/|Z|}-1\right), \tag{4.25}$$

The required transmitted power due to different values of $|Z|$ is plotted in Figure 4.5. The ratio $\frac{\eta}{G_{m\_\mathrm{BE}}^n}$ is taken as *constant value*, under the assumption that the noise level present in each RB is not directly affected by allocating extra RBs, since all operations are performed on a per RB basis. Moreover, to improve system performance, the propagation conditions (e.g., frequency selective fading) of the new allocated RBs should be similar or better than the current allocated RB as we will show later in the chapter.

In Figure 4.5, we can see that increasing the number of RBs always provides transmission power savings at different SNR values, since a significant decrease in transmission power is observed as the value of $|Z|$ increases. Nevertheless, in Figure 4.6 it can be seen that this behavior does not remain the same when overall power consumption is considered by including the model in (4.14). Adding extra resource blocks is not an energy efficient solution at low SNR levels (e.g., SNR $\leq$ 6 [dB]). Therefore, transmitting with only one RB is the most energy efficient

solution in this regime. This is because in a low SNR regime a low required transmitted power is also required. Thus, using the BB and the RF modules to transmit in more than one RB is not an energy efficient solution. Moreover, we can see that $|Z| = 2$ tends to be the most energy efficient solution from 6 to 15 [dB]. Finally, using more than two RBs provides the most power savings for high SNR levels (e.g., SNR $\geq$ 15 [dB]). This is because, under the assumption that $\frac{\eta}{G^n_{m\_\mathrm{BE}}}$ is taken as *constant value* in (4.25), in a high SNR regime a high transmitted power is also required. Hence, the circuit power consumption for using the RF and the BB to transmit in multiple RBs is justified in this case.

Moreover, when channel effects are considered, it should be understood when it is worthwhile to add extra RBs to a specific user, since channel propagation conditions such as frequency selective fading may not remain the same within different RBs. Hence, in terms of transmitted power this requirement can be represented by [20]:

$$P^n_m \geq \sum_{n \in Z} P^n_{m\_\mathrm{BE}}. \tag{4.26}$$

In terms of circuit consumed power(4.14), Eq. (4.26) becomes:

$$P^n_{m\_\mathrm{circ}}(P^{n\,*}_m) \geq \sum_{n \in Z} P^n_{m\_\mathrm{circ\_BE}}({P^n_{m\_\mathrm{BE}}}^*). \tag{4.27}$$

where ${P^n_{m\_\mathrm{BE}}}^*$ and $P^{n\,*}_m$ represent the value of $P^n_{m\_\mathrm{BE}}$ and P^n_m converted to [dBm].

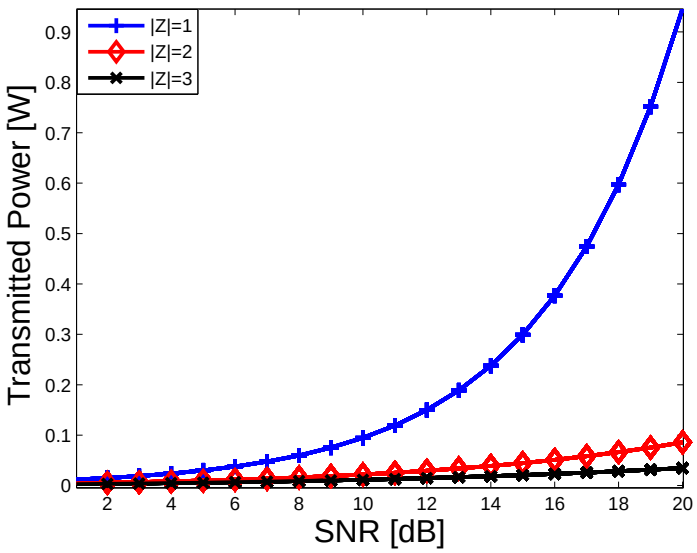

Figure 4.5: *Transmitted power plotted for different bandwidth expansion factors* $|Z|$.

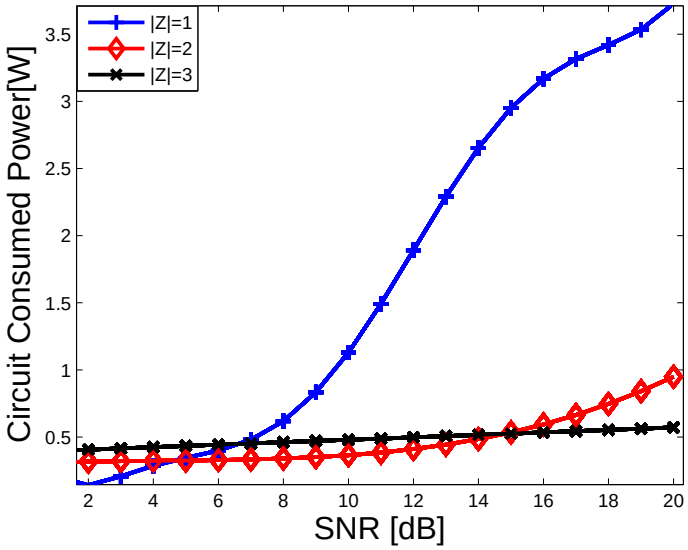

Figure 4.6: *Overall power consumption for different bandwidth expansion factors* $|Z|$.

4.5 Distributed Resource Allocation Framework

In order to obtain energy savings, we model the *virtual MIMO coalition* formation and the *bandwidth expansion* process by a game theoretic approach derived from the concept of stable marriage with incomplete lists (SMI) [95]. The SMI framework is used to find a *stable match* between two sets (MSs and RSs) or (MSs and RBs) respectively. A match is said to be *stable* when no better alternative pairing exists in the other set compared with the currently matched elements. Thereby, the SMI reaches a *stable* solution for each process [95].

4.5.1 Virtual MIMO Coalition Formation

In our approach, one set contains M mobiles and the other one contains R relay stations. Furthermore, each single device's list consists of a subset of the members of the opposite set ordered by *preference*. A matching $\bar{E}$ is a tuple (MS, RS) such that each single antenna device belongs to exactly one tuple. If $(m, r) \in \bar{E}$, we say that the r-th RS is the m-th MS partner in $\bar{E}$ and vice versa. The distributed RS selection procedure is as follows:

1) First, each MS in the system sends a broadcast message on the short range (cooperative) link, in order to find the subset of RSs close enough to cooperate with it, which is denoted as $S_m \in R$.

2) After the broadcast message, the RSs willing to form a MIMO link share their channel

statistics for their uplink (path loss, shadowing, and channel fading coefficient) and their channel statistics in the cooperative link (path loss) with the subset of mobile stations willing to cooperate with them, which for the r-th RS is denoted by $S_r \in M$. Mobiles only exchange with the RSs their channel statistics in the uplink. Hence, each MSs is able to rank its preferred subset of RSs, S_m, by using the following utility function:

$$U_{mr\_\mathrm{diversity}}(\gamma_{\mathrm{target}}) = P^n_{m\_\mathrm{simo}}(\gamma_{\mathrm{target}}) - P^n_{m\_\mathrm{mimo\_diversity\_total}}(\gamma_{\mathrm{target}}), \tag{4.28}$$

where U_{mr} is computed as the difference between the power spent by the m-th MS acting on its own or making a coalition with the r-th RS, and γ_{target} represents a target SNR that both SIMO and MIMO users aim to achieve. Hence the higher the utility value, the more the m-th MS will be willing to cooperate with the r-th RS. Additionally, if the utility becomes negative the MS will ignore the RS for coalition formation, since forming a virtual MIMO link will degrade the user's performance. Furthermore, the MS preference list L_m is formed by evaluating each element of the subset S_m by Eq. (4.28). MSs that do not obtain any benefit from cooperating with any of the relays in their preferred subset, S_m, are allowed to act in SIMO mode. The RSs need to compute how important or necessary is their cooperation with the MSs to form a virtual MIMO link. Thus, RSs rank their suitable candidates as follows:

$$U_{rm}(\gamma_{\mathrm{target}}) = P^n_{m\_\mathrm{circ}}\left(\frac{P^n_m(\gamma_{\mathrm{target}})\|w_{\mathrm{rs}}\|^2}{M_t}\right) - P^n_{m\_\mathrm{circ}}\left(\frac{P^n_m(\gamma_{\mathrm{target}})\|w_{\mathrm{ms}}\|^2}{M_t}\right), \tag{4.29}$$

where U_{rm} is computed as the difference between the power spent by the RS and the MS when forming a virtual MIMO link. Thus, a high value in the utility means that the RS carries most of the power expenditure for the virtual link, since its channel to the BS experiences better instantaneous conditions than the MS channel. Moreover, the RS' preference list, L_r, is formed by evaluating each element of S_r by Equation (4.29).

3) After the ranking is done, the SMI procedure given in Algorithm 1 [95], can be applied.

4.5.2 Bandwidth Expansion Process

In our proposed framework, the set of spare RBs in the system consists of F RBs, thus $F \in N$ and the other set represents the M mobile stations. Moreover, in order to perform the bandwidth expansion process every element in each set should build a list which consists of the members of the opposite set ordered by *preference*. A matching pair E is a tuple (MS, RB)

Algorithm 1: Stable Marriage with incomplete lists (SMI).

Initialization: All MSs transmit in only one RB and with only one antenna;
In the following algorithm the term *resource* may refer to an RB or RS;
while *There is a spare resource willing to be allocated to the* m*-th MS;*
do
  MS_h is the highest ranked MS in the i-th spare *resource* preference list, L_f or L_r respectively, to whom it has not yet proposed;
  if MS_h *is free* **then**
    the spare i-th *resource* and the MS_h become engaged;
  else
    MS_h is already engaged with a j-th spare *resource* (where $i \neq j$) ;
    if MS_h *prefers the* i*-th spare resource to the one that it is currently engaged in its preference list,* L_m*;* **then**
      the i-th spare *resource* becomes engaged, and the j-th spare *resource* becomes free;
    else
      MS_h remains engaged to the j-th spare *resource*;
      MS_h is deleted from the list of the i-th spare *resource*, L_f or L_r respectively;
    end
  end
end

such that each MS and f-th spare RB belong exactly to one tuple. If $(m, f) \in E$, we say that the f-th spare RB is the m-th MS's partner in E and vice versa. The distributed BE procedure is modeled as follows:

1) First, the channel quality information is obtained at the BS side by Sounding Reference Signals (SRS) transmitted by the MS [34].

2) Further, this information may be forwarded to the MSs through the feedback channel. Thereby, MSs are able to compute the benefit of using the BE method with each of the spare RBs in the F subset by Eq. (4.27).

$$U_{mf}(\gamma_{\text{target}}) = P^{n}_{m\_\text{circ}}(P^{n}_{m}{}^{*}(\gamma_{\text{target}})) - \sum_{j \in Z} P^{j}_{m\_\text{circ\_BE}}(P^{j}_{m\_\text{BE}}{}^{*}(\gamma_{\text{target}})), \tag{4.30}$$

where Z represents the subset of allocated RBs to the m-th MS, and γ_{target} is the target SNR that all the users independent of transmitting in one or multiple RBs aim to achieve. Thus, Eq. (4.30) represents the difference in power expenditure when using the currently allocated n-th RB compared with the BE method. Hence, the higher the utility value, the more willing is the m-th MS to use more than one RB for transmission. Moreover, if the utility becomes negative the MS will avoid using the spare RB contained in the Z subset, since the power consumption in the uplink increases when the BE is used. Furthermore, the MS preference list L_m is formed

by evaluating the elements of the subset F with Eq. (4.30). MSs not obtaining any benefit from using the BE method with any of the spare RBs in the subset, F, should transmit in a single RB.

3) In addition, the RBs in the F subset need to compute the suitability for the BE process with a specific MS. Thus, each RB ranks the available MSs in the network as follows:

$$U_{fm}(\gamma_{\text{target}}) = \sum_{j=1, j\neq m}^{M} \mathbb{1} P^{f}_{m\_\text{circ}}(P^{f\,*}_{m}(\gamma_{\text{target}})) \leq P^{f}_{j\_\text{circ}}(P^{f\,*}_{j}(\gamma_{\text{target}})), \tag{4.31}$$

where U_{fm} is an utility function which consists of the pairwise comparisons of the f-th RB when allocated to the m-th MS against any other j-th MS in the network, where $j \in M$. The operator $^{\mathbb{1}}(A \leq B)$ provides an output of 1 when the proposed condition holds, and 0 in any other case. Thus, a high utility value means that allocating the f-th RB to the m-th MS will contribute to higher energy savings in the system. Moreover, the RB's preference list, L_f, is formed by evaluating each m-th MS with Equation (4.31).

4) After the ranking is done, the SMI procedure given in Algorithm (1) [95], can be applied.

4.6 Comparison Schemes and Simulation Scenario

In this section, we describe the comparison schemes that were utilized in the simulations. The first part presents the comparison methods employed for virtual MIMO coalition formation. In the latter, the comparison schemes when expanding the bandwidth of the m-th user for transmission in the uplink are described.

4.6.1 Virtual MIMO coalition formation

In order to evaluate the proposed method, this section describes two distributed coalition formation schemes, which allow the mobiles and relays to cooperate in order to form a virtual MIMO link. Additionally, we present a baseline scheme where all the MSs transmit in SIMO mode. Finally, a centralized global optimum scheme, which is coordinated from the BS, is computed based on an exhaustive search approach.

4.6.1.1 Minimum Relaying Hop (MRH) Path Loss Selection

In [99], the authors propose an RS selection method as a function of path loss. Thus, the best RS to form a coalition is the one with the least path loss to the m-th MS, which is the relay that has the most energy efficient cooperative link:

$$RS_c = \text{argmin}\left(d_{mr}^{\kappa}\right), \tag{4.32}$$

4.6.1.2 Best Worst (BW) Channel Selection

In order to form a virtual MIMO link, each MS should take into consideration the quality of the cooperative link, and the RS channel statistics on the uplink. This is because both have a direct influence on the total energy expenditure to form the virtual MIMO link. In [99], the best worst channel is used in which the relay whose worse channel is the best is selected:

$$\text{argmin}\left(\|h_r, \frac{1}{d_{mr}^{\kappa}}\|\right), \tag{4.33}$$

where h_r is the fading coefficient between the r-th RS and the BS, path loss and shadowing are not considered for the decision making process, since we assume that the other RS candidates are close enough to the MS to experience the same shadowing and path loss.

4.6.1.3 Stable marriage

By using the method described in Algorithm (1), the virtual MIMO coalition formation through stable marriage can be applied to increase the energy efficiency in the network.

4.6.2 Simulation scenario

Monte Carlo simulations are performed using the parameters listed in Table 4.1. This is done in order to compare the performance of our method with the schemes presented above. The simulation is comprised of a single cell with the mobile stations and relays distributed uniformly over the cell. The cell is served by a multi-antenna BS. Furthermore, the system is only noise limited, thus each coalition transmits in an independent RB. In our simulation, we assume that all the *coalitions* (SIMO or MIMO) try to achieve the same target SNR.

Parameter	Value
MSs per macro-cell, M	20
RSs per macro-cell, R	120
Number of antennas at the receiver, M_r	5
Cell radius	350m
Number of available RBs, N	20
Number of cells, D	1
Subcarriers per RB, k_{sc}	12
Symbol rate per subcarrier, ϱ_s	15ksps
P_{Tx}	31.8dBm
P_{con}	23.8dBm
P_{BB} for $\varepsilon = 3.90\ \frac{\text{bits}}{\text{symbol}}$	11.7dBm
Maximum user transmit power	23dBm
Shadowing, Std. Dev., σ	3dB
γ_{target},	14dB
ε for 14dB SNR	$3.90\ \frac{\text{bits}}{\text{symbol}}$
κ	3.5

Table 4.1: *Virtual MIMO simulation parameters.*

4.6.3 Bandwidth Expansion Process

To evaluate the performance of the SMI algorithm. In this section, three BE schemes which can allocate spare RBs to reduce the power expenditure in the uplink are described. In addition, a baseline scheme where all the MSs transmit in a single RB is considered.

4.6.3.1 Arbitrary RB allocation (ARBA)

In this scheme, the extra RBs used by the m-th MS for transmission in the uplink are chosen on a random basis.

4.6.3.2 Stable marriage

By using Algorithm (1), the BE expansion process through stable marriage can be applied to increase the energy efficiency in the network.

4.6.3.3 Centralized global optimum

A centralized global optimum approach, which is based on an exhaustive search coordinated from the BS side, is implemented in order to find the price of anarchy for the distributed BE

Parameter	Value
MSs per macro-cell, M	20
Number of antennas at the receiver, M_r	5
Cell radius	150m
Number of available RBs, N	45
Number of cells, D	1
Subcarriers per RB, k_{sc}	12
Symbol rate per subcarrier, ϱ_s	15ksps
P_{Tx}	31.8dBm
P_{con}	23.8dBm
P_{BB} for $\varepsilon = 3.90\ \frac{\text{bits}}{\text{symbol}}$	11.9dBm
Maximum user transmit power	23dBm
Shadowing, Std. Dev., σ	3dB
γ_{target},	14dB
ε for 14dB SNR	$3.90\ \frac{\text{bits}}{\text{symbol}}$
BE factor, $\lvert Z \rvert$	2

Table 4.2: *Bandwidth expansion simulation parameters.*

method. The price of anarchy is computed as the difference in performance when comparing a distributed with a centralized method [100].

4.6.3.4 Simulation scenario

Monte Carlo simulations are performed using the parameters listed in Table 4.2. This allows comparison of the performance of the proposed method with the other schemes presented above. The simulation is comprised of a single cell with the MSs uniformly distributed over the cell. The cell is served by a multi-antenna BS. Furthermore, the system is thermal noise limited. We assume low network load conditions (e.g., 40% to 60% of the maximum capacity) thus spare RBs are available in the network. In our simulation, we assume that all the users in the network should achieve the same target SNR.

4.7 Results

In this section, simulations results are presented to show the advantages in performance of the stable marriage framework when compared to the other proposed methods. In the first part the SMI is used as a coalition formation framework for an energy efficient virtual MIMO link. The latter show the results in system performance when the SMI framework is employed in an energy efficient BE process.

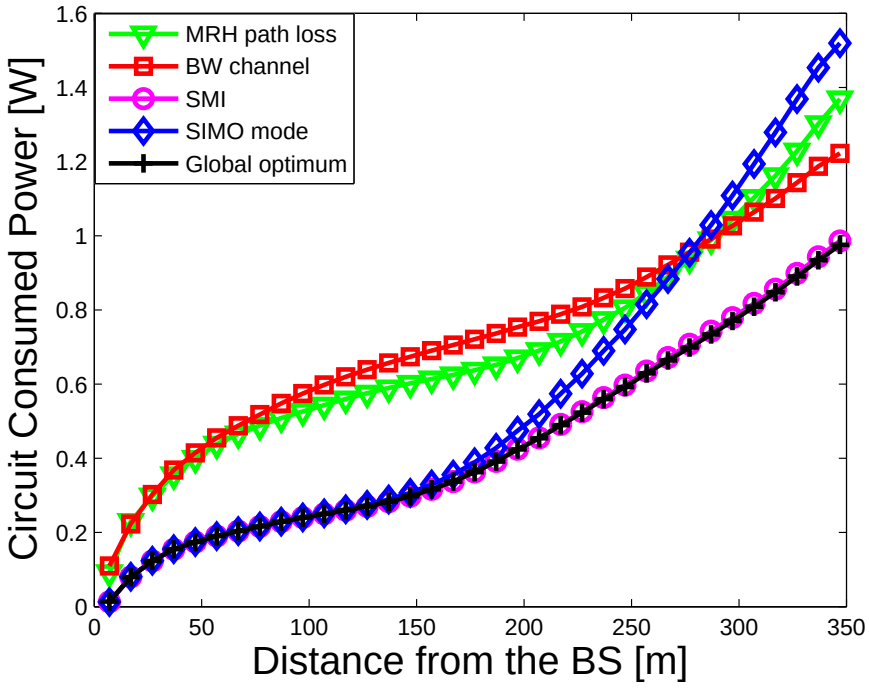

Figure 4.7: *User overall consumed power vs distance from the BS.*

4.7.1 Virtual MIMO Coalition Formation

The cumulative distribution function (CDF), and the graphs that show the distribution of the user overall consumed power at different distances from the BS for the schemes described in Section 4.6.1 have been generated. In Figure 4.7, we plot the user overall consumed power. We observe, that when the MSs are close to the BS (up to 160 m), the overall power consumption of the SIMO scheme matches the SMI and the global optimum curve. This is because the MSs are able to experience better transmission conditions when they are close to the BS. Thus, turning on the RF transmitter of the relay stations is less power efficient than transmitting with only one antenna. Furthermore, due to the design of the MS's utility function (4.28) for the SMI case, MSs are able to switch to SIMO mode when it provides power savings. In the case of the other two distributed approaches (MRH path loss selection and the BW channel selection), both schemes always try to form a virtual MIMO link even if the MSs experience favorable transmission conditions to the BS. Hence, they consume more power for small distances to the BS than for the other three approaches.

Additionally, the system energy efficiency in Figure 4.8 is shown. At the 50^{th} percentile, the SMI scheme shows improvements of 37%, 42%, and 44% compared to the SIMO transmission, the MRH path loss and the BW channel respectively. Hence, the proposed SMI approach is

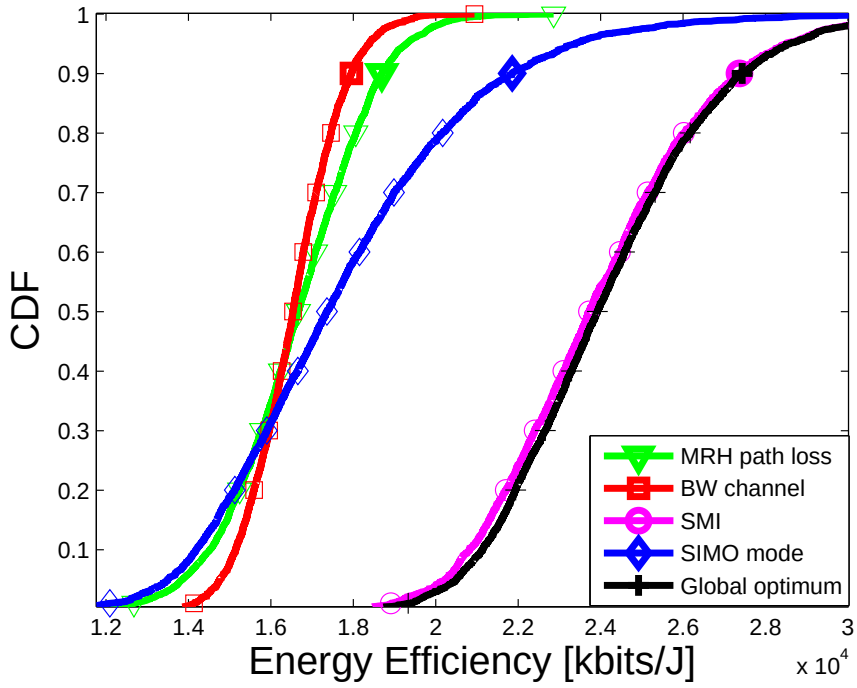

Figure 4.8: *System CDF energy efficiency.*

more energy efficient than the other two distributed approaches and the baseline case. Furthermore, the price or anarchy for the SMI is only 2%, this can be seen as the loss in performance, when the SMI algorithm is compared with the global optimum. Thus, the performance of our distributed approach is similar when compared to a centralized scheme.

4.7.2 Bandwidth Expansion Process

In this section, we compare the performance in terms of energy efficiency and overall power expenditure for the schemes presented in Section 4.6.3. Figure 4.9 plots the overall power expenditure against different distances from the BS. It can be observed that when MSs are close to the cell center, the users' power consumption of the centralized global optimum and SMI schemes overlap with the baseline method. This is because mobile users are able to experience more favorable propagation conditions when they are close to the cell center. Thus, as shown in Section 4.4 the generated power cost due to the BB and RF modules when transmitting with more than one RB does not become an optimal solution in a low power transmission regime. Moreover, since the SMI scheme performance is based on optimizing the utility function, Eq. (4.30), it allows the proposed algorithm to use more than one RB only when it gener-

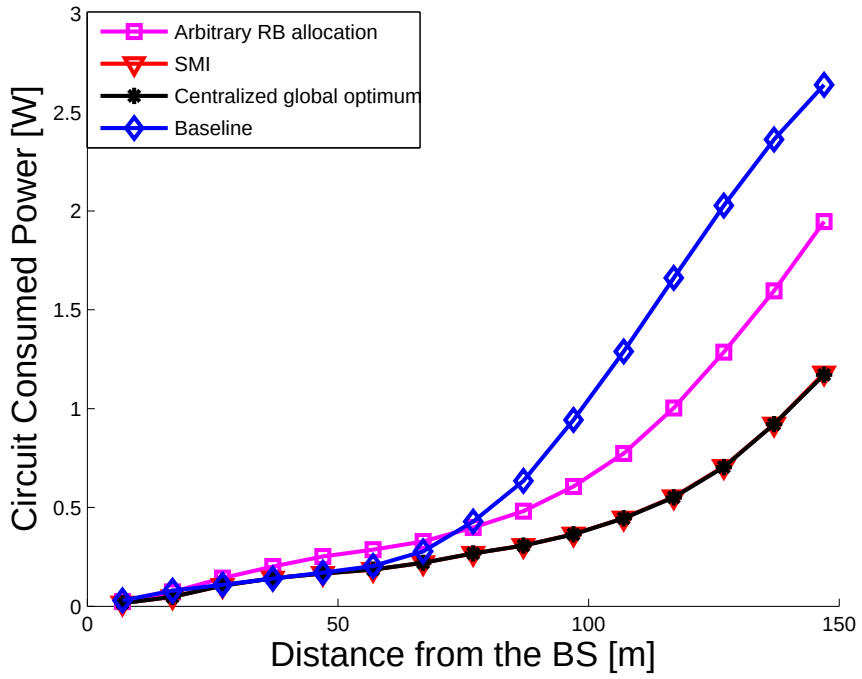

Figure 4.9: *User overall consumed power vs distance from the BS.*

ates significant power savings. In the case of the arbitrary RB allocation (ARBA) scheme, it can be seen how at close distances from the BS, this method consumes more power to achieve the same rate constraints than other approaches. This difference in performance is because ARBA allocates more than one RB when transmitting at close distances from the BS. Furthermore, for users close to the cell edge (e.g., 140 m), we can observe that less power is required when more than one RB are allocated to them. This is clear, since the other presented methods require less overall consumed power than the baseline. Thus, it can be understood that in order to reduce energy consumption in the system, the extra RBs should be allocated mostly for users close to the edge rather than for cell center users.

Additionally, Figure 4.10 shows the system energy efficiency. At the 50^{th} percentile, the SMI and the centralized method show performance improvements of 115% and 72% when compared to the baseline and ARBA, respectively. Hence, the proposed SMI approach is more energy efficient than the other two approaches. Such gains in energy efficiency for the SMI and the centralized method compared to the other approaches are because both schemes allocate efficiently most of the RBs at the cell edge rather than at the cell center. Furthermore, notice that the performance of the centralized optimum method is the same as for the SMI scheme. Thus, for this case the price of anarchy of the proposed approach is zero.

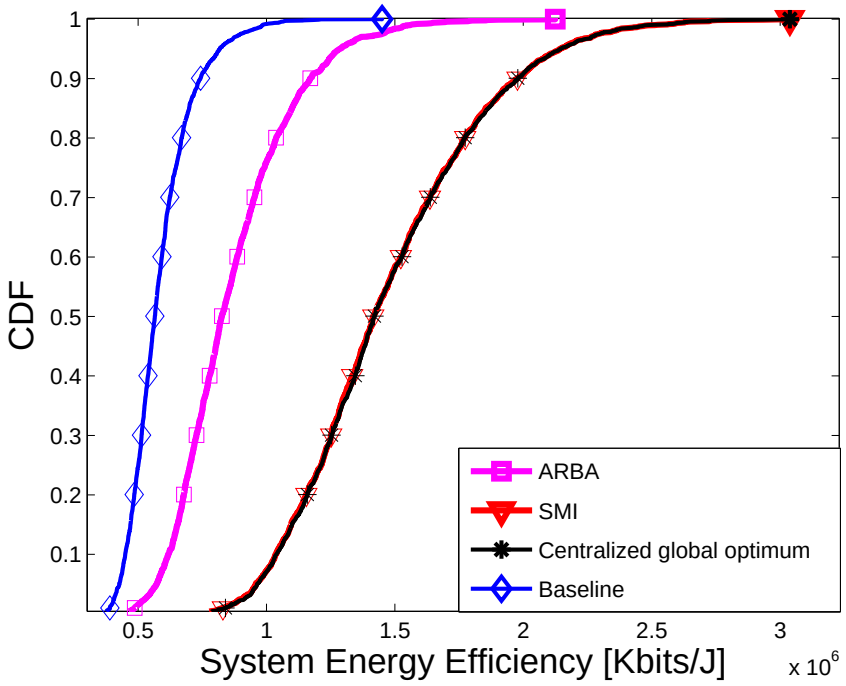

Figure 4.10: *System CDF energy efficiency.*

4.7.3 Computational Complexity

To conclude the comparison, a discussion of the computational complexity of the SMI and the centralized approach is presented. Big $\mathcal{O}$ notation is used to describe the growth rate of both schemes. Thus, it can be seen that the SMI method bases its optimization on Eqs (4.30) and (4.31), which induces a complexity of $\mathcal{O}(|F|)$ and $\mathcal{O}(M)$ respectively, where $|.|$ defines the cardinality of the subset. Furthermore, the bandwidth expansion scheme is based on the assumption of having more RBs available than MSs present in the system, thus the complexity of the algorithm is bounded by the number of RBs rather than by the number of MSs. So, the complexity induced by the computation of the utility functions is $\mathcal{O}(|F|)$. Moreover, forming the preference lists L_m and L_f and performing Algorithm (1) requires a sorting and a binary search operation respectively, thus a complexity of $\mathcal{O}|(F|\log(|F|))$ and a complexity of $\mathcal{O}(\log(|F|))$ is induced for each calculation. The dominant factor will be the one with the largest exponent, therefore the complexity of SMI is upper bounded by $\mathcal{O}(|F|\log(|F|))$. The complexity increases linearly with the number of MSs, M, in the system. Hence, the complexity of the SMI is denoted by $\mathcal{O}(M \times |F|\log(|F|))$. In the case of the centralized method, an exhaustive

search approach, where the number of elements is discrete, is considered $\mathcal{NP}$-complete [35]. The optimal solution between the spare set of RBs, F, and the M MSs is computed through permutations between both sets in order to find the match which provides the optimal energy efficient solution for the system. After all the permutations are done, the system chooses the most optimal solution. The total number of permutations is upper bounded by the number of spare RBs, F. Thus, the number of required permutations in the system is $|F|!$. The circuit power that is consumed when using the BE is obtained considering the right-hand side of Eq (4.27). Thus, an arithmetic operation is required which induces a complexity of $\mathcal{O}(|F|!)$ for the method. Thereby, the final complexity for the centralized scheme is $\mathcal{O}(|F|!)$, which is a much higher order complexity that the one required by the SMI method.

4.8 Summary

A low complexity distributed framework for resource allocation derived from the SMI concept is proposed in this chapter. The SMI method has been employed for virtual MIMO coalition formation and as an energy efficient bandwidth expansion tool. When the SMI is employed as a virtual MIMO coalition formation framework, it allows each MS and RS to independently pick up the best partner to reduce the power consumption in the uplink without the involvement of a central authority. Thus, based on the presented results, the proposed approach is a more energy efficient solution with improvements of 42%, 44%, and 37% when compared to the MRH path loss, the BW channel, and the SIMO mode scheme respectively. The price of anarchy of our proposed method is only of 2%. Furthermore, it is shown that when the overall consumed power is considered for the optimization process and under a given set of conditions, transmitting in SIMO mode is more energy efficient than forming a virtual MIMO link. In its counterpart, utilizing the SMI in the BE process allows each RB and mobile user in the system to be considered as an independent entity which takes an active role in the decision making process. From the results obtained, it is shown that the SMI method is a more energy efficient solution with improvements of 115% and 72% when compared to the baseline and the ARBA scheme respectively. The performance of the method is the same in bits per Joule as the centralized global optimum, thus the price of anarchy in this case is zero. Furthermore, it is shown analytically and by simulation that when the mobile user experience favorable propagation conditions in the uplink, the overall consumed power is reduced by transmitting in one RB rather than using an RB expansion technique. Finally, in this chapter it is shown how through the SMI framework the network infrastructure can be utilized in an efficient way to implement spatial

diversity through relays with the aim of increasing the energy efficiency metric in the network. Moreover, it has been discussed how the stable marriage framework can be used as a useful optimization tool at the protocol stack level by allocating extra RBs to the mobile users in the uplink to reduce the power expenditure.

Chapter 5
A Distributed Virtual MIMO Coalition Formation Framework for Energy Efficient Wireless Networks

5.1 Introduction

The stable marriage framework imposes restrictions regarding the number of elements that can participate in the coalitions, typically two entities. In this chapter, a more powerful tool is introduced called the college admissions framework for virtual MIMO coalition formation. This framework does not impose any restriction on the number of elements participating in the coalitions. In this chapter, we again focus on coalitions of antennas which enhance single user performance rather than multiuser performance by using a multiuser configuration. Moreover, power savings are obtained through the use of multiantenna arrays by implementing the concepts of spatial diversity and spatial multiplexing for uplink transmission. As in the previous chapter the proposed approach focuses on optimizing the circuit consumed power rather than just the transmitted power of the network devices. Furthermore, it is shown by system level simulations and mathematical derivations that when circuit consumed power is optimized the energy efficiency of the wireless entities is not always improved by forming a virtual MIMO array. Hence, single antenna devices may prefer to transmit at their own when channel conditions are favorable.

The rest of the chapter is structured as follows: Section 5.2 provides an extensive literature review, Section 5.3 describes the problem scenario, Section 5.4 presents the power consumption model and performance metrics. In Section 5.5, the cooperative framework is shown. Moreover, in Section 5.6 a theoretical analysis of the consequences arising when optimizing overall consumed power rather that transmitted power when implementing spatial diversity and spatial multiplexing in multi-antenna systems is presented. A summary of the comparison schemes

and the simulation scenario is described in Section 5.7. Simulation results are presented in Section 5.8. Finally, Section 5.9 offers concluding remarks.

5.2 Literature Review

The use of multiple antennas in wireless links has emerged as an effective way to enhance the energy efficiency. It has been shown in [2] that multi-antenna systems require less transmitted power to achieve the same capacity requirements than single antenna devices. In networks such as Long Term Evolution (LTE), a base station (BS) may support multiple antennas. However, mobile stations (MSs) may not be equipped with more than one single antenna due to physical constraints [25, 34]. Hence, implementing effective solutions that allow MSs to benefit from the advantages of multi-antenna systems without the extra burden of having multiple antennas physically present at the users' side, has become a major issue for current communication systems.

Cooperative communications have recently attracted significant attention as an effective way to improve the performance of wireless networks [29]. By the use of cooperative techniques wireless devices are allowed to share and utilize the network resources in a more efficient way [3, 6, 27, 29, 56–58]. As an example, the authors in [56] present a cooperative method to share the network resources and manage interference among femtocells in a distributed manner. Hence, femtocells form coalitions to improve their performance by sharing spectral resources and maximizing the spatial reuse. In [58], the authors consider the consequences that arise when two multi-antenna systems share the same spectrum band. They demonstrate that if cooperation between the two systems is possible, they may achieve a performance close to the maximum sum-rate.

An important application of cooperative techniques is the formation of virtual multi-antenna arrays. In this context, a number of single antenna devices may cooperate with each other by forming virtual multiple-input multiple-output (MIMO) transmitters or receivers to reap some of the benefits of multi-antenna systems [59]. The theoretical aspects of virtual MIMO have previously been covered in [59, 101]. Papers on virtual MIMO which consider energy efficiency as an optimization constraint can be found in [25–27]. The authors in [26, 27] illustrate the energy savings obtained when virtual MIMO techniques are used compared with non-cooperative approaches in wireless sensor networks. They argue that at certain ranges from the destination node, cooperative MIMO results in a more energy efficient solution that also reduces the total delay compared with the non-cooperative case. In [25], an approach to optimize the power

allocation between transmitter and relay in order to minimize the overall energy per bit consumption in the system is presented. Moreover, it is shown that by using an optimal power allocation, the virtual MIMO case achieves an energy efficiency performance close to the ideal MIMO system.

As mentioned previously, most of the current research in energy efficient virtual MIMO tackles the problem of "why to cooperate". Nevertheless, there are two questions that remain unanswered namely "when to cooperate" and "with whom to cooperate". Thereby, the aim of this work is to provide an answer for both questions by providing a coalition formation framework that allows single antenna devices to decide with whom to cooperate in order to obtain energy savings in the uplink transmission.

In addition, the implementation of cooperative solutions may face many challenges due to the large scale nature of wireless systems. Cooperation comes along with costs such as power expenditure that may limit or reduce the system's performance. Moreover, if cooperation between the users is regulated by a centralized entity, a significant amount of wireless signaling overhead is required between the users and the network. Furthermore, it is well known that the use of centralized techniques entails extra implementation costs and an increase in system's complexity [7, 102, 103]. Thus, the design of effective techniques that allow the single antenna devices to *autonomously* decide when and with whom to cooperate is a matter of vital importance for current networks [28]. In this regard, game theory provides a powerful mathematical tool for the design of distributed solutions in cooperative communications [3, 28, 29, 31]. Through the use of coalitional game theory, the authors in [28] propose a merge and split distributed algorithm to form multi-antenna coalitions among single antenna devices. The aim of their work is to maximize the users' rate while accounting for the cost of cooperation in terms of power. In Chapter 4, an energy efficient solution for virtual MIMO coalition formation is proposed, where cooperation is modeled as a game theoretical approach derived for the concept of stable marriage with incomplete lists. An optimal relay is selected to minimize the MS's power expenditure. A major drawback of the proposed framework in Chapter 4 is that the number of elements that can join the coalition is constrained to a limited number, typically two.

The main contributions of this chapter are: (1) to provide a distributed low complexity virtual MIMO coalition formation algorithm for energy efficient networks; (2) the proposed solution can support any number of transmitters participating in the coalitions; (3) we focus on enhancing the mobile station (MS) performance by forming virtual coalitions with the RSs; (4) the proposal is analyzed from both diversity and capacity perspectives; (5) the proposed solution focuses on reducing the overall device consumed power rather than the transmitter radio

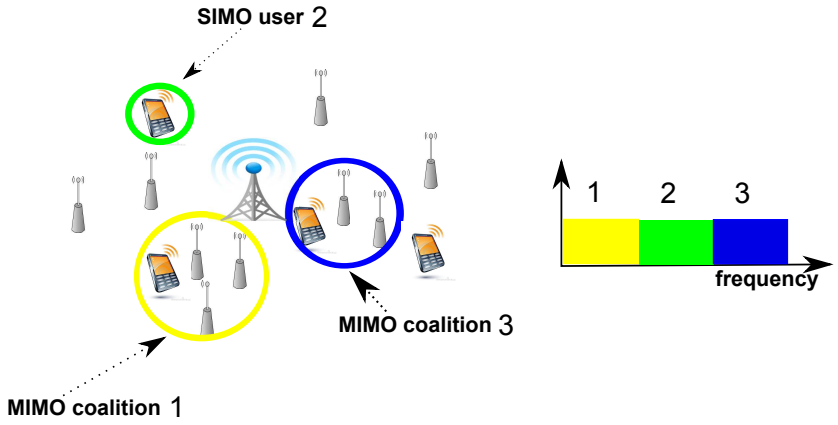

Figure 5.1: *User cooperation example coalitions considering an OFDMA transmission model.*

frequency (RF) power, thus the power consumption of the RF components such as the power amplifiers and the base band (BB) module is taken into account.

5.3 System Scenario

In this section, the scenario adopted in this chapter is described. We consider a system with M single antenna mobile stations (MSs) that transmit data to a multi-antenna base station. In addition, R single antenna relay stations (RSs) are uniformly distributed through the cell, assuming $R \gg M$. In order to improve the user's performance, single antenna devices (MSs and RS) are allowed to cooperate by forming virtual $M_t \times M_r$ MIMO coalitions, where M_r is the number of antennas at the base station (BS), and M_t is the number of single antenna devices forming a virtual MIMO link. If cooperation is not feasible, MSs will prefer to transmit to their own to the BS in single-input multiple-output (SIMO) mode.

An orthogonal frequency division multiple access (OFDMA) system is constructed, where the system bandwidth B (Hz) is divided into N resource blocks (RBs). Each RB is assigned to each user independently to avoid mutual interference. An RB defines the basic time-frequency unit with bandwidth $B_{RB} = B/N$ (Hz). In Figure 5.1, an illustration of the OFDMA system scenario is shown.

5.3.1 Virtual MIMO Link

Figure 5.2(a) and Figure 5.2(b) show a virtual $M_t \times M_r$ MIMO link which implements spatial diversity and spatial multiplexing respectively. At the first time slot, the MS forwards the

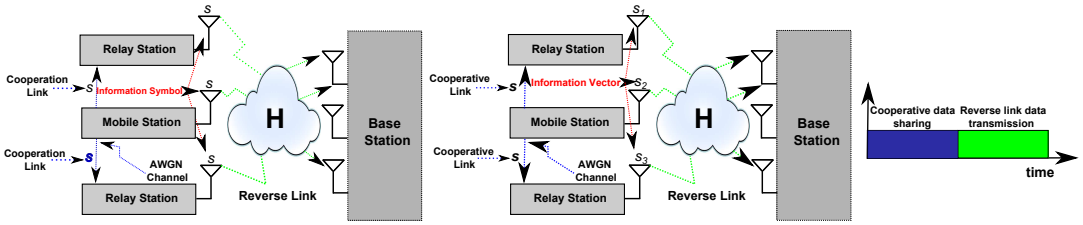

(a) Spatial Diversity (b) Spatial Multiplexing

Figure 5.2: *A Virtual $M_t \times M_r$ MIMO link.*

information symbol s or vector $\mathbf{s}$ to its peers by using the cooperative link. In the following slot, the MS and RSs will transmit the information symbol s or vector $\mathbf{s}$ on the uplink through the MIMO channel. In addition, to avoid mutual interference the uplink and the cooperative link should be designed to be orthogonal to each other. When spatial multiplexing is implemented as shown in Figure 5.2(b), it is assumed that the cooperative link has sufficient bandwidth for information transmission, thus MSs can transmit their signal vector $\mathbf{s}$ to the cooperating peers and they can demultiplex it into independent information streams for simultaneous transmission in the next time slot.

5.3.2 Cooperative Link

For the single antenna devices (MSs and RSs) to cooperate among each other, the set up and maintenance of a cooperative link is required. The cooperative link is based on a short range transmission, which is primarily used for information exchange between the transmitting peers. Thus, the channel between the m-th MS and the r-th RS can be modeled as a κ^{th}-power path loss (loss $\approx \frac{1}{d_{mr}^{\kappa}}$) with additive white Gaussian noise (AWGN). Accordingly, the received power Pr_{mr} at the r-th RS, transmitted from the m-th MS is given by:

$$Pr_{mr} = P_{mr} d_{mr}^{-\kappa} \tag{5.1}$$

where d_{mr} is the distance between the r-th RS and the m-th MS, and P_{mr} is the transmitted power for cooperation. Hence, the signal-noise ratio (SNR) at the RS side is represented by

$$\gamma_{mr} = \frac{Pr_{mr}}{\eta}. \tag{5.2}$$

where η is the noise power. Moreover, due to the broadcast nature of the wireless channel, when the MS broadcasts its information to the farthest RS in the coalition, all other RSs can also receive and decode this information simultaneously. Thus, define $S'_m \in R$ as the subset of RSs which have formed a coalition with the m-th MS. The cost of cooperation can be defined as the MS's maximum transmitted power to reach the farthest RS in the coalition. Thereby, define the set of distances between the m-th MS and its S'_m subset of RSs as

$$\begin{aligned} D^*_{mr} &= \{d_{m(1)}, d_{m(2)}, \ldots, d_{m(J)}\}, \\ \text{s.t } d_{m(1)} &\leq d_{m(2)} \leq \ldots \leq d_{m(J),} \end{aligned} \tag{5.3}$$

where $J = |S'_m|$, and $|.|$ defines the cardinality of the sub-set. Thus, by using Equations (5.1) and (5.2) the power spent for cooperation may be represented by

$$P_{\text{tcop}} = \gamma_{m(J)} d^{\kappa}_{m(J)} \eta. \tag{5.4}$$

5.3.3 Uplink channel model

The channel coefficient between a multi-antenna BS separated by a distance d_m from the m-th MIMO coalition is determined by path loss, log-normal shadowing, and channel variations caused by frequency selective fading. In this work, a fading Rayleigh channel is considered, thus the fading coefficients for an $M_t \times M_r$ MIMO channel can be represented by a matrix.

$$\mathbf{H}^n_m = \begin{bmatrix} h^n_{1,1} & h^n_{1,2} & \cdots & h^n_{1,M_t} \\ h^n_{2,1} & h^n_{2,2} & \cdots & h^n_{2,M_t} \\ \vdots & \vdots & \ddots & \vdots \\ h^n_{M_r,1} & h^n_{M_r,2} & \cdots & h^n_{M_r,M_t} \end{bmatrix}, \tag{5.5}$$

where each matrix element defines a zero mean circular symmetric complex Gaussian (ZMC-SCG) random variable with unit variance [2]. If the MS prefers to transmit in SIMO mode the channel can be defined by the following vector:

$$\mathbf{h}^n_m = [h^n_1, h^n_2, \ldots, h^n_{M_r}]^T. \tag{5.6}$$

Furthermore, path loss and shadowing are considered to attenuate the transmitted signal, thus, the received power P_r at the BS side is given by [4]

$$Pr_m^n = P_m^n 10^{\frac{-L(d_m)+X_\sigma}{10}}, \tag{5.7}$$

where P_m^n represents the transmitted power, X_σ is the log-normal shadowing value (dB) with standard deviation σ, and $L(d_m)$ is the distance dependent path loss (dB) which is calculated as follows:

$$L(d_m) = a + b \log_{10}(d_m) \text{ [dB]}. \tag{5.8}$$

where $a = 15.3$ and $b = 37.6$ are pathloss constants for a micro urban cell scenario. Moreover, since single antenna devices utilize a short range transmitter for information exchange, a valid assumption is to consider that the elements involved in a MIMO coalition are sufficiently closely spaced to experience the same channel statistics. Thereby, shadowing and path loss remain the same for all devices forming a virtual link. In addition, the receiver and transmitter are assumed to know the channel coefficients between them. The state-of-the-art wireless solutions such as LTE may implement closed loop techniques to obtain current channel state information [54]. In this work, coalitions are formed to reduce the uplink power consumption in the network by using the concepts of spatial diversity and spatial multiplexing. In the case of spatial diversity, the required equations to compute the SNR for a SIMO (4.6), and a MIMO user (4.10), are previously given in Section 4.3. For the spatial multiplexing, these are shown below.

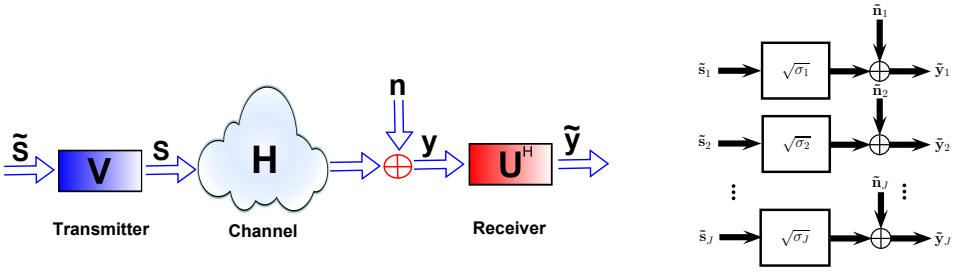

(a) Linear processing of the transmitted signal (b) Modal decomposition of the channel

Figure 5.3: *Linear processing of the transmitted signal by using modal decomposition of the channel, when channel knowledge is assumed at transmitter and receiver side.*

5.3.3.1 Spatial Multiplexing

When channel knowledge is assumed, the individual spatial channel modes may be accessed through linear processing at the transmitter and receiver side [2]. Therefore, a signal vector $\mathbf{s}$ of dimension $\omega \times 1$ which is transmitted from the m-th MIMO coalition through a rank ω MIMO channel, $\mathbf{H}_m^n$, is processed as shown in Figure 5.3(a). By using the singular value decomposition (SVD) the channel matrix can be represented as $\mathbf{H}_m^n = \mathbf{U}_m^n \Sigma \mathbf{V}_m^{n\,H}$, where the columns of $\mathbf{V}_m^n$ and $\mathbf{U}_m^n$ are known as the input and output singular value vectors respectively. Thus, the signal vector $\mathbf{s}$ is multiplied by the matrix $\mathbf{V}_m^n$ of dimensions $M_t \times \omega$ at the transmitter side. Moreover, at the receiver side, the signal is multiplied by the matrix $\mathbf{U}_m^{n\,H}$ of dimensions $M_r \times \omega$. Thus, the signal after linear processing is given by

$$\begin{aligned} \tilde{\mathbf{y}}_m^n &= \sqrt{\frac{Pr_m^n}{M_t}} \mathbf{U}_m^{n\,H} \mathbf{H}_m^n \mathbf{V}_m^n \mathbf{s} + \mathbf{U}_m^{n\,H} \mathbf{n}, \\ &= \sqrt{\frac{Pr_m^n}{M_t}} \Sigma \mathbf{s} + \tilde{\mathbf{n}} \end{aligned} \tag{5.9}$$

where $\tilde{\mathbf{y}}_m^n$ and $\tilde{\mathbf{n}}$ are the received signal and the ZMCSCG noise vector after processing respectively, with dimensions $\omega \times 1$, and $\Sigma = \mathrm{diag}\{\sigma_1, \sigma_2, ..., \sigma_\omega\}$ with $\sigma_i \geq 0$, where σ_i is the i-th singular value of the channel. The transmitted signal vector $\mathbf{s}$ must satisfy: $\mathbf{E}\{\mathbf{s}\mathbf{s}^{\mathbf{H}}\} = M_t$, to constrain the total transmitted power. Furthermore, Figure 5.3(b) shows how $\mathbf{H}_m^n$ is decomposed into ω parallel SISO channels under the assumption of channel knowledge at the transmitter side, where each parallel sub-channel satisfies

$$y_i^n = \sqrt{\frac{Pr_m^n}{M_t}} \sqrt{\sigma_i} s_i + \tilde{n}_i, \quad i = 1, 2, ..., \omega. \tag{5.10}$$

Hence, the total uplink user throughput will become the sum of the individual parallel SISO channel capacities, where the SNR of the i-th spatial channel (SC) is given by

$$\gamma_{i\_SC}^n = \frac{Pr_m^n \zeta_i \sigma_i}{M_t \eta}, \tag{5.11}$$

where $\zeta_i = \mathbf{E}\{\|s_i\|^2\}$ $i = 1, 2, ..., \omega$, represents the transmitted power in the i-th SISO parallel sub-channel and must satisfy $\sum_{i=1}^{\omega} \zeta_i = M_t$.

Furthermore, since the transmitter may access multiple parallel SISO channels, the problem becomes how to allocate the power in a way that maximizes the mutual information. The optimal value of ζ_i is found iteratively through the use of the waterpouring method, which is explained in detail in Table 5.1. When cooperation is not suitable, the MSs will transmit in

1. Obtain the value of the constant τ Set the iteration count f to one, in order to obtain the value of τ as follows: $\tau = \frac{M_t}{\omega - f + 1}[1 + \frac{\eta}{Pr_m^n} \sum_{i=1}^{\omega - f + 1} \frac{1}{\sigma_i}]$
2. Allocate power to the i-th subchannel By using the value of τ, the power allocation for the i-th subchannel is obtained as: $\zeta_i = (\tau - \frac{M_t \eta}{Pr_m^n \sigma_i}), i = 1, 2, ..., \omega - f + 1$
3. Check for a negative value in the power allocation of the subchannel with the lowest gain If the power allocation of the subchannel with the lowest gain is negative, $\zeta_{(\omega - f + 1)} < 0$. The channel is eliminated from consideration by setting: $\zeta_{(\omega - f + 1)} = 0$.
4. The counter f increments by one Repeat steps 1 to 3 until the power allocated to each subchannel is non-negative.

Table 5.1: *Waterpouring method, after [5].*

SIMO mode, where the achievable SNR is defined by Eq. (4.6).

5.4 Power Consumption Model and Performance Metrics for Optimizing Overall Consumed Power

In this chapter, the aim is to optimize the overall power consumption of the MS's components rather than only the transmitted power. For the MIMO user case, it considers the power expenditure in both the uplink and the cooperative link. For the cooperative link case, we only consider the power that is spent for coding the transmitted signal, since the decoding power spent due to the BB system module at the RS side is significantly small, thus it can be neglected from the calculations [97]. When cooperation is not feasible, MSs would prefer to transmit in SIMO mode, hence only the uplink power expenditure is taken into account. The uplink and cooperative link power consumption mainly depend on components such as the radio frequency (RF) parts and the base-band (BB) signal processing module [97]. The RF module incorporates the power expenditure of power amplifiers, and the BB module comprises the power consumption for channel coding/decoding and modulation/demodulation. For modeling the RF and BB module, the model previously presented in Section 4.3.3 is considered. Therefore, the overall consumed power in SIMO mode, P_{m_simo}, depends primarily of the transmitted power in the

uplink P_m^n.

$$P^n_{m\_\text{simo}}(P_m^n) = P^n_{\text{circ}}(P_m^n) \tag{5.12}$$

Furthermore, the total consumed power to form a virtual MIMO link becomes a function of the transmitted power in the uplink P_m^n, and how is distributed between the mobile and the relay stations, which is defined by the water filling coefficients ζ_i , $i = 1, 2, ..., \omega$, for the spatial multiplexing case. Thus, the total consumed power in the uplink is obtained as follows:

$$P^n_{m\_\text{mimo\_capacity}}(P_m^n) = \sum_{i=1}^{M_t} P^n_{\text{circ}}\left(\frac{P_m^n \zeta_i}{M_t}\right) \tag{5.13}$$

where P^n_{circ}, Eq. (4.14), defines the circuit power in the uplink spent by each single antenna device such as MSs or RSs forming the virtual MIMO link. In addition, the power expenditure due to the cooperative link, P_{circop}, given in Eq. (4.16) should be added to Eq. (5.13). Thereby, the total power expenditure to form the virtual MIMO link when implementing spatial multiplexing is given by:

$$P^n_{m\_\text{mimo\_capacity\_total}}(P_m^n, P_{\text{tcop}}) = P^n_{\text{circop}}(P_{\text{tcop}}) + \sum_{i=1}^{M_t} P^n_{\text{circ}}\left(\frac{P_m^n \zeta_i}{M_t}\right) \tag{5.14}$$

where P_{tcop} is computed using Eq. (5.4).

5.4.1 Performance Metrics to Optimize Overall Consumed Power

The achievable throughput on the link between the m-th coalition and the BS when spatial multiplexing is implemented is calculated as [4]:

$$T^n_{m\_\text{capacity}}(\gamma^n_{i\_pipe}) = n_m^{RB} k_{sc} \varrho_s \sum_{i=1}^{\omega} \varepsilon(\gamma^n_{i\_SC}) \ \ [\text{bits/s}]\,, \tag{5.15}$$

where $\gamma^n_{i\_\text{SC}}$ is the SNR in the i-th individual parallel SISO channel previously given in (5.11) and ω is defined as the rank of the channel. Notice that in any case, if the MS prefers to transmit in SIMO mode, the capacity is computed by using (4.17), where γ_m^n is substituted by (4.7).
The user energy efficiency $\beta^n_{m\_\text{capacity}}$ measures the user throughput per unit of consumed energy.

$$\beta^n_{m\_\text{capacity}} = T^n_{m\_\text{capacity}} / \bar{P}^n_{m\_\text{total}} \ \ [\text{bits/J}]\,. \tag{5.16}$$

This is based on the total consumed power $\bar{P}^n_{m\_\text{total}}$, where $\bar{P}^n_{m\_\text{total}}$ is replaced by P_{m_simo} in (5.12) when the coalition acts in SIMO mode, and to $P^n_{m\_\text{mimo\_capacity}}$ in (5.14), when a virtual MIMO link is constructed to implement spatial multiplexing. Additionally, the system energy efficiency β_{sys} is defined as the ratio between the total user throughput and the total power spent by all the users in the system:

$$\beta_{sys} = \frac{\sum_{m=1}^{M} T^n_{m\_\text{capacity}}}{\sum_{m=1}^{M} \bar{P}^n_{m\_\text{total}}} \ [\text{bits/J}] \,. \tag{5.17}$$

5.5 College admission framework for distributed virtual MIMO coalition formation

In this chapter, cooperation is modeled using a game theory approach derived from the college admissions problem [104]. The college admission framework (CAF) is used to find a stable match between two sets of elements (MSs and RSs). The CAF is a generalization of the stable marriage (SM) problem [95]. However, coalitions are not limited only to two participants as in the SM case [31]. As described in [104], the CAF involves a set of colleges and a set of applicants. Each applicant lists in order of preference those institutions she/he aims to attend and each institution lists in order of preference those applicants it is willing to admit. Additionally, each institution has a limit in the number of applicants that is able to admit. Thus, the problem becomes to assign applicants to institutions in a way that takes into account both preferences and constraints. For this case, the M MSs take the role of colleges and the R RSs become the applicants. Hence, RSs are assigned to MSs to form virtual MIMO coalitions with the aim of reducing the total energy consumption of the MSs. This case is studied in order to reduce the power consumption by allowing coalitions to implement spatial diversity or spatial multiplexing respectively. An important property of the CAF is that it leads the system to a stable solution as described in [105]. Stability means that there are no RSs or MSs in the system such that both of the following assumptions are true:

- The RS is not included into any coalition or would prefer to form a virtual MIMO link with a different MS to the one that it is currently matched with;
- The MS is able to include another RS into its MIMO coalition or would prefer to cooperate with a different RS to one of its current partner RSs.

A mapping E' is a tuple of one MS with a subset of one or more RSs, such that each single antenna device (MS or RS) belongs exactly to one tuple. Hence, if $(m, S'_m) \in E'$, the S'_m subset of RSs is the cooperative partner set of the m-th MS in E' and vice versa, where $S'_m \in R$. The distributed coalition formation algorithm is described as follows:

1. At the beginning of the algorithm, each MS in the system sends a broadcast message through the cooperative link to find the subset of RSs willing to cooperate and form a virtual MIMO link, which for the m-th MS is denoted by $S_m \in R$.

2. Moreover, the RSs in the system exchange their channel statistics in the uplink (fading coefficient, path-loss and shadowing) and the channel statistics in the cooperative link (path loss) with the subset of MSs willing to cooperate with them, which for the r-th RS is denoted by $S_r \in M$. Thereafter, each mobile station has the means to rank its subset of suitable RSs, S_m, by using the utility function defined in Eq. (4.28) when diversity is enhanced. In the case when implementing spatial multiplexing, each m-th MS ranks each r-th RS from its S_m subset by:

$$U_{mr\_\text{capacity}}(T_{\text{target}}) = P^n_{m\_\text{simo}}(T_{\text{target}}) - P^n_{m\_\text{mimo\_capacity\_total}}(T_{\text{target}}), \qquad (5.18)$$

where U_{mr_capacity} represents the difference in energy efficiency performance when the m-th MS transmits on its own or forms a coalition with the r-th RS, and T_{target} represents the target transmission rate for SIMO and MIMO users. Thus, as in the case when diversity is enhanced, Eq. (4.28), the higher the value of the utility the more the m-th MS will be willing to form a virtual MIMO link with the r-th RS. The m-th MS's preference list L_m is formed by evaluating the utility for each of the RS in S_m by using Eqs. (4.28) or (5.18) for the diversity or the capacity case respectively. Moreover, the RSs of the m-th MS's preference list, L_m, must be sorted in descending order as follows:

$$\begin{aligned} L_m &= \{\text{RS}_{m(h)}, \text{RS}_{m(2)}, \ldots, \text{RS}_{m(1)}\}, \qquad (5.19) \\ \text{s.t } U_{m(1)} &\leq U_{m(2)} \leq \ldots \leq U_{m(h)}, \end{aligned}$$

where $U_{m(r)}$ represents the pairwise comparisons between the m-th MS and the r-th RS. These are the values obtained from Eqs. (4.28) or (5.18) when the preference list is built to implement spatial diversity or spatial multiplexing respectively. Notice that when the value of $U_{m(r)}$ becomes negative, the m-th MS will not consider the r-th RS for coalition formation, thus the r-th RS will not be contained in the m-th MS ranking list, L_m.

3. Mobiles are only required to exchange their channel statistics in the uplink with the RSs willing to cooperate with them. Based on this information, RSs are able to rank their subset of MSs, S_r, by using the following utility function when spatial multiplexing is implemented.

$$U_{rm\_\text{capacity}} = P^n_{\text{circ}}\left(\frac{P^n_m \zeta_{\text{rs}}}{M_t}\right) - P^n_{\text{circ}}\left(\frac{P^n_m \zeta_{\text{ms}}}{M_t}\right), \tag{5.20}$$

Equation (5.20) represents the difference in power expenditure between the r-th RS and

Algorithm 2: College admission framework (CAF), after [105].

Initialization: All MSs must be operating in SIMO mode;
while *There is an MS-n wanting to form a MIMO link;*
do
  $MS_r(h)$ is the highest ranked MS in the RS-r preference list, L_r, to whom the RS-r has not proposed yet;
  if *RS-r is contained in the $MS_r(h)$'s preference list;* **then**
    if *$MS_r(h)$ is free;* **then**
      the $MS_r(h)$ and the RS-r become engaged;
    else
      $MS_r(h)$ is already engaged with a subset of RSs, $\bar{S_n} \in R$;
      if *If adding the RS-r to the $MS_r(h)$ current subset of RSs, $\bar{S_n}$, provides energy savings;* **then**
        RS-r becomes engaged;
      end
      if *If adding the RS-r to the $MS_r(h)$ current subset of RSs, $\bar{S_n}$, does not provides extra energy savings. Nevertheless, $MS_r(h)$ prefers RS-r to the RS-t in its preference list, $L_r(h)$, where RS-$t \in \bar{S_n}$;* **then**
        RS-r becomes engaged;
        RS-t becomes free;
      else
        $MS_r(h)$ is deleted from the list of the RS-r, L_r;
      end
    end
  end
end

the m-th MS when forming a virtual MIMO link. Thus, the larger the value of the utility the larger the power expenditure of the RS due to its better channel conditions in the uplink when compared to the MS. Furthermore, the RS's preference list, L_r, is obtained by evaluating each of the elements in the S_r subset by Equations (4.29) or (5.20) when implementing spatial diversity or spatial multiplexing respectively. The elements of L_r are also sorted in descending order as the L_m case described previously in (5.19).

4. After the preference lists for MSs and RSs are obtained, Algorithm (2) from [105] can be performed.

5.6 Analysis of the consequences in performance of MIMO systems when optimizing overall consumed power

In this section, a theoretical analysis is provided of the consequences that arise in terms of energy efficiency when overall power consumption is considered as an optimization metric rather than transmitted power. Hence, to show the effects on user performance, we analytically derive the statistics of the transmitted and overall consumed power when implementing spatial diversity or spatial multiplexing respectively. While these statistics can be obtained experimentally, we derive them in closed form.

5.6.1 Spatial Diversity Approach

From Eq. (5.7) it can be seen that the transmitted power of any signal, P_m^n, can be obtained by

$$P_m^n = \frac{Pr_m^n}{10^{\frac{-L(d_m)+X_\sigma}{10}}}, \tag{5.21}$$

Moreover, if Eq. (4.10) is combined with Eq. (5.21), we obtain the transmitted power for a MIMO user.

$$P_{m\_\text{mimo}}^n = \frac{\gamma_{m\_\text{mimo\_diversity}}^n \eta}{\sigma_{max}^2 10^{\frac{-L(d_m)+X_\sigma}{10}}}. \tag{5.22}$$

Given that, on average, $\mathbf{E}\{\sigma_{max}^2\} \leq M_t \times M_r$, and $X_\sigma = 0$ [2], this allows us to re-write Eq. (5.22) as follows:

$$P_{m\_\text{mimo}}^n = \frac{\gamma_{m\_\text{mimo\_diversity}}^n \eta}{M_t \times M_r 10^{\frac{-L(d_m)}{10}}}. \tag{5.23}$$

To obtain the statistics for the transmitted power of a MIMO user $P_{m\_\text{mimo}}^n$, it is assumed that the MSs are uniformly distributed in the cell. Therefore, for a circular cell of radius R it is known that the probability distribution function (PDF) of the distance of any point from the center is [27]:

$$f_{d_m}(d_m) = \frac{2d_m}{R^2} \;\; d_m \in [0, R] \tag{5.24}$$

In addition, from Eq. (5.8) it is observed that pathloss is an element which is a function of distance, thus to derive its PDF the transformation of random variables is used. Thereby, the

inverse relationship of the distance as a function of pathloss is obtained as follows:

$$d_m(L) = 10^{\left(\frac{L-a}{b}\right)}, \tag{5.25}$$

Hence, the pathloss PDF $f_L(L)$ may be derived by

$$f_L(L) = \left|\frac{dd_m}{dL}\right| f_{d_m}(d_m(L)) \;\; L \in [-\infty, a + b\log_{10}(R)][dB], \tag{5.26}$$

$$f_L(L) = \frac{2\log(10)}{bR^2} 10^{\frac{2(L-a)}{b}}. \tag{5.27}$$

After the statistics for the pathloss are obtained, the PDF of the transmitted power is derived. From Eq. (5.23), it is obtained the inverse relationship of the pathloss as a function of the transmitted power for a MIMO user, $P^n_{m\_\text{mimo}}$.

$$L(P^n_{m\_\text{mimo}}) = -10\log_{10}\left(\frac{\gamma^n_{m\_\text{mimo\_diversity}}\eta}{M_t M_r P^n_{m\_\text{mimo}}}\right), \tag{5.28}$$

Thus, the PDF of the transmitted power for a MIMO user can be obtained as follows:

$$f_{P^n_{m\_\text{mimo}}}(P^n_{m\_\text{mimo}}) = \left|\frac{dL}{dP^n_{m\_\text{mimo}}}\right| f_L(L(P^n_{m\_\text{mimo}})) \;\; P^n_{m\_\text{mimo}} \in \left[0, \frac{\gamma^n_{m\_\text{mimo\_diversity}}\eta}{M_t M_r 10^{-\left(\frac{a+b\log_{10}(R)}{10}\right)}}\right], \tag{5.29}$$

$$f_{P^n_{m\_\text{mimo}}}(P^n_{m\_\text{mimo}}) = \frac{20}{bR^2 P^n_{m\_\text{mimo}}} 10^{\frac{-2}{b}\left(10\log_{10}\left(\frac{\gamma^n_{m\_\text{mimo\_diversity}}\eta}{M_t M_r P^n_{m\_\text{mimo}}}\right)+a\right)}. \tag{5.30}$$

From Eq. (4.14), it can be seen that the circuit consumed power, P^n_{circ}, depends of the transmitted power when converted to [dBm]. Thus, the inverse relationship of the transmitted power, $P^n_{m\_\text{mimo}}$, in function of the transmitted power in [dBm], $P^n_{m\_\text{mimo\_dBm}}$, for a MIMO user case is given by:

$$P^n_{m\_\text{mimo}}(P^n_{m\_\text{mimo\_dBm}}) = 1e^{-3} \times 10^{\frac{P^n_{m\_\text{mimo\_dBm}}}{10}}, \tag{5.31}$$

Thereby, the PDF of the transmitted power in [dBm], $P^n_{m\_\text{mimo\_dBm}}$ is:

$$\begin{aligned} f_{P^n_{m\_\text{mimo\_dBm}}} &= \left|\frac{dP^n_{m\_\text{mimo}}}{dP^n_{m\_\text{mimo\_dBm}}}\right| f_{P^n_{m\_\text{mimo}}}(P^n_{m\_\text{mimo}}(P^n_{m\_\text{mimo\_dBm}})) \\ P^n_{m\_\text{mimo\_dBm}} &\in [-\infty, 10\log_{10}\left(\frac{1e^3 \times \gamma^n_{m\_\text{mimo\_diversity}}\eta}{M_t M_r 10^{-(a+b\log_{10}(R))}}\right)], \end{aligned} \tag{5.32}$$

$$f_{P^n_{m\_\text{mimo\_dBm}}} = \frac{2\log(10)}{bR^2} 10^{\frac{-2}{b}\left(10\log_{10}\left(\frac{1e^3 \times \gamma^n_{m\_\text{mimo\_diversity}}\eta}{M_t M_r 10^{\frac{P^n_{m\_\text{mimo\_dBm}}}{10}}}\right)+a\right)} \tag{5.33}$$

Moreover, It can be observed that the input of P_{circ} in Eq. (4.12) is the transmitted power for each antenna in [dBm]. Thereby, by using the assumption that the total transmitted power for a MIMO user, $P^n_{m\_\text{mimo}}$, is divided evenly between each antenna as was proposed for this derivation. The PDF of the transmitted power per antenna in [dBm], $P^{n}_{m}*$, is given by:

$$\begin{aligned} P^{n}_{m}* &= \frac{2\log(10)}{bR^2}10^{\frac{-2}{b}\left(10\log_{10}\left(\frac{1e^3\times\gamma^n_{m\_\text{mimo\_diversity}}\eta}{M_t^2M_r10^{\frac{P^{n}_{m}*}{10}}}\right)+a\right)} \\ P^{n}_{m}* &\in \left[-\infty, 10\log_{10}\left(\frac{1e^3\times\gamma^n_{m\_\text{mimo\_diversity}}\eta}{M_t^2M_r10^{-(a+b\log_{10}(R))}}\right)\right], \end{aligned} \tag{5.34}$$

Finally, the inverse relationship of the transmitted power per antenna in [dBm] is derived as a function of the circuit consumed power in the uplink by combining Eqs. (4.12) and (4.14) as follows:

$$P^{n}_{m}*(P_{m\_\text{mimo\_diversity}}) = \begin{cases} \frac{\varpi+A-2}{0.005} & 14 \geq P^{n}_{m}*, \\ \frac{4\varpi+(A-\frac{3P_{BB}}{4})-1.2}{0.117} & 17 \geq P^{n}_{m}* > 14, \\ \frac{2\varpi+(A-P_{BB})-1.2}{0.117}, & 20 \geq P^{n}_{m}* > 17, \\ \frac{\varpi+A-1.2}{0.117} & 24 \geq P^{n}_{m}* > 20. \end{cases} \tag{5.35}$$

where $\varpi = \frac{P^n_{m\_\text{mimo\_diversity}}}{M_t}$. Hence, by using the transformation of random variables, the PDF of the circuit consumed power in the uplink for a MIMO user is shown below:

$$f_{P^n_{m\_\text{mimo\_diversity}}} = \begin{cases} \frac{363\log(10)}{bR^2M_t}10^{\frac{-2}{b}\left(10\log_{10}\left(\frac{1e^3\times\gamma^n_{m\_\text{mimo\_diversity}}\eta}{M_t^2M_r10^{\frac{\varpi+A-2}{0.05}}}\right)+a\right)} & \\ P^n_{m\_\text{mimo\_diversity}} \in [0, M_t(2+0.005Z1-A)], & \\ \frac{68\log(10)}{bR^2M_t}10^{\frac{-2}{b}\left(10\log_{10}\left(\frac{1e^3\times\gamma^n_{m\_\text{mimo\_diversity}}\eta}{M_t^2M_r10^{\frac{4\varpi+A-0.75P_{BB}-1.2}{1.17}}}\right)+a\right)} & \\ P^n_{m\_\text{mimo\_diversity}} \in [M_t(2+0.005Z1-A), M_t(\frac{1.2+0.117Z1-Z2}{4})], & \end{cases} \tag{5.36}$$

$$f_{P^n_{m\_\text{mimo\_diversity}}} = \begin{cases} \frac{34\log(10)}{bR^2M_t} 10^{\frac{-2}{b}\left(10\log_{10}\left(\frac{1e^3\times\gamma^n_{m\_\text{mimo\_diversity}}\eta}{M_t^2M_r 10^{\frac{2\varpi+A-P_{BB}-1.2}{1.17}}}\right)+a\right)} \\ \\ P^n_{m\_\text{mimo\_diversity}} \in [M_t(\frac{1.2+0.117Z1-Z2}{4}), M_t(\frac{1.2+0.117Z1-Z3}{2})], \\ \\ \frac{17\log(10)}{bR^2M_t} 10^{\frac{-2}{b}\left(10\log_{10}\left(\frac{1e^3\times\gamma^n_{m\_\text{mimo\_diversity}}\eta}{M_t^2M_r 10^{\frac{\varpi+A-1.2}{1.17}}}\right)+a\right)} \\ \\ P^n_{m\_\text{mimo\_diversity}} \in [M_t(\frac{1.2+0.117Z1-Z3}{2}), M_t(1.2+0.117Z1-A)]. \end{cases}$$

where $Z1 = 10\log_{10}\left(\frac{1e^3\times\gamma^n_{m\_\text{mimo\_diversity}}\eta}{M_t^2M_r 10^{-(a+b\log_{10}(R))}}\right)$, $Z2 = A - (0.75 \times P_{BB})$ and $Z3 = A - P_{BB}$.

Finally, by integrating the PDFs of the transmitted and circuit consumed power over its respective ranges, the cumulative distribution functions (CDFs) for transmitted and overall consumed power are obtained, which are shown in Figure 5.4(a) and 5.4(b) respectively. In addition, the empirical CDFs are also obtained to compare them with the theoretical derivations. Moreover, as an example, we consider SIMO and MIMO users with three and six antennas. Furthermore, the users are required to achieve the same target SNR $\gamma_{\text{target}} = 17\ dB$, whether SIMO or MIMO mode is used, in order to make fair comparisons in terms of power expenditure. It should be noticed that for obtaining the statistics of the overall consumed power for the SIMO case, a similar procedure is followed as the one shown for the MIMO user. For the required values to evaluate the statistics and perform the simulations, the values shown in Table 5.2 are considered. These results are discussed further in Subsection 5.6.3 below.

5.6.2 Spatial Multiplexing Approach

For the following derivations, Shannon's capacity formula is used. Thus, Eq. (5.15) can be re-written as follows:

$$T^n_{m\_\text{capacity}} = \sum_{i=1}^{\omega} \log_2(1+\gamma^n_{i\_SC}) = \sum_{i=1}^{\omega} \log_2(1+\frac{Pr^n_m\zeta_i\sigma_i}{M_t\eta}), \tag{5.37}$$

Moreover, if equal gain conditions between the multiple parallel SISO channels are assumed: $\zeta_i = 1$, $\mathbf{E}\{\|\mathbf{H}\|_F^2\} = M_rM_t = \omega\sigma_i$ [2], Equation (5.37) may be re-written in the following

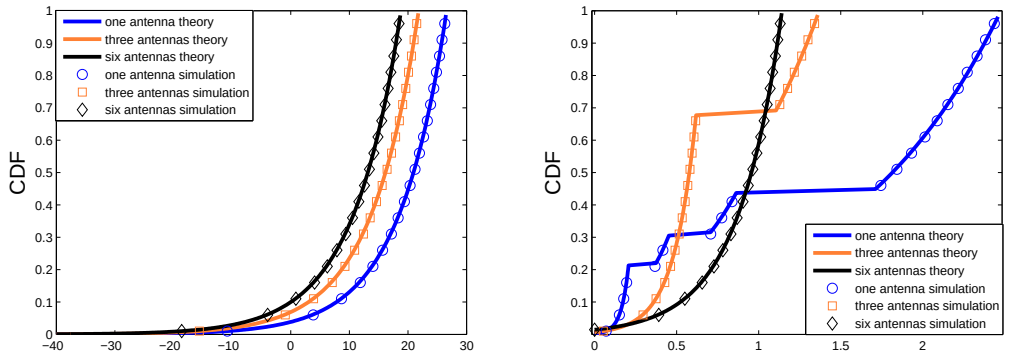

(a) Transmitted Power (dBm)

(b) Overall Consumed Power (W)

Figure 5.4: *User performance differences, when enhancing diversity and optimizing transmitted 5.4(a) and overall consumed power 5.4(b) respectively*

way:

$$T^n_{m\_\text{capacity}} = \sum_{i=1}^{\omega} \log_2(1+\gamma^n_{i\_pipe}) = \omega \log_2(1+\frac{Pr^n_m M_r}{\omega\eta}), \tag{5.38}$$

Thus, by combining Eq. (5.21) and Eq. (5.38), the required transmitted power is obtained as:

$$P^n_m = \frac{\beta}{M_r 10^{\frac{-L(d_m)}{10}}}, \tag{5.39}$$

where $\beta = \left(2^{\frac{T^n_{m\_\text{capacity}}}{\omega}} - 1\right)\omega\eta$. To obtain the statistics of the transmitted power P^n_m, it is assumed that the MSs are uniformly distributed over the cell. Moreover, from Eq. (5.39) the inverse relationship of the pathloss in function of the transmitted power is obtained.

$$L(P^n_m) = -10\log_{10}\left(\frac{\beta}{M_r P^n_m}\right), \tag{5.40}$$

Thus, by using a similar approach as the one used in Eq. (5.29), the PDF of the transmitted power may be obtained.

$$f_{P^n_m} = \frac{20}{R^2 b P^n_m} 10^{\frac{-2}{b}\left(a+10\log_{10}\left(\frac{\beta}{M_r P^n_m}\right)\right)} \quad P^n_m \in \left[0, \frac{\beta}{M_r 10^{-(\frac{a+b\log_{10}(R)}{10})}}\right], \tag{5.41}$$

Furthermore, the transmitted power in [dBm] is required. Thus, the inverse relationship of the transmitted power, P^n_m, in function of the transmitted power in [dBm], $P^n_{m\_\text{dBm}}$, is given by:

$$P^n_m(P^n_{m\_\text{dBm}}) = 1e^{-3} 10^{\frac{P^n_{m\_\text{dBm}}}{10}}, \tag{5.42}$$

Thereby, by using a similar approach as the used in Eq. (5.32), the PDF of the transmitted power in [dBm] is derived as follows.

$$f_{P^n_{m\_\mathrm{dBm}}} = \frac{20\log(10)1^{-3}}{R^2 b} 10^{\frac{-2}{b}\left(a+10\log_{10}\left(\frac{\beta}{1e^{-3}M_r 10^{\frac{P^n_{m\_\mathrm{dBm}}}{10}}}\right)\right)} \quad P^n_{m\_\mathrm{dBm}} \in \left[-\infty, 10\log_{10}\left(\frac{1e^3\times\beta}{M_r 10^{-(\frac{a+b\log_{10}(R)}{10})}}\right)\right], \tag{5.43}$$

As in the diversity case, it should be observed that in order to compute the circuit consumed power P^n_{circ}, Eq(4.14). The transmitted power per each antenna is required. Thus, by using the assumption that the transmitted power is divided evenly over all the antennas. The PDF of the transmitted power per antenna in [dBm] is:

$$f_{P^{n*}_m} = \frac{20\log(10)}{R^2 b} 10^{\frac{-2}{b}\left(a+10\log_{10}\left(\frac{\beta}{M_r M_t 1e^{-3} 10^{\frac{P^{n*}_m}{10}}}\right)\right)} P^{n*}_m \in \left[-\infty, 10\log_{10}\left(\frac{1e^3\times\beta}{M_t M_r 10^{-(\frac{a+b\log_{10}(R)}{10})}}\right)\right], \tag{5.44}$$

Finally, the inverse relationship of the transmitted power per antenna in [dBm] is derived as a function of the circuit consumed power in the uplink by combining Eqs. (5.13) and (4.14) as shown:

$$P^{n*}_m(P^n_{m\_\mathrm{mimo\_capacity}}) = \begin{cases} \frac{\psi+A-2}{0.005} & 14 \geq P^{n*}_m, \\ \frac{4\psi+(A-\frac{3P_{BB}}{4})-1.2}{0.117} & 17 \geq P^{n*}_m > 14, \\ \frac{2\psi+(A-P_{BB})-1.2}{0.117}, & 20 \geq P^{n*}_m > 17, \\ \frac{\psi+A-1.2}{0.117} & 24 \geq P^{n*}_m > 20. \end{cases} \tag{5.45}$$

where $\psi = \frac{P^n_{m\_\mathrm{mimo\_capacity}}}{M_t}$. Hence, by using the transformation of random variables, the PDF of the circuit consumed power is shown below:

$$f_{P^n_{m\_\mathrm{mimo\_capacity}}} = \begin{cases} \frac{363\log(10)}{bR^2M_t} 10^{\frac{-2}{b}\left(10\log_{10}\left(\frac{1^3\beta}{M_t M_r 10^{\frac{\psi+A-2}{0.05}}}\right)+a\right)} \\ P^n_{m\_\mathrm{mimo\_capacity}} \in [0, M_t(2+0.005Z1-A)], \\ \frac{68\log(10)}{bR^2M_t} 10^{\frac{-2}{b}\left(10\log_{10}\left(\frac{1^3\beta}{M_t M_r 10^{\frac{4\psi+A-0.75P_{BB}-1.2}{1.17}}}\right)+a\right)} \\ P^n_{m\_\mathrm{mimo\_capacity}} \in [M_t(2+0.005Z1-A), M_t(\frac{1.2-0.117Z1-Z2}{4})], \end{cases} \tag{5.46}$$

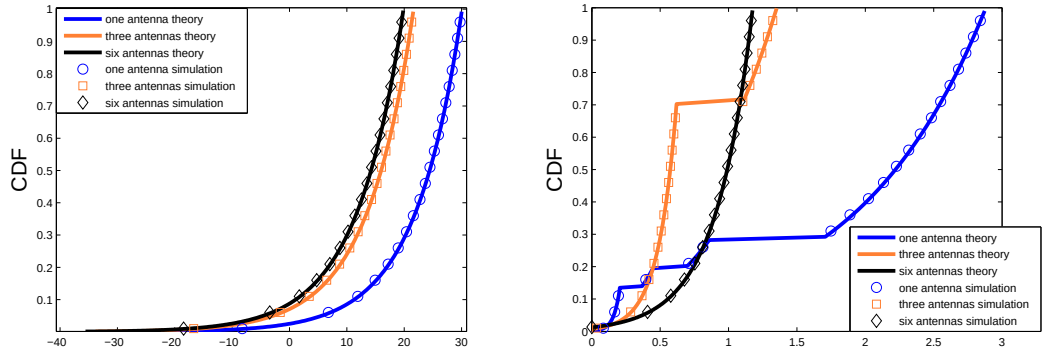

(a) Transmitted Power (dBm)

(b) Overall Consumed Power (W)

Figure 5.5: *User performance differences, when implementing spatial multiplexing and optimizing transmitted power 5.5(a) and overall consumed power 5.5(b) respectively*

$$f_{P^n_{m\_\text{mimo\_capacity}}} = \begin{cases} \frac{34\log(10)}{bR^2M_t} 10^{\frac{-2}{b}\left(10\log_{10}\left(\frac{1^3\beta}{M_tM_r 10^{\frac{2\psi+A-P_{BB}-1.2}{1.17}}}\right)+a\right)} \\ P^n_{m\_\text{mimo\_capacity}} \in [M_t(\frac{1.2-0.117Z1-Z2}{4}), M_t(\frac{1.2+0.117Z1-Z3}{2})], \\ \frac{17\log(10)}{bR^2M_t} 10^{\frac{-2}{b}\left(10\log_{10}\left(\frac{1^3\beta}{M_tM_r 10^{\frac{\psi+A-1.2}{1.17}}}\right)+a\right)} \\ P^n_{m\_\text{mimo\_capacity}} \in (M_t(\frac{1.2+0.117Z1-Z3}{2}), M_t(1.2+0.117Z1-A)]. \end{cases}$$

where $Z1 = 10\log_{10}\left(\frac{1^3\beta}{M_rM_t 10^{-(\frac{a+b\log_{10}(R)}{10})}}\right)$, $Z2 = A - (0.75 \times P_{BB})$ and $Z3 = A - P_{BB}$.

Finally as in the diversity case, by integrating the PDFs of the transmitted and circuit consumed power over its respective ranges, the cumulative distribution functions (CDFs) for transmitted and circuit consumed power are obtained, which are shown in Figure 5.5(a) and 5.5(b) respectively. In addition, the empirical CFDs are also found to compare them with the theoretical derivations. As an example, SIMO and MIMO users carrying three and six antennas are considered. Furthermore, the users independently of SIMO or MIMO try to achieve the same transmission rate $T_{\text{target}} = 910$ kbps, in order to make fair comparisons in terms of power expenditure. To evaluate the statistics and perform the simulations, the values shown in Table 5.2

are considered.

5.6.3 Analysis

From Figures. 5.4(a) and 5.5(a), it is easy to see that increasing the number of antennas provides power savings at all percentiles of the CDF when only transmitted power is optimized. However, this trend does not remain the same when optimizing overall power consumption. In Figure 5.4(b) in the case of diversity, it can be seen that the SIMO curve intersects the MIMO curves when transmitting with three and six antennas at the 30^{th} and 45^{th} percentile respectively. Moreover, for the capacity case in Figure 5.5(b), it can be observed that the SIMO curve intersects the MIMO curves when transmitting with three and six antennas at the 20^{th} and 28^{th} percentile respectively. This intersection point represents than in the diversity case SIMO is more power efficient for 30% and 45% of the users in the cell when compared to MIMO when transmitting with three and six antennas respectively. The same relation holds for the spatial multiplexing case. This is because the MSs are able to experience better transmission conditions, when they are close to the BS. Thus, turning on the RF transmitter and the BB module of the relay stations is less power efficient than transmitting with only one antenna. Nevertheless, as the users get close to the cell edge increasing the number of transmit antennas tends to be an energy efficient solution when overall power consumption is optimized. This fact can be seen from Figures. 5.4(b) and 5.5(b), since as the number of antennas increases, it allows the three and six antennas curves to converge faster to the tail of the distribution. The presented analysis in this section will be useful to understand the performance of the proposed framework in Section 5.8.

5.7 Comparison Schemes and Simulation Scenario

To evaluate the performance of the proposed method four distributed relay selection algorithms, which allow MSs and RSs to cooperate to form MIMO coalitions with the purpose of reducing the energy consumption in the uplink, are described. In addition, a baseline scheme is presented where all MSs transmit on their own in SIMO mode. Finally, a centralized global optimum approach which is coordinated from the BS and based on an exhaustive search is presented. For all the described methods, the communication between the MSs and RSs is made through the cooperative link. Thus, the subset of RSs willing to cooperate with the m-th MS is limited

by the range of the cooperative link, which naturally limits the complexity of the relay selection.

5.7.1 Minimum Relaying Hop (MRH) Path Loss Selection scheme

In [99], the authors propose a relay selection method as a function of path loss. Hence, the best RS for coalition formation is the one with the least path loss to the MS, this method always chooses the RS with the most energy efficient cooperative link.

$$RS_c = \text{argmin}\{d_{mr}^{\kappa}\} \tag{5.47}$$

From (5.47), it should be noticed that for performing the RS selection it is just required to know the channel statistics of the cooperative link.

5.7.2 Best Worst (BW) Channel Selection scheme

The BW method considers the quality of the cooperative link and the uplink of each RS. This is because both links have a direct influence on the total consumed energy for forming the virtual MIMO link. In [99], the best worst channel is used in which the relay whose worse channel is the best is selected:

$$\text{argmin}\{\|G_r, \frac{1}{d_{mr}^{\kappa}}\|\}, \tag{5.48}$$

where $G_r = \|\mathbf{h}_r^n\|_F^2 10^{\frac{-L(d_r)+X_\sigma}{10}}$ represents the channel path gain between the r-th RS and the BS, and d_r defines the distance between the r-th Rs and the BS.

5.7.3 Stable Marriage (SMI) scheme

In Chapter 4, a distributed RS selection algorithm is presented which is based on the stable marriage process. This method, as in the BW channel selection scheme, requires the channel statistics from the RSs for both the uplink and cooperative link plus the channel statistics of the MSs in the uplink. Thereby, each MS and RS is able to rank its respective candidates for coalition formation. It should be noticed that the SMI method has the same limitation as MRH and BW methods in that each MS is only able to select one RS.

5.7.4 SIMO transmission

A baseline scheme is presented, where all the MSs in the network transmit in SIMO mode.

5.7.5 College Admissions Framework (CAF) scheme

This method implements, the RS selection method described previously in Section 5.5.

5.7.6 Centralized optimum scheme

A centralized global optimum scheme, based on an exhaustive search approach, is presented. Thus, the BS collects the required channel statistics from RSs and MSs in order to form optimal coalitions. This centralized approach is implemented with the aim of finding the *price of anarchy* for the proposed scheme. The price of anarchy is computed as the difference in performance between a centralized and a distributed approach [100].

5.7.7 Simulation scenario

Monte Carlo simulations are performed using the parameters presented in Table 5.2. This is done to compare the performance of the proposed method with the schemes presented above. The simulation is comprised of a single cell with the MSs and RSs distributed uniformly over the cell area. The cell is served by a multi-antenna BS. Moreover, the system is noise limited, hence each coalition transmits in an independent RB to avoid co-channel interference. For the case when diversity is enhanced, it is assumed that all the *users* (SIMO or MIMO), independent of their distance to the BS try to achieve the same target SNR. In the case when spatial multiplexing is used, it is assumed that all the users in the network aim to achieve the same data rate.

5.8 Results

From the simulations the cumulative distribution functions (CDFs) and the graphs, that illustrate the performance in terms of *overall power expenditure* for the schemes presented in Section 5.7, are generated.

When diversity is enhanced in Figure 5.6, it is shown the overall consumed power at different distances from the BS, where all the users in the cell aim to achieve the same target SNR. It can be observed that the distributed and centralized approaches exhibit a similar performance when compared to the baseline method at close distances from the BS (up to 75 m). This is because as mentioned in the analysis presented in Section 5.6.1, MSs experience good transmission conditions close to the cell center. Thus, turning on the BB and RF module of the RSs

Parameter	Value
MSs per macro-cell, M	20
RSs per macro-cell, R	95
Number of antennas at the receiver, M_r	6
Cell radius	150m
Number of available RBs, N	20
Number of cells, D	1
Subcarriers per RB, k_{sc}	12
Symbol rate per subcarrier, ϱ_s	15ksps
P_{Tx}	31.8dBm
P_{con}	23.8dBm
P_{BB}	11.7dBm
Maximum user transmit power	24dBm
Shadowing, Std. Dev., σ	3dB
γ_{target},	17dB
T_{target}	910 kbps
ε for 17dB SNR	4.5 $\frac{\text{bits}}{\text{symbol}}$
κ	3.5
Pathloss constant, a	15.3
Pathloss constant, b	37.6

Table 5.2: *Simulation parameters.*

becomes less power efficient than transmitting with only one antenna. Conversely, when channel conditions are no longer so beneficial (e.g., after 75 m), it can be seen that as the MSs move away from the BS, the increase from one to a higher number of transmit antennas allows the MS to obtain potential energy savings. Furthermore, from the analysis shown in Section 5.6.1 and the results presented Figure 5.6, it can confirmed that, when overall power consumption is optimized and spatial diversity is enhanced, by increasing the number of antennas the obtained power savings are more visible at the cell edge than at the cell center. In Figure 5.7, the system energy efficiency, given by Equation (5.17), is evaluated. Notice that at the 50^{th} percentile the CAF scheme is more energy efficient compared to the benchmark, the MRH pathloss, the BW channel, and the SMI framework with improvements of 58%, 15%, 10% and 5% respectively. Nevertheless, the CAF scheme has losses of 10% compared to the centralized global optimum scheme. These losses are tolerable in practice due to the significant reductions in complexity for the CAF method compared to the centralized optimum scheme: this is discussed further at the end of this section. Moreover, the better performance in energy efficiency terms for the CAF and centralized optimum method when compared to the other distributed approaches can be easily understood as a direct consequence of the bigger number of antenna elements than can be involved in the coalition.

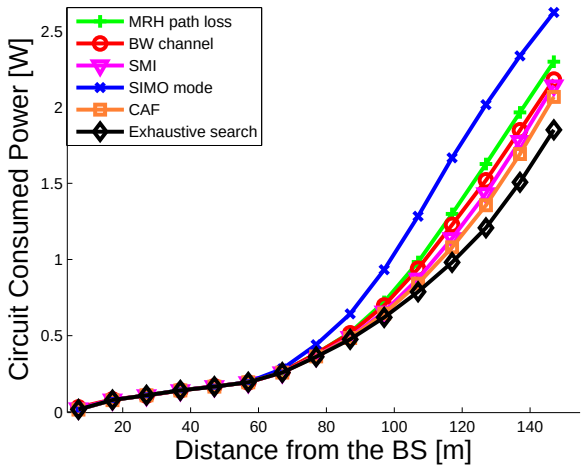

Figure 5.6: *User overall consumed power against distance from the BS for a SNR=17 dB*

When spatial multiplexing is used, the aim is to obtain gains in energy efficiency by dividing

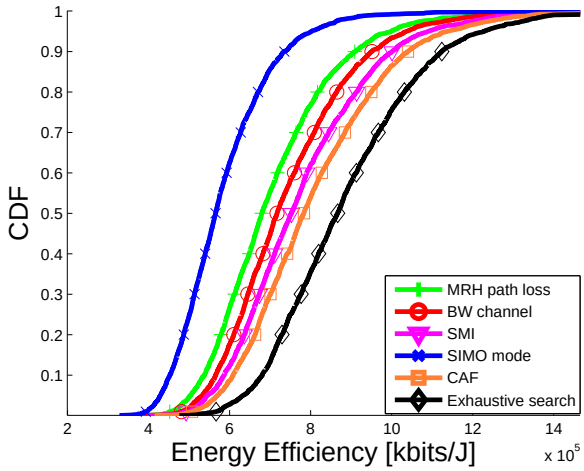

Figure 5.7: *System CDF energy efficiency.*

the total data rate requirements between the elements forming the virtual MIMO link. Thereby, as in the diversity case it can be observed from Figure 5.8 that the most of the power savings due to coalition formation are observed at the cell border. This is because, it is more power efficient to deliver high transmission rates for SIMO users when close to the BS than when close to the cell edge due to the improved propagation conditions. Thus, using a lower modulation order for transmitting from each antenna in a coalition when close to the cell edge becomes more power efficient that using a single transmitter. Hence, from the results shown in Section 5.6.2 and Figure 5.8, it can be understood than increasing the number of transmit antennas to split the total rate requirement among the transmitters to implement spatial multiplexing is more power

efficient in terms of overall power consumption at the cell border than at the cell center.

Finally, in Figure 5.9 it is shown the performance in terms of energy efficiency for the ap-

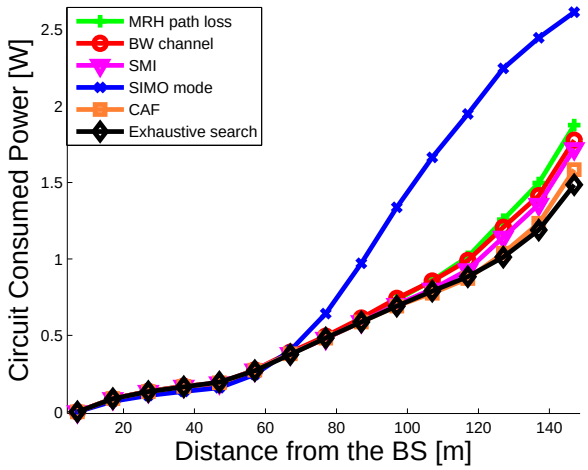

Figure 5.8: *User overall consumed power against distance from the BS for a bit rate of 910 kbps.*

proaches presented in Section 5.7 when spatial multiplexing is implemented. It is observed that the centralized global optimum is 2% more energy efficient when contrasted to the CAF. Moreover, when comparing the CAF with the other distributed approaches it can be seen that the CAF method has improvements of 14%, 9%, 5%, and 91% over MRH pathloss, BW channel, SMI and the baseline SIMO mode respectively. Thereby, it can be confirmed that increasing the number of antennas in order to use a lower modulation order results in an energy efficient solution for the network.

To conclude the comparison, the complexity of the centralized global optimum approach is compared with the proposed CAF method. On one hand, for the CAF method each MS in the system has to evaluate each RS in its preferred subset of suitable candidates, S_m, by using Eqs. (4.28) or (5.18) depending on whether diversity or capacity are enhanced. Furthermore, each RS evaluates its preferred subset S_r of RSs by using Eqs. (4.29) or (5.20). Big $\mathcal{O}$ notation is used to describe the growth rate of both schemes. Thus, arithmetic operations with a complexity of $\mathcal{O}(|S_m|^2)$ and $\mathcal{O}(|S_r|^2)$ are performed by the system when candidate MSs or RS are ranked respectively, where $|.|$ defines the cardinality of the subset. If we assume that $R \gg M$, the complexity of the candidate ranking process is bounded by the number of RSs in the system rather than by the number of MSs. Thereby, this will allow us to upper bound the complexity of the candidate ranking by $\mathcal{O}(|S_m|^2)$ operations. Moreover, forming the MS's preference list, L_m, (5.19) requires a sorting operation which induces a complexity of $\mathcal{O}(|S_m|\log(|S_m|))$ oper-

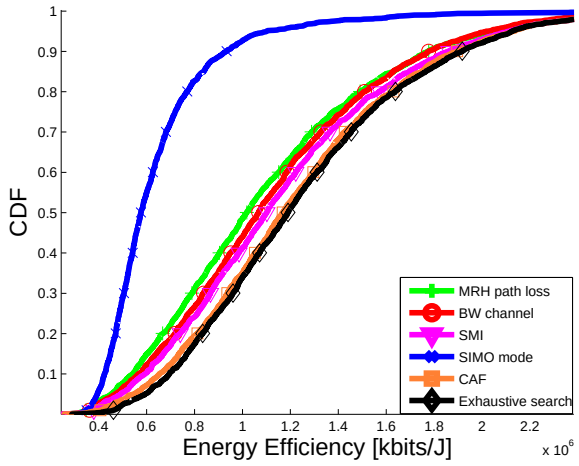

Figure 5.9: *System energy efficiency when enhancing capacity.*

ations. Finally, the complexity of the decision making Algorithm (2) can be upper bounded by a binary search operation which requires a complexity of $\mathcal{O}(\log(|S_m|))$ operations. Therefore, the dominant factor which determines the CAF scheme complexity will be the one with the largest exponent, thus the complexity of the method will be upper bounded by order $\mathcal{O}(|S_m|^2)$ operations.

On the other hand, the centralized global optimum scheme is based on enumerating all possible alternatives for virtual MIMO coalition formation between the m-th MS and its preferred subset of candidate RSs, S_m. This is done with the purpose of finding the optimal number of transmit antennas that would minimize the overall power consumption in the uplink. Therefore, to guarantee that a given feasible solution is optimal, the solution should be compared with any other feasible solutions. In general, an exhaustive search approach, when the number of elements is discrete, is considered $\mathcal{NP}$-complete [35]. A notable characteristic of $\mathcal{NP}$-complete problems is that the required time to solve the problem increases very quickly as the size of the problem grows [35]. To implement the exhaustive search scheme, each MS in the system will evaluate the total number of possible combinations in its preferred subset of candidate RSs, S_n. Hence, the total number of possible combinations is computed by $\sum_{k=1}^{|S_m|} \binom{|S_m|}{k}$, where $\binom{|S_m|}{k} = \frac{|S_m|!}{k!(|S_m|-k)!}$. Moreover, each combination is evaluated by Eqs. (4.13) or (5.14) depending if diversity or capacity are enhanced respectively. Thus, it induces a complexity of $\mathcal{O}\left(\left(\sum_{k=1}^{|S_m|} \binom{|S_m|}{k}\right)^2\right)$ for the system. In addition the complexity of both presented methods (exhaustive search and CAF) increases linearly with the number of MSs in the system, M. Hence, the exhaustive search method has a complexity of $\mathcal{O}\left(M \times \left(\sum_{k=1}^{|S_m|} \binom{|S_m|}{k}\right)^2\right)$ which is a higher

order complexity when compared to the complexity of $\mathcal{O}(M \times |S_m|^2)$ for the CAF scheme. Furthermore, Figure 5.10 shows how the complexity of the system changes for both methods as the number of RSs increases in the system. It can be easily seen that as the number of RSs increases, the computational complexity of the exhaustive search increases exponentially, therefore it may not be a suitable solution for being implemented in real time systems.

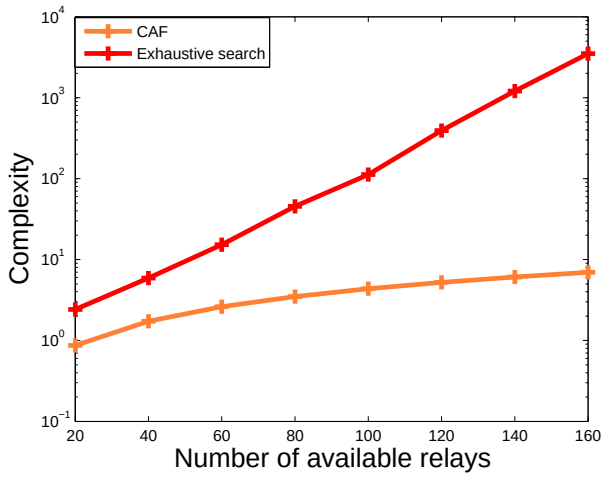

Figure 5.10: *Complexity of the centralized optimum approach compared to the CAF method.*

5.9 Summary

In this chapter, a low complexity virtual MIMO coalition formation algorithm is considered, which is based on game theory. The proposed framework allows MSs to select the most suitable RSs which provides the most power savings in the network. Thereby, energy efficient coalition formation is studied by using the concepts of diversity and spatial multiplexing respectively. It is shown analytically and by simulation that increasing the number of transmit antennas is a more energy efficient solution for users close to the cell edge rather than for cell center users, when overall terminal power consumption is optimized. Furthermore, by performance comparisons we have proven than the proposed coalition formation algorithm is more energy efficient compared to the benchmark, the MRH pathloss, the BW channel, and the SMI framework with improvements of 58%, 15%, 10% and 5% for the spatial diversity case. When implementing spatial multiplexing the CAF method has improvements of 14%, 9%, 5%, and 91% over MRH, BW, SMI, and the baseline SIMO mode. It experiences only small performance losses of 10% and 2% when compared to an exhaustive search approach when implementing diversity or spatial multiplexing respectively. In addition, a complexity analysis is presented, which shows that

the complexity of the proposed method increases linearly as the number of RSs grows in the network. This is a much lower order complexity when compared to the exponential growth of the exhaustive search scheme. Thus, the proposed game theory framework achieves a similar performance compared to a centralized scheme with a much lower order of complexity. Hence, it may be a suitable energy efficient solution for practical applications.

Chapter 6
Conclusions and Future work

This thesis has contributed to the design of low complexity resource allocation methods with emphasis on energy efficiency. In this chapter, Section 6.1 will emphasize the key contributions of the thesis. Moreover, in Section 6.2 some limitations of the work and suggestions for future work will be given.

6.1 Conclusions

This thesis models the radio resource allocation in wireless networks through the use of game theory. Radio resource management techniques such as: interference mitigation, resource block allocation and virtual MIMO coalition formation are studied with the aim of reducing the power consumption in the uplink. The key contributions of this work are summarized as follows.

6.1.1 Interference protection

The traditional uplink power control challenge is reevaluated and investigated from the view point of interference mitigation rather than power minimization. A low complexity distributed resource allocation scheme for reducing the uplink co-channel interference (CCI) is proposed. The presented approach forces users with good propagation conditions to reduce transmission power, in order to protect users experiencing high levels of interference. Thus, the MSs' uplink throughputs are equalized under the max-min fairness optimization criterion. This distributed scheme obtains a similar performance in terms of fairness and energy efficiency when compared to a centralized signal interference noise ratio balancing scheme. In addition, system level simulations suggests that schemes that consider a fair distribution of the system resources achieve a higher performance in terms of energy efficiency that those that aim to maximize the system's capacity. Finally, it is shown by a mathematical analysis and performance simulations that improvements in energy efficiency are directly related with improvements in fairness at the system level. Thus, an increase in the fairness index produces an increase in the system energy efficiency metric for the network.

6.1.2 Resource block allocation

A distributed resource allocation framework which reduces the power expenditure during low network load periods is proposed. Extra resource blocks (RBs) are allocated to mobile users in the reverse link. Thereby, the users rate demands are split among its allocated RBs in order to transmit in each of them by using a simpler modulation scheme. The resource block allocation is modeled by a game theory framework derived from the concept of stable marriage with incomplete lists (SMI). Hence, each RB and mobile user in the system are considered as an independent entity which takes an active role in the decision making process. The proposed solution optimizes the circuit consumed power rather than the transmitter power. Moreover, it is shown that the distributed approach achieves a similar performance in terms of bits per Joule when compared to a centralized method which is coordinated at the base station side. In addition, mathematical analysis and system level simulations suggest that when circuit power consumption is optimized and mobile users experiences favorable transmission conditions in the reverse link, the energy efficiency is optimized by transmitting in one RB rather than in multiple RBs.

6.1.3 Virtual MIMO coalition formation

A coalition formation framework for distributed virtual Multiple-input Multiple-output (MIMO) is proposed. Cooperation between single antennas devices such as mobile and relays stations is modeled by a game theoretic approach derived from the concept of the college and admissions framework. Thus, single antenna devices interact in a distributed way to form virtual MIMO coalitions to implement spatial diversity or spatial multiplexing respectively with the aim of reducing the power expenditure in the reverse link. The presented solution optimizes the circuit consumed power rather than the transmitter power. The low complexity solution achieves a similar performance in bits per Joule when compared to an exhaustive search scheme. Moreover, the proposed scheme presents a linear growth in complexity as the number of single antenna devices increases which is much less than the exponential growth of the exhaustive search approach. Additionally, mathematical analysis and system performance simulations suggest that forming a virtual MIMO link to implement spatial diversity or spatial multiplexing in the reverse link is only beneficial at the cell border in terms of energy efficiency. Thus, relay stations should be deployed mostly at the cell edge rather than at the cell center to obtain energy savings.

6.2 Future work

This thesis has identified promising schemes for radio resource allocation in green wireless networks. However, the proposed schemes have some limitations due to the initial modeling assumptions. Thus, there are several research directions that can be extended. Some suggestions are listed below:

- In Chapter 3, an interference mitigation framework is proposed which obtains energy savings by equalizing the uplink user throughputs under the max-min fairness optimization criterion. However, the system is assumed to be Single-input Single-output (SISO) system rather than a multi-antenna one. Thus, to model the multi-antenna case the non-cooperative game at the user level might be modified to consider the interference generated by the mutiple antenna case. Moreover, an analysis of the convergence and uniqueness of the Nash equilibrium should be provided for this scenario. The theoretical analysis at the system level which proves that improvements in energy efficiency are directly related with improvements in fairness may lead to a similar insight for the multi-antenna case. Since, the assumption of reducing the transmitted power for users at the cell center to reduce interference for users at the cell border will also hold in the multi-antenna scenario.

- The system model considered in Chapter 5 is a noise limited system. Thus, future research may tackle the problem of virtual MIMO formation in an interference limited scenario. Moreover, the college admission framework imposes certain restrictions in the coalition formation process, for example a relay station (RS) cannot form a coalition with more than one mobile in the system. This is an important issue since in some practical scenarios RSs may be able to serve many MSs in order to use more efficiently the current network infrastructure. Moreover, it is assumed that the RSs that cooperate with the mobiles are close enough to experience the same channel statistics such as pathloss and shadowing. A more realistic scenario may assume that shadowing is not correlated between the single antenna devices. Thereby, an uncorrelated shadowing scenario may have a significant impact in the design of the coalition formation framework.

- In Chapters 4 and 5, the resource allocation process is modeled trough the use of game theory frameworks such as the stable marriage with incomplete lists and the college and admission framework. Both schemes may be a suitable solution to model scenarios beyond the scope of resource allocation. For example, they may be used to model coalition

formation in smart grids. Thus, the use of both frameworks beyond the resource allocation domain is an open field in research that should be studied deeply.

Appendix A
Existence and uniqueness of the equilibrium for the user level framework

At the *equilibrium*, all the users should be satisfied with the utilities that they obtain from the NCG, if so the *equilibrium* point is called *Nash Equilibrium* [45, 66, 67].

Definition 1: A power vector $\mathbf{p}^n = (P_1^n \dots P_D^n)$ is a *Nash equilibrium* of the NCG, $G = [D, \{P\}, \{U_m^n(\cdot)\}]$ if, for every $m \in D$, $U_m^n(P_m^n, \mathbf{p}_{-m}^n, \mu_m^n) \geq U_m^n(P_m'^n, \mathbf{p}_{-m}^n, \mu_m^n)$ for all $P_m^n \in P$.

Theorem 1: A *Nash equilibrium* exists in the game $G = [D, \{P\}, \{U_m^n(\cdot)\}]$ if, for all $m = 1, \dots, D$:

1) P is a nonempty, convex, and compact subset of some Euclidean space $\Re^n$

2) $U_m^n(P_m^n, \mathbf{p}_{-m}^n, \mu_m^n)$ is continuous in P and quasi-concave [106], in P_m^n.

For the first part of *Theorem 1*, we have already stated in Section 3.5, that P is a compact convex set. For the second part using (3.1) and (3.10), it is easy to show that U_m^n is twice differentiable over P_m^n and the second derivative is always negative for any value of P_m^n. Therefore, the second order conditions for concavity are fulfilled [106]. Hence, the inner solution if it exists, is the unique point maximizing the cost function and it is defined by (A.1). The boundary solution $P_m^n = 0$, is the other possible maximization point for the optimization problem. If the user utility function $U_m^n(P_m^n, \mathbf{p}_{-m}^n, \mu_m^n)$ reaches a value less than zero, the optimal solution will be the boundary point.

$$P_m^{n\cdot} = \frac{1}{\mu_m^n \log(2)} - \frac{I_m^n + \eta}{\nu G_{md}^n}. \tag{A.1}$$

Theorem 2: The NCG has a unique equilibrium.

This proof follows a similar procedure as the one proposed previosuly in [66, 107].

For notational convenience, let us denote a user specific parameter α_m^n, which is defined as follows:

$$\alpha_m^n = \frac{G_{md}^n \nu}{\mu_m^n \log(2)} - \eta. \tag{A.2}$$

Hence, the optimal response $B_m^n(\mathbf{p}_{-m}^n)$ of the m-th user in the n-th RB is defined as:

$$B_m^n(\mathbf{p}_{-m}^n) = \begin{cases} \frac{1}{\nu G_{md}^n}\left[\alpha_m^n - I_m^n\right], & \alpha_m^n \geq I_m^n \\ 0, & \text{otherwise.} \end{cases} \tag{A.3}$$

The solution for the maximization problem will be the best response of the m-th user to the other users strategies, which are denoted by $\mathbf{p}_{-m}^n$.

Definition 2: The best response $B_m^n(\mathbf{p}_{-m}^n)$ of the m-th player to the profile strategies $\mathbf{p}_{-m}^n$ is the strategy P_m^n such that

$$B_m^n(\mathbf{p}_{-m}^n) = \left\{P_m^n \in P : \operatorname{argmax} U_m^n(P_m^n, \mathbf{p}_{-m}^n, \mu_m^n)\right\}. \tag{A.4}$$

A *Nash equilibrium* for the NCG can be stated as the power vector $\mathbf{p}^n$ which fulfills: $P_m^n \in B_m^n(\mathbf{p}_{-m}^n)$. When conditions of *Theorem 1* are satisfied, the correspondence $B_m^n(\cdot)$ is nonempty, convex-valued, and upper semi-continuous for all m. Thus, there exists a vector $\mathbf{p}^n$ such that $P_m^n \in B_m^n(\mathbf{p}_{-m}^n)$ for all $m \in D$ [67]. This vector is by definition the *Nash equilibrium*. From (A.3), the set of linear fixed point equations which converges to the equilibrium solution, if it exists, can be written in matrix form as:

$$\begin{aligned} \begin{bmatrix} 1 & \frac{G_{21}^n}{\nu G_{11}^n} & \frac{G_{31}^n}{\nu G_{11}^n} & \cdots \frac{G_{D1}^n}{\nu G_{11}^n} \\ \frac{G_{12}^n}{\nu G_{22}^n} & 1 & \frac{G_{32}^n}{\nu G_{22}^n} & \cdots \frac{G_{D2}^n}{\nu G_{22}^n} \\ \vdots & \vdots & \vdots & \ddots \vdots \\ \frac{G_{1D}^n}{\nu G_{DD}^n} & \frac{G_{2D}^n}{\nu G_{DD}^n} & \frac{G_{3D}^n}{\nu G_{DD}^n} & \ldots 1 \end{bmatrix} \begin{bmatrix} P_1^n \\ P_2^n \\ \vdots \\ P_D^n \end{bmatrix} &= \begin{bmatrix} \frac{\alpha_1^n}{\nu G_{11}^n} \\ \frac{\alpha_2^n}{\nu G_{22}^n} \\ \vdots \\ \frac{\alpha_D^n}{\nu G_{DD}^n} \end{bmatrix}, \\ \mathbf{A}^n \mathbf{p}^n &= \mathbf{w}^n. \end{aligned} \tag{A.5}$$

For *Theorem 2*, we need to show that the $D \times D$ matrix $\mathbf{A}^n$ is non-singular. This means that the system has a unique solution given by $\mathbf{p}^n = (\mathbf{A}^n)^{-1}\mathbf{w}^n$. Therefore if $(\mathbf{A}^n)^{-1}$ exists, it is equivalent to prove that $\mathbf{A}^n\mathbf{x} = 0 \rightarrow \mathbf{x} = 0$. Hence, there should not exist a non zero vector $\mathbf{x}= (x_1, x_2, \ldots, x_D)^T \neq 0, \mathbf{x} \in P$ such that $\mathbf{A}^n\mathbf{x} = 0$. This condition can be written as follows:

$$G_{dd}^n x_d(\nu - 1) + \sum_{j=1}^{D} H_{jd}^n x_j = 0, \ d \in D, \tag{A.6}$$

Summing up this set of equations for the D users in the n-th RB, we have:

$$(\nu - 1)\sum_{d=1}^{D} H_{dd}^n x_d + \sum_{d=1}^{D}\sum_{j=1}^{D} H_{jd}^n x_j = 0. \tag{A.7}$$

In Equation (A.7), the channels path gains (3.7) and ν as we have stated before are greater than 0. Thus, the only value that can fulfill the conditions for the equality in (A.7) is the vector $\mathbf{x}$. If $\mathbf{x} = 0$, we are at the boundary solution of our problem, which means that no mobile will be active. For any other case $\mathbf{A}^{-1}$ exists, provided that the rows of $\mathbf{A}$ are linearly independent. Hence, the matrix $\mathbf{A}$ is non-singular and the system has a unique solution given by $\mathbf{p}$.

Appendix B
Increase in energy efficiency and fairness in the system based on power reductions applied to users with good propagation condition

To show the improvements in energy efficiency, Shannon's capacity formula will be used for ease of analysis and without loss of generality. In the following demonstration, it is considered that all the mobiles transmit in the n-th RB, hence the index n will be removed from the following derivations. Thus, the energy efficiency metric, equation (3.4), can be re-written in the following way:

$$\beta_m = \frac{\log_2(1+\nu\gamma_m)}{P_m} \left[\frac{\text{bits}}{\text{J}}\right]. \tag{B.1}$$

It will be shown that the user energy efficiency metric $\beta_{P_{HSE}}$ for users with high spectral efficiency (HSE), transmitting at power P_{HSE}, can be improved if the transmission strategy is changed to $P_{HSE} - \Delta P_{HSE}$, which we have defined as P^*_{HSE} in our derivations, where $P_{HSE} - \Delta P_{HSE} \leq P_{HSE}$. Since, a substantial reduction in transmitted power ΔP_{HSE} for HSE users will bring as consequence a slightly reduction in HSE users' capacity, due to the fact that the degradation of cell center users' capacity is logarithmic. Hence, the condition presented in equation (B.2) should be met.

$$\beta_{P^*_{HSE}} \geq \beta_{P_{HSE}} \quad \text{or} \quad \frac{\beta_{P^*_{HSE}}}{\beta_{P_{HSE}}} \geq 1. \tag{B.2}$$

where $\beta_{P^*_{HSE}}$ is the user energy efficiency metric after the change of power strategy for HSE users from P_{HSE} to P^*_{HSE}. Thus, by substituting equation (B.1) in (B.2), the following expression is obtained:

$$\frac{P_{HSE}\log_2(1+\frac{\nu P^*_{HSE}G_{md}}{I_m+\eta})}{P^*_{HSE}\log_2(1+\frac{\nu P_{HSE}G_{md}}{I_m+\eta})} \geq 1. \tag{B.3}$$

Define the variables $K = \frac{\nu P_{HSE} G_{md}}{I_m + \eta}$ and $R = \frac{P^*_{HSE}}{P_{HSE}}$. After introducing the new variables, the above equation may be re-written in the following way:

$$\frac{\log_2(1+KR)}{R\log_2(1+K)} \geq 1, \tag{B.4}$$

$$\log_2(1+KR) \geq R\log_2(1+K), \tag{B.5}$$

By using logarithm identities the equation above is written as follows:

$$\log_2(1+KR) \geq \log_2(1+K)^R. \tag{B.6}$$

By removing the logarithm, the following expression is obtained:

$$(1+KR) \geq (1+K)^R,\ 0 < R \leq 1,\ K \geq 0. \tag{B.7}$$

The Bernoulli inequality can be used to prove the inequality above, which states

$$(1+x\alpha) \geq (1+x)^\alpha,\ 0 < \alpha \leq 1,\ x \geq -1. \tag{B.8}$$

Furthermore, if we replace: K by x and R by α in (B.8), the Bernoulli inequality (B.8) is exactly (B.7). Thus, by proving (B.7), it has been shown that (B.2) is indeed true. Moreover, we have shown that due to the logarithmic degradation of the high spectral efficiency (HSE) users' capacity, a reduction in transmission power leads to an increase in energy efficiency for these users. Additionally, after the power for HSE users is reduced, this will reduce the CCI for users with low spectral efficiency (LSE), so their energy efficiency metric $\beta_{P_{LSE}}$ will be increased without changing their power strategies P_{LSE}. Therefore, the total system energy efficiency is improved after the change in power strategies for HSE users:

$$\beta^{system}_{P^*_{HSE}} \geq \beta^{system}_{P_{HSE}}, \tag{B.9}$$

where $\beta^{system}_{P^*_{HSE}}$ denotes the system energy efficiency after the HSE users change their power level from P_{HSE} to P^*_{HSE} and $\beta^{system}_{P_{HSE}}$ is the system energy efficiency before the change in power level.

Additionally, in order to show the improvements in system fairness, we use the Jain's fairness index, equation (3.6), and the uplink throughput, equation (3.3). Thus, if the HSE users power strategy P_{HSE} is changed to P^*_{HSE}, the system fairness should be increased. For simplicity, we will consider a two user case. Furthermore, if the total system fairness is improved, the

following condition must hold:

$$\Gamma(T_{P^*_{HSE}}, T_{P^*_{LSE}}) - \Gamma(T_{P_{HSE}}, T_{P_{LSE}}) \geq 0, \tag{B.10}$$

where $T_{P^*_{HSE}}, T_{P^*_{LSE}}$ stands for the MS's throughput for HSE and LSE users respectively after the change of the power strategy from P_{HSE} to P^*_{HSE}, and $T_{P_{HSE}}, T_{P_{LSE}}$ stands for the user's throughput before the change of power strategy. Thus after combining (3.6) and (B.10) the following equation is obtained:

$$\frac{(T_{P^*_{HSE}} + T_{P^*_{LSE}})^2}{{T_{P^*_{HSE}}}^2 + {T_{P^*_{LSE}}}^2} - \frac{(T_{P_{HSE}} + T_{P_{LSE}})^2}{{T_{P_{HSE}}}^2 + {T_{P_{LSE}}}^2} \geq 0. \tag{B.11}$$

After some algebraic manipulations, equation (B.11) can be re-written as follows:

$$\begin{aligned}({T_{P_{HSE}}}^2 + {T_{P_{LSE}}}^2) \times (T_{P^*_{HSE}} \times T_{P^*_{LSE}}) \geq \\ ({T_{P^*_{HSE}}}^2 + {T_{P^*_{LSE}}}^2) \times (T_{P_{HSE}} \times T_{P_{LSE}})\end{aligned} \tag{B.12}$$

Definition 3: The function $T_m(\gamma_m)$ is monotonically increasing and strictly concave in γ_m, and γ_m is a function of the transmitted power of the m-th user. A change in the power transmission strategy for HSE users from P_{HSE} to P^*_{HSE} will produce a reduction in throughput $\Delta T_{P_{HSE}}$, if the power strategies of the remaining users are unchanged. Furthermore, this reduction on power will indirectly reduce the interference levels for the remaining LSE users, so their throughput measurements will be increased by $\Delta T_{P_{LSE}}$. Hence, equation (B.12) can be re-written in the following way:

$$\begin{aligned}({T_{P_{HSE}}}^2 + {T_{P_{LSE}}}^2) \times ((T_{P_{HSE}} - \Delta T_{P_{HSE}}) \times (T_{P_{LSE}} \\ +\Delta T_{P_{LSE}})) \geq ((T_{P_{HSE}} - \Delta T_{P_{HSE}})^2 \\ +(T_{P_{LSE}} + \Delta T_{P_{LSE}})^2) \times (T_{P_{HSE}} \times T_{P_{LSE}})\end{aligned} \tag{B.13}$$

After some algebraic manipulations, we obtain the following expression.

$$\begin{aligned}(T_{P_{HSE}} \times \Delta T_{P_{LSE}} + T_{P_{LSE}} \times \Delta T_{P_{HSE}}) \times ({T_{P_{HSE}}}^2 \\ -{T_{P_{LSE}}}^2) \geq 0\end{aligned} \tag{B.14}$$

As we can observe from the left hand side of equation (B.14), the first part of the term will be always positive, the second part is only negative if $T_{P_{HSE}} \leq T_{P_{LSE}}$, which is not practically possible. Thus equation (B.10) is indeed true, so we conclude the proof of *Theorem 1*.

Definition 4: If the power weighting factor μ_m^n for HSE users is increased, this will consequently increase their cost for transmitting at high power, thus their transmission power will be reduced. Therefore, improvements in energy efficiency and fairness in the system will be obtained, if the power levels of the remaining users are unchanged.

Therefore, if we change the pricing factor μ_m^n according to *Theorem 1* and *Definition 4*, the users' uplink throughput will be distributed in a *fairer* way in the n-th RB. Moreover, the Jain's fairness index (3.6) measures the *equality* of throughput allocation for each user. Thus, as the equality increases, fairness increases as well [85]. This suggests that a similar way to use (B.10) for a case where more than two users are considered in the n-th RB will lead the proof to a similar insight.

Appendix C
Publication List

Journal

1. Rodrigo Vaca, John Thompson, Eitan Altman, and Víctor Ramos; "A Distributed Virtual MIMO Coalition Formation Framework for Energy Efficient Wireless Network;"Submitted to *IEEE Transactions on Communications.*

2. Rodrigo Vaca, John Thompson, and Víctor Ramos; " Non-cooperative Uplink Interference Protection Framework for Fair and Energy Efficient Orthogonal Frequency Division Multiple Access Networks;" *IET Communications Journal* , vol.7, no.18, pp.2015-2025, December 2013.

Conference

1. Rodrigo Vaca, John Thompson, Eitan Altman, and Víctor Ramos;" A Game Theory Framework for a Distributed and Energy Efficient Bandwidth Expansion Process;" To appear in the Proceedings of the *2014 IEEE INFOCOM Workshop on Green Cognitive Communications and Computing Networks*, May, 2014.

2. Rodrigo Vaca, Eitan Altman, John Thompson and Víctor Ramos, " A Stable Marriage Framework for Distributed Virtual MIMO Coalition Formation;" Proceedings of the *24th Annual IEEE International Symposium on Personal Indoor and Mobile Radio Communications (PIMRC)*, vol., no., pp.2722-2727, September, 2013.

3. Rodrigo Vaca, John Thompson and Víctor Ramos; "Uplink Interference Protection as a Non-cooperative Game over OFDMA Networks;" Proceedings of the *72th IEEE Vehicular Technology Conference (VTC)*, vol., no., pp.1-5, September 2012.

Bibliography

[1] J. Jang, "Virtual-mimo systems with compress-and-forward cooperation," *University of Edinburgh PhD Thesis*, p. 157, Nov 2011.

[2] A. Paulraj, R. Nabar, and D. Gore, *Introduction to space-time wireless communications*, C. U. Press, Ed. Cambridge University Press, Jul. 2003.

[3] W. Saad, Z. Han, M. Debbah, A. Hjorungnes, and T. Basar, "Coalitional game theory for communication networks," *Signal Processing Magazine, IEEE*, vol. 26, no. 5, pp. 77–97, 2009.

[4] H. Burchardt, Z. Bharucha, G. Auer, and H. Haas, "Uplink interference protection and scheduling for energy efficient OFDMA networks," *EURASIP Journal on Wireless Communications and Networks*, vol. 2012, no. 180, p. 19, 2012.

[5] T. Cover and J. Thomas, *Elements of Information Theory*, Wiley, Ed. Wiley-Interscience, Aug. 1991.

[6] C. Han and S. Armour, "Energy efficient radio resource management strategies for green radio," *IET Communications*, vol. 5, no. 18, pp. 2629–2639, Dec 2011.

[7] R. Vaca, J. Thompson, and V. Ramos, "Non-cooperative uplink interference protection framework for fair and energy efficient Orthogonal Frequency Division Multiple Access networks," *IET Communications*, vol. 7, no. 18, pp. 2015–2025, 2013.

[8] X. Cong, G. Li, L. Yalin, C. Yan, and X. Shugong, "Energy-efficient design for downlink ofdma with delay-sensitive traffic," *IEEE Transactions on Wireless Communications*, vol. 12, no. 6, pp. 3085–3095, June 2013.

[9] X. Cong, G. Li, Z. Shunqing, C. Yan, and X. Shugong, "Energy-efficient resource allocation in ofdma networks," *IEEE Transactions on Communications*, vol. 60, no. 12, pp. 3767–3778, December 2012.

[10] R. Kwan and C. Leung, "A survey of scheduling and interference mitigation in LTE," *Journal of Electrical Computer Engineering*, vol. 2010, no. 273486, p. 10, 2010.

[11] J. Zander, "Performance of optimum transmitter power control in cellular radio systems," *IEEE Transactions on Vehicular Technology*, vol. 41, no. 1, pp. 57–62, 1992.

[12] M. Shaat and F. Bader, "Efficient resource allocation algorithm for uplink in multicarrier-based cognitive radio networks with fairness consideration," *IET Communications*, vol. 5, no. 16, pp. 2328 –2338, 2011.

[13] S. Videv, J. S. Thompson, H. Haas, and P. M. Grant, "Resource allocation for energy efficient cellular systems," *EURASIP Journal on Wireless Communications and Networking*, no. 2012:181, 2012.

[14] E. Jorswieck, H. Boche, and S. Naik, "Energy-aware utility regions: Multiple access pareto boundary," *IEEE Transactions on Wireless Communications*, vol. 9, no. 12, pp. 2216–2226, Jul. 2010.

[15] F. Meshkati, H. V. Poor, and S. C. Schwartz, "Energy-efficient resource allocation in wireless networks," *IEEE Signal Processing Magazine*, vol. 24, no. 3, pp. 58–68, May 2007.

[16] G. Miao, N. Himayat, Y. Li, and D. Bormann, "Energy efficient design in wireless OFDMA," *IEEE International Conference on Communications, 2008. ICC '08*, pp. 3307 –3312, May 2008.

[17] D. Wu, L. Zhou, and Y. Cai, "Energy-efficient resource allocation for uplink orthogonal frequency division multiple access systems using correlated equilibrium," *IET Communications*, vol. 6, no. 6, pp. 659 –667, 2012.

[18] D. W. Kwan, E. S. Lo, and R. Schober, "Energy-efficient resource allocation in multi-cell OFDMA systems with limited backhaul capacity," *IEEE Transactions on Wireless Communications*, vol. 11, no. 10, pp. 3618–3631, 2012.

[19] ——, "Energy-efficient resource allocation in OFDMA systems with large numbers of base station antennas," *IEEE Transactions on Wireless Communications*, vol. 11, no. 9, pp. 3292–3304, 2012.

[20] S. Videv and H. Haas, "Energy-efficient scheduling and bandwidth-energy efficiency trade-off with low load," in *IEEE International Conference on Communications (ICC)*, 2011, pp. 1–5.

[21] B. Badic, T. O'Farrrell, P. Loskot, and J. He, "Energy efficient radio access architectures for green radio: Large versus small cell size deployment," in *Vehicular Technology Conference Fall (VTC 2009-Fall), 2009 IEEE 70th*, Sept 2009, pp. 1–5.

[22] X. Chen, H. Zhang, T. Chen, and M. Lasanen, "Improving energy efficiency in green femtocell networks: A hierarchical reinforcement learning framework," in *2013 IEEE International Conference on Communications (ICC),*, June 2013, pp. 2241–2245.

[23] R. Krishna, Z. Xiong, and S. Lambotharan, "A cooperative mmse relay strategy for wireless sensor networks," *IEEE Signal Processing Letters*, vol. 15, pp. 549–552, 2008.

[24] R. Krishna, K. Cumanan, X. Zhilan, and S. Lambotharan, "A novel cooperative relaying strategy for wireless networks with signal quantization," *IEEE Transactions on Vehicular Technology*, vol. 59, no. 1, pp. 485–489, Jan 2010.

[25] J. Jiang, M. Dianati, M. Imran, and Y. Chen, "Energy efficiency and optimal power allocation in virtual-MIMO systems," in *Proceedings of the IEEE 76th Vehicular Technology Conference*, Sep. 2012, pp. 1–6.

[26] S. Cui, A. Goldsmith, and A. Bahai, "Energy efficiency of MIMO and Cooperative MIMO Techniques in Sensor Networks," *IEEE Journal on Selected Areas in Communications*, vol. 10, no. 10, p. 35, 2004.

[27] S. Hussain, A. Azim, and J. Park, "Energy efficient virtual MIMO communication for wireless sensor networks," *Telecommunication Systems*, vol. 42, no. 1-2, pp. 139–149, 2009.

[28] W. Saad, Z. Han, and M. Debbah, "A distributed coalition formation framework for fair user cooperation in wireless networks," *IEEE Transactions on Wireless Communications*, vol. 8, no. 9, pp. 4580–4593, Sep. 2009.

[29] Z. Han, D. Niyato, T. Başar, and A. Hjørungnes, *Game Theory in Wireless and Communication Networks*. Cambridge University Press, Oct. 2012.

[30] R. Vaca, J. Thompson, E. Altman, and V. Ramos, "A game theory framework for a distributed and energy efficient bandwidth expansion process," in *Proceedings of the INFOCOM Workshop on Green Cognitive Communications and Computing Networks*, May 2014.

[31] R. Vaca, E. Altman, J. Thompson, and V. Ramos, "A stable marriage framework for distributed virtual MIMO coalition formation," in *Proceedings of the 24th Annual IEEE International Symposium on Personal Indoor and Mobile Radio Communications (PIMRC),*, Sep. 2013, pp. 2722–2727.

[32] R. Vaca, J. Thompson, E. Altman, and V. Ramos, "A distributed virtual mimo coalition formation framework for energy efficient wireless networks," *Submitted to IEEE Transaction on Communications*, 2014.

[33] C. Cox, *An introduction to LTE, LTE-advanced, SAE and 4G mobile communications*, 1st ed., C. Wiley, Ed. Wiley, Chichester, 2012.

[34] S. Sesia, I. Toufik, and M. Bake, *LTE-The UMTS Long Term Evolution From Theory to Practice*, 1st ed., C. Wiley, Ed. Wiley, Chichester, 2009.

[35] Z. Han and K. J. R. Liu, *Resource Allocation for Wireless Networks*, C. U. Press, Ed. Cambridge University Press, Jul. 2008.

[36] R. Wang, "Energy-efficient lte transmission techniques–introducing green radio from resource allocation perspective," *University of Edinburgh PhD Thesis*, p. 126, March 2011.

[37] K. Gilhousen, I. Jacobs, R. Padovani, A. Viterbi, L. Weaver, and C. Wheatley, "On the capacity of a cellular cdma system," *IEEE Transactions on Vehicular Technology*, vol. 40, no. 2, pp. 303–312, May 1991.

[38] M. Guowang, N. Himayat, G. Y. Li, and S. Talwar, "Low-complexity energy-efficient scheduling for uplink ofdma," *IEEE Transactions on Communications*, vol. 60, no. 1, pp. 112–120, January 2012.

[39] A. Fu, E. Modiano, and J. Tsitsiklis, "Optimal energy allocation for delay-contrained data transmission over a time-varying channel," in *Twenty-Second Annual Joint conference of the IEEE Computer and Communications, INFOCOM 2003*, vol. 2, March 2003, pp. 1095–1105 vol. 2.

[40] R. Madan and S. Ray, "Uplink resource allocation for frequency selective channels and fractional power control in lte," in *2011 IEEE International Conference on Communications (ICC)*, June 2011, pp. 1–5.

[41] A. Simonsson and A. Furuskar, "Uplink power control in lte - overview and performance, subtitle: Principles and benefits of utilizing rather than compensating for sinr variations," in *IEEE 68th Vehicular Technology Conference VTC 2008-Fall*, Sept 2008, pp. 1–5.

[42] M. Elmusrati, R. Jantti, and H. Koivo, "Multiobjective distributed power control algorithm for cdma wireless communication systems," *IEEE Transactions on Vehicular Technology*, vol. 56, no. 2, pp. 779–788, March 2007.

[43] F. Cao and Z. Fan, "Downlink power control for femtocell networks," in *IEEE 77th Vehicular Technology Conference (VTC Spring)*, June 2013, pp. 1–5.

[44] M. Kubisch, H. Karl, A. Wolisz, Z. L, and J. Rabaey, "Distributed algorithms for transmission power control in wireless sensor networks," in *WCNC 2003 IEEE Wireless Communications and Networking Conference*, vol. 1, March 2003, pp. 558–563 vol.1.

[45] R. Vaca, J. Thompson, and V. Ramos, "Uplink interference protection as a non-cooperative game over OFDMA networks," *In the Proceedings of the IEEE 76th Vehicular Technology Conference*, Sep. 2012.

[46] R. Mullner, C. Ball, K. Ivanov, J. Lienhart, and P. Hric, "Contrasting open-loop and closed-loop power control performance in utran lte uplink by ue trace analysis," in *The IEEE International Conference on Communications*, June 2009, pp. 1–6.

[47] F. Rashid-Farrokhi, K. Liu, and L. Tassiulas, "Downlink power control and base station assignment," *IEEE Communications Letters*, vol. 1, no. 4, pp. 102–104, July 1997.

[48] V. Douros and G. Polyzos, "Review of some fundamental approaches for power control in wireless networks," *Elsevier Computer Communications*, vol. 34, no. 13, pp. 1580–1592, 2011.

[49] A. Rao, "Reverse link power control for managing inter-cell interference in orthogonal multiple access systems," in *IEEE 66th Vehicular Technology Conference, VTC 2007.*, Sept 2007, pp. 1837–1841.

[50] T. Cover and A. Gamal, "Capacity theorems for the relay channel," *IEEE Transactions on Information Theory*, vol. 25, no. 5, pp. 572–584, Sep 1979.

[51] C. Tao, K. Haesik, and Y. Yang, "Energy efficiency metrics for green wireless communications," in *International Conference on Wireless Communications and Signal Processing (WCSP)*, Oct 2010, pp. 1–6.

[52] L. Zhao, G. Zhao, and T. O'Farrell, "Efficiency metrics for wireless communications," in *IEEE 24th International Symposium on Personal Indoor and Mobile Radio Communications (PIMRC)*, Sept 2013, pp. 2825–2829.

[53] C. Han, T. Harrold, S. Armour, I. Krikidis, S. Videv, P. M. Grant, H. Haas, J. Thompson, I. Ku, C.-X. Wang, T. A. Le, M. Nakhai, J. Zhang, and L. Hanzo, "Green radio: radio techniques to enable energy-efficient wireless networks," *IEEE Communications Magazine*, vol. 49, no. 6, pp. 46–54, 2011.

[54] Q. Li, G. Li, W. Lee, M. il Lee, D. Mazzarese, B. Clerckx, and Z. Li, "MIMO techniques in WiMAX and LTE: a feature overview," *IEEE Communications Magazine*, vol. 48, no. 5, pp. 86–92, 2010.

[55] S. Alamouti, "A simple transmit diversity technique for wireless communications," *IEEE Journal on Selected Areas in Communications*, vol. 16, no. 8, pp. 1451–1458, Oct 1998.

[56] F. Pantisano, M. Bennis, W. Saad, R. Verdone, and M. Latva-aho, "Coalition formation games for femtocell interference management: A recursive core approach," in *Wireless Communications and Networking Conference (WCNC), 2011 IEEE*, 2011, pp. 1161–1166.

[57] A. Ibrahim, A. Sadek, W. Su, and K. Liu, "Cooperative communications with relay-selection: when to cooperate and whom to cooperate with?" *IEEE Transactions on Wireless Communications*, vol. 7, no. 7, pp. 2814–2827, 2008.

[58] E. Larsson and E. Jorswieck, "Competition versus cooperation on the MISO interference channel," *Selected Areas in Communications, IEEE Journal on*, vol. 26, no. 7, pp. 1059–1069, 2008.

[59] K. Yazdi, E. Gammal, and P. Schitner, "On the desing of cooperative transmission schemes," in *Allerton Conference on Communications, Control and Computing*, 2003.

[60] Z. Zhu, J. Tang, S. Lambotharan, W. Chin, and Z. Fan, "An integer linear programming and game theory based optimization for demand-side management in smart grid," in *2011 IEEE GLOBECOM Workshops*, Dec 2011, pp. 1205–1210.

[61] Z. He, S. Yuelong, P. Lihui, and Y. Danya, "A review of game theory applications in transportation analysis," in *International Conference on Computer and Information Application (ICCIA)*, Dec 2010, pp. 152–157.

[62] A. Rouskas, A. Kikilis, and S. Ratsiatos, "Admission control and pricing in competitive wireless networks based on non-cooperative game theory," in *IEEE Wireless Communications and Networking Conference*, vol. 1, April 2006, pp. 205–210.

[63] C. Man-Hon and V. Wong, "Interference pricing for sinr-based random access game," *IEEE Transactions on Wireless Communications*, vol. 12, no. 5, pp. 2292–2301, May 2013.

[64] M. Kibria and A. Jamalipour, "Game theoretic outage compensation in next generation mobile networks," *IEEE Transactions on Wireless Communications*, vol. 8, no. 5, pp. 2602–2608, May 2009.

[65] J. Nash, "Equilibrium points in n-person games," *Proc. in the National Academy of Sciences of the United States of America*, vol. 36, no. 1, pp. 48–49, May 1950.

[66] T. Alpcan, T. Basar, R. Srikant, and E. Altman, "CDMA uplink power control as a noncooperative game," in *Proc. 40th IEEE Conf. on Decision and Control*, Dec. 2001, pp. 197–202.

[67] C. Saraydar *et al.*, "Efficient power control via pricing in wireless data networks," *IEEE Trans. Commun.*, vol. 50, no. 2, pp. 291–303, Feb. 2002.

[68] E. Larsson and E. Jorswieck, "Competition versus cooperation on the miso interference channel," *IEEE Journal on Selected Areas in Communications*, vol. 26, no. 7, pp. 1059–1069, September 2008.

[69] A. Garcia-Saavedra, P. Serrano, A. Banchs, and M. Hollick, "Balancing energy efficiency and throughput fairness in IEEE 802.11 WLANs," *Pervasive and Mobile Computing*, vol. 8, no. 5, pp. 631 – 645, 2012.

[70] J. Thompson and C. Khirallah, "Overview of green radio research outcomes," in *2012 1st IEEE International Conference on Communications in China Workshops (ICCC)*, Aug 2012, pp. 69–73.

[71] IDATE, "Green telecom-calling for a Better Future," *News 453*, May. 2009.

[72] Z. Hasan, H. Boostanimehr, and V. Bhargava, "Green cellular networks: A survey, some research issues and challenges," *IEEE Communications Surveys and Tutorials*, vol. 13, no. 4, pp. 524–540, april 2011.

[73] R. Wang, J. Thompson, H. Haas, and P. Grant, "Sleep mode design for green base stations," *IET Communications*, vol. 5, no. 18, pp. 2606 –2616, 2011.

[74] Vision 2020, "Enabling the Digital Future," *Mobile VCE Vision Group*, 2007.

[75] C. Lima, M. Bennis, K. Ghaboosi, and M. Latva-aho, "Interference management for self-organized femtocells towards green networks," in *2010 IEEE 21st International Symposium on Personal Indoor and Mobile Radio Communications Workshops (PIMRC Workshops)*, Sept 2010, pp. 352–356.

[76] Y. Xinmin, W. Tong, H. Jing, and W. Ying, "A non-cooperative game approach for distributed power allocation in multi-cell OFDMA-relay networks," in *VTC Spring 2008 IEEE Vehicular Technology Conference*, May 2008, pp. 1920–1924.

[77] A. Anandkumar, S. Lambotharan, and J. Chambers, "A game-theoretic approach to transmitter covariance matrix design for broadband mimo gaussian interference channels," in *SSP '09. IEEE/SP 15th Workshop on Statistical Signal Processing, 2009*, Aug 2009, pp. 301–304.

[78] V. Shah, N. B. Mandayam, and D. J. Goodman, "Power control for wireless data based on utility and pricing," in *The Ninth IEEE International Symposium on Personal Indoor and Mobile Radio Communications*, 1998, pp. 1427–1432.

[79] S. Gunturi and F. Paganini, "Game theoretic approach to power control in cellular CDMA," *IEEE 58th Vehicular Technology Conference, VTC 2003-Fall*, pp. 2362–2366, oct. 2003.

[80] Z. Han and R. Liu, "Non-cooperative power-control game and throughput game over wireless networks," *IEEE Transactions on Communications*, vol. 53, no. 10, pp. 1625–1629, 2005.

[81] D. Goodman and N. Mandayam, "Power control for wireless data," *IEEE Personal Communications*, vol. 7, no. 2, pp. 48–54, Apr. 2000.

[82] A. Zapone, G. Alfano, S. Buzzi, and M. Meo, "Energy-efficient non-cooperative resource allocation in multi-cell OFDMA systems with multiple base station antennas," in *Proceedings of the 2011 IEEE Online Conference on Green Communications,*, 2011, pp. 82–87.

[83] F. Nan, M. Siun-Chuon, and N. Mandayam, "Pricing and power control for joint network-centric and user-centric radio resource management," *IEEE Transactions on Communications*, vol. 52, no. 9, pp. 1547–1557, Sept 2004.

[84] S. Sesia, I. Toufik, and M. Bake, *LTE-The UMTS Long Term Evolution From Theory to Practice*, 1st ed., C. Wiley, Ed. Wiley, Chichester, 2009.

[85] R. Jain, D.-M. Chiu, and W. Hawe, "A quantitative measure of fairness and discrimination for resource allocation in shared computer systems," *CoRR*, vol. cs.NI/9809099, 1998.

[86] 3GPP, "Simulation Assumptions and Parameters for FDD HeNB RF Requirements," 3GPP TSG RAN WG4 R4-092042, July 2008. [Online]. Available: http://www.3gpp.org/ftp/Specs/

[87] WINNER, "Final Report on Link Level and System Level Channel Models," D5.4 V1.4 IST-2003-507581 WINNER, Nov 2005. [Online]. Available: http://www.ist-winner.org/DeliverableDocuments/D5.4.pdf

[88] Q. Jing and Z. Zheng, "Distribute resource allocation based on game theory in multicell OFDMA systems," *International Journal of Wireless Information Networks*, vol. 16, pp. 44–50, 2009.

[89] S. Koskie and Z. Gajic, "A Nash game algorithm for SIR-Based power control in 3G wireless CDMA networks," *IEEE/ACM Transactions on Networking*, vol. 13, no. 5, pp. 1017–1026, 2005.

[90] Y. Chen, S. Zhang, and S. X. and, "Fundamental trade-offs on green wireless networks," *IEEE Communications Magazine*, vol. 49, no. 6, pp. 30–37, June 2011.

[91] M. Butt, B. Schubert, M. Kurras, K. Borner, T. Haustein, and L. Thiele, "On the energy-bandwidth trade-off in green wireless networks: System level results," in *1st IEEE International Conference on Communications in China Workshops (ICCC)*, Aug 2012, pp. 91–95.

[92] S. Sohaib and D. So, "Energy allocation for green multiple relay cooperative communication," *EURASIP Journal on Wireless Communications and Networks*, vol. 2012, no. 291, p. 11, 2012.

[93] S. Jayaweera, "Energy efficient virtual MIMO-based cooperative communications for wireless sensor networks," in *Proceedings of 2005 International Conference on Intelligent Sensing and Information Processing*, Jan 2005, pp. 1–6.

[94] F. Meshkati, V. Poor, and S. Schwartz, "Energy-efficient resource allocation in wireless networks: An overview of game-theoretic approaches," *CoRR*, vol. abs/0705.1787, 2007.

[95] K. Iwama, , and S. Miyazaki, "A survey of the stable marriage problem and its variants," in *Proceedings of the International Conference on Informatics Research for Development of Knowledge Society Infrastructure*, Jan 2008, pp. 131–136.

[96] A. Lozano and N. Jindal, "Transmit diversity vs. spatial multiplexing in modern MIMO systems," *IEEE Transactions on Wireless Communications*, vol. 9, no. 1, pp. 186–197, 2010.

[97] A. Jensen, M. Lauridsen, P. Mogensen, T. Srensen, and P. Jensen, "LTE UE power consumption model for system level energy and performance optimization," in *Proceedings of the IEEE 76th Vehicular Technology Conference*, Sep. 2012, pp. 1–6.

[98] K. Bobae, K. Cholho, and L. Jongsoo, "A dual-mode power amplifier with on-chip switch bias control circuits for LTE handsets," *IEEE Transactions on Circuits and Systems*, vol. 58, no. 12, pp. 857–861, 2011.

[99] V. Sreng *et al.*, "Relayer selection strategies in cellular networks with peer-to-peer relaying," in *Proceedings of the IEEE 58th Vehicular Technology Conference*, Oct. 2003, pp. 1949–1953.

[100] E. Larsson, E. Jorswieck, J. Lindblom, and R. Mochaourab, "Game theory and the flat-fading gaussian interference channel," *IEEE Signal Processing Magazine*, vol. 26, no. 5, pp. 18–27, September 2009.

[101] N. Jindal, U. Mitra, and A. Goldsmith, "Capacity of ad-hoc networks with node cooperation," in *Information Theory, 2004. ISIT 2004. Proceedings. International Symposium on*, 2004, p. 271.

[102] Z. Han *et al.*, *Game Theory in Wireless and Communication Networks*, C. U. Press, Ed. Cambridge University Press, Oct. 2012.

[103] Z. Han and R. Liu, "Fair multiuser channel allocation for OFDMA networks using Nash bargaining solutions and coalitions," *IEEE Transactions on Communications*, vol. 53, no. 8, pp. 1366–1376, 2005.

[104] D. Gale and M. Sotomayor, "Some remarks on the stable matching problem," *Discrete Applied Mathematics*, vol. 11, no. 3, pp. 223 – 232, 1985.

[105] D. Gale and L. S. Shapley, "College admissions and the stability of marriage," *The American Mathematical Monthly*, vol. 69, no. 1, pp. 9 – 15, 1962.

[106] A. W. Roberts *et al.*, *Convex Functions*. New York: Academic, 1973.

[107] S. Ren and M. V. der Schaar, "Pricing and distributed power control in wireless relay networks," *IEEE Transactions on Signal Processing*, vol. 59, no. 6, pp. 2913–2926, 2011.